The assessment of waveform distortion in power systems: Validation of methods based on single-point measurements

---

A dissertation presented to The School of
Electrical, Electronic and Computer Engineering
North-West University

In partial fulfilment of the requirements for the degree Magister Ingeneriae in Electrical engineering

by

Duan Serfontein

Supervisor: Prof. A.P.J. Rens

November 2011

Potchefstroom Campus

DECLARATION

I hereby declare that all the material incorporated in this thesis is my own original unaided work except where specific reference is made by name or in the form of a numbered reference. The work herein has not been submitted for a degree at another university.

Signed: ……

Date: ……..

SUMMARY

The portion of energy converted by non-linear loads in the modern power system is increasing due to the energy-efficiency and sophistication possible with power electronics. Higher voltage and energy ratings are continuously forthcoming. These devices draw non-linear currents resulting in voltage waveform distortion at the Point of Common Coupling due to non-zero supply impedances between voltage source and the PCC. With the increase in waveform distortion comes the demand for better Quality of Supply management.

The verification and quantification of the origin of waveform distortion in a power system is a continuous field of study and forms a critical part of the mitigation design. Methods utilizing single-point measurements, usually taken at the Point of Common Coupling, for the assessment of the harmonic distortion generated by loads are continuously being published. It's been proven by means of computer simulations and laboratory experiments that in an interconnected network where multiple sources of distortion exist that loads have the ability to exchange harmonic active power between each other. This project investigates the latter statement by conducting practical experiments to conclude that loads have the ability to exchange harmonic active power and that multiple synchronized measurements should be taken to assess the harmonic distortion due to a load.

Laboratory experiments are carried utilizing an acknowledged single point measurement method. The results are compared to the direction of harmonic active power obtained from utilizing multiple synchronized measurements. To further the information obtained from the laboratory experiments, practical experiments were conducted utilizing the same methods. The results obtained coincided with the results of previously conducted experiments of which the results were published.

From the results obtained it was concluded that in an interconnected network where multiple sources of distortion exist that loads have the ability to exchange harmonic active power between each other. Furthermore it was proven that the single point measurement method investigated presented inconsistent results. Ultimately it was concluded that the reason for the inconsistency was due to the fact that loads have

the ability to exchange harmonic active power and that the single point measurement failed to acknowledge this.

Keywords

Harmonic Emission, Harmonic Vector Method, Harmonic Active Power, Localization of harmonic sources, Synchronization of instruments.

ACKNOWLEDGEMENTS

I would like to acknowledge the following people, in no particular order, for their contribution and support during the course of my studies and this project.

- *Hester Maria Viljoen for turning a dream into an opportunity.*
- *Professor Johan Rens, my supervisor, for the guidance, opportunities and inspiration that motivated me during this project.*
- *My brothers Reon and Jaendre Serfontein, who showed me every day that success comes from hard work.*
- *My parents Isabel and Henning van Wyk, for all their love and for supporting me through the years.*
- *My grandparents Basie and Magriet Venter, for always listening and caring.*
- *The Lourens family for caring and supporting me.*
- *Leigh Thornhill for her love, support and understanding.*

I can do all things through Christ which strengthens me.

Php 4:13.

Table of content

List of Figures

List of Tables

List of abbreviations

DC	Direct Current
EMF	Electromagnetic Frequency
EMI	Electromagnetic Interference
FFT	Fast Fourier Transform
GPS	Global Positioning System
HAP	Harmonic Active Power
JHAP	Joint Harmonic Active Power
LED	Light Emitting Diode
PCC	Point of Common Coupling
PPS	Pulse per second
QoS	Quality of Supply
RMS	Root Mean Square
SMPS	Switch Mode Power Supply
THD_X	Total Harmonic Distortion. This can either refer to the total current (subscript X is I) or voltage (subscript X is V) harmonic distortion.
UML	Unified Modelling Language

Chapter 1
Introduction

This chapter provides introductory information on the harmonic emission assessment techniques in general. It also provides the problem statement and discusses some of the issues that will be addressed with this project.

1.1 Background

Solid-state power electronics enhances high levels of sophistication and efficiency in energy conversion. The principle of operation is inherently non-linear and harmonic load currents have to be sustained by the supply impedances. The result is voltage waveform distortion, and as the energy levels at which these solid-state devices operate remain on the increase so does the voltage distortion generated by them. The increase in the harmonic levels has numerous negative effects on a network such as vibrations, heat losses, flicker etc. The assessment of the harmonic emission due to a specific source, remains an interesting academic and industrial problem. New academic and professional literature claiming to be able to assess how much a single source of waveform distortion is contributing in an interconnected power system are continuously forthcoming. An accurate and reliable method will be valuable as management of distortion levels overall will benefit from such knowledge.

1.1.1 Harmonic emission assessment techniques

Most of the harmonic assessment techniques use measurements obtained at a single point in the power system network [**1**], [**2**], [**3**], [**4**], [**5**]. Some of the single point measurements, lack practical application and contribute at most on a scientific level. A method that utilizes single point measurements and which is claiming practical application is the Harmonic Vector method reviewed by the CIGRE-CIRED joint working group C4.109 [**1**], [**2**]. This method requires a reference harmonic impedance from the supply source, and phasor information on harmonic voltage and current phasors to assess the harmonic distortion contributed to the network by a single source of distortion [**2**], [**4**]. The method seems practical, as precise information on

the harmonic impedance at the source of distortion or the supply network is not needed. The method requires synchronized measurements of the voltage and current phasors, but is possible with modern instrumentation.

Other methods used for the evaluation of harmonic emission due to loads, utilizes multi-point measurements. It is well known that the evaluation of distorting loads can be done by inspecting the direction of the Joint Harmonic Active Power (JHAP) [**6**],[**7**], [**8**], [**9**] if a single source of distortion exists. The JHAP method is derived from basic fundamental power theory for which a general agreement exist. However practical application is a challenging, as all nodes in the power system under study have to be characterized by means of synchronized measurements. A single-point measurement in the localisation of distortion sources in an interconnected power system is useless when Harmonic Active Power (HAP) is used in the assessment [**6**], [**7**].

1.2 Problem statement

It is generally agreed that the direction of (HAP) commensurate with the location of the source [**6**], [**8**] if a single source of distortion exists. However, it was shown [**6**], [**7**] that a single-point measurement and HAP cannot be used to further reliable information on the contribution of a specific non-linear load to the Voltage Total Harmonic Distortion (THD_V) at the Point of Common Coupling (PCC), if non-linear loads are distributed all over the power system.

Nevertheless single-point measurements are still claimed in literature (for example [**10**]) to be able to qualify and quantify the extent by which a specific load contributes to the THD_V at a PCC. Even though it was shown in [**6**], [**7**], by means of simulations and laboratory measurements, that when more than one source of waveform distortion exist in an interconnected power system, all nodes connecting a load or a source have to be studied by means of synchronous measurements as non-linear loads have the ability to exchange HAP between each other and not only between load and source.

This project's aim is to prove by means of practical measurements that loads have the ability to exchange HAP. Proving this will aid and conclude the findings in previous studies [**6**], [**7**]. Furthermore this project evaluates the harmonic emission

assessment technique as reviewed by the CIGRE-CIRED working group C4.109 [**2**] by application in a practical power system but with variables controlled and mostly known. If such single-point measurements can be used to further reliable information on the contribution of a specific non-linear load to the Total Harmonic Distortion (THD) at the PCC when non-linear loads are distributed all over the power system, it will find valuable application into practical engineering application in the management of harmonic waveform distortion.

1.3 Issues to be addressed and methodology

1.3.1 Exchange of harmonic active power

To date the concept of the exchange of HAP between loads has only be investigated by means of simulations and laboratory experiments where it was proved valid. To use the exchange of HAP as an argument in an attempt to validate the practicality of the Harmonic Vector method, it must be proved by means of practical measurements that loads have the ability to exchange HAP.

1.3.2 Practicality of harmonic vector method and jhap

To investigate the practicality of the Harmonic Vector method a practical network must be constructed that will provide control over the harmonic emission due to the utility and the loads in a network. By doing this the harmonic emission due to a specific load can be changed and investigated using both the Harmonic Vector and the JHAP methods. The harmonic orders that will be investigated will be the dominant harmonics, obtained by means of signal processing.

1.3.3 Data capturing

1.3.3.1 Instruments

To assure that accurate measurements are used for the validation of a method it is essential that calibrated instruments of class A are used for the experiments. With these instruments accurate transducers with a wide bandwidth must be used which will be able to measure high order harmonics. Measurements must be taken for a

time that will represent the different operating conditions of the network under investigation.

1.3.3.2 Measurements

Voltages and currents waveforms will be captured at the PCC and in each line connecting a load. All the instruments and measurement will be synchronized and each measurement will contain 11 periods of each waveform which will then be used to calculate the different harmonic components in the network.

To utilize the direction of JHAP for the assessment of harmonic emission caused by a non-linear load, it is necessary that multiple synchronized measurements are taken. The synchronisation of instruments placed at different locations in a network is essential and if not achieved will bring about erroneous results. Global Positioning Systems (GPS) are well known for their ability to synchronize devices and a reliable system utilizing GPSs will be developed to obtain synchronisation between the instruments.

1.3.4 Data processing

A large amount of data will be captured and stored with the power quality instruments and all this data will need to be processed. A program will be developed in MathCAD^{TM} that will process the data in a quick and accurate manner. This will avoid tedious and time consuming calculations. The results will then be presented in such a manner that it will aid the process of evaluating the different harmonic emission assessment techniques.

1.3.5 Validation of data

1.3.5.1 The exchange of harmonic active power

After the results are obtained from practical measurements it must be compared to the results obtained in previous studies which made use of simulations and laboratory measurements to prove that loads have the ability to exchange HAP. Apart from the dominant harmonics, the fundamental frequency will also be analysed and compared to the given network information.

1.3.5.2 Harmonic Vector method

The results obtained with the Harmonic Vector method will be compared to results obtained from applying the JHAP method. Emphasis will be placed on the direction of the dominant harmonic active powers and the corresponding harmonic vector magnitudes obtained with the JHAP and the Harmonic Vector method respectively.

1.4 Thesis overview

Chapter 2 discusses the literature of the project. The chapter contains an in-depth literature study on harmonics in voltage and current waveforms, a phenomena found in power quality. This chapter will also provide an overview of basic power theory, the negative effects harmonics have on power systems and the methods used to verify and quantify the presence of harmonics.

Chapter 3 is the methodology chapter and discusses the development of the practical models, to investigate the exchange of HAP between loads and the evaluation of the Harmonic Vector Method. The development of the MathCAD™ program, used to process the data, and the circuit board, used to synchronise the power quality instruments, are also provided.

Chapter 4 provides the results obtained during the practical experiment and analyses it. Typical results discussed in this chapter are the fundamental active powers, harmonic active powers and phasor diagrams at each point of evaluation. Investigating the direction of the HAP with practical measurements will indicate if loads have the ability to exchange HAP in a practical environment.

Chapter 5 provides the results obtained during the laboratory experiment. The HAP and Harmonic Vector results are analysed and compared. Comparing the results will provide an indication of the Harmonic Vector method's practical limitations due to the use of single point measurements.

Chapter 6 contains the conclusion of the project and discusses the results obtained in the experiments. The chapter will also provide recommendations for future studies.

Chapter 2

Literature Study

This chapter contains an in-depth literature study on harmonics in voltage and current waveforms, a phenomena found in power quality. Topics in this chapter include basic power theory, the negative effects harmonics have on power systems and the methods used to verify and quantify the presence of harmonics.

2.1 Basic power theory

This section discusses the fundamental and basic power theory of power systems.

2.1.1 Single-phase voltage and current definitions

The instantaneous voltage and current in an electrical power network can generally be expressed as

$$\boldsymbol{v}(t) = V_m \cos(\omega \boldsymbol{t} + \alpha) \tag{2.1}$$

and

$$\boldsymbol{i}(t) = I_m \cos(\omega t + \beta) \tag{2.2}$$

where V_m and I_m are the maximum voltage and current magnitude respectively, ω is the angular frequency in radians per second (rad/s) and can be expressed as

$$\omega = 2\pi f \tag{2.3}$$

where f is the fundamental frequency. The initial phase shifts of the voltage and current waveforms are given by α and β respectively. The time that the waveforms take to complete one cycle is called the period of the waveforms and is represented by T where (Figure 2.1)

$$T = \frac{1}{f}. \tag{2.4}$$

The root-mean-square (RMS) value of the voltage or current waveform is

$$V = \frac{V_m}{\sqrt{2}} \tag{2.5}$$

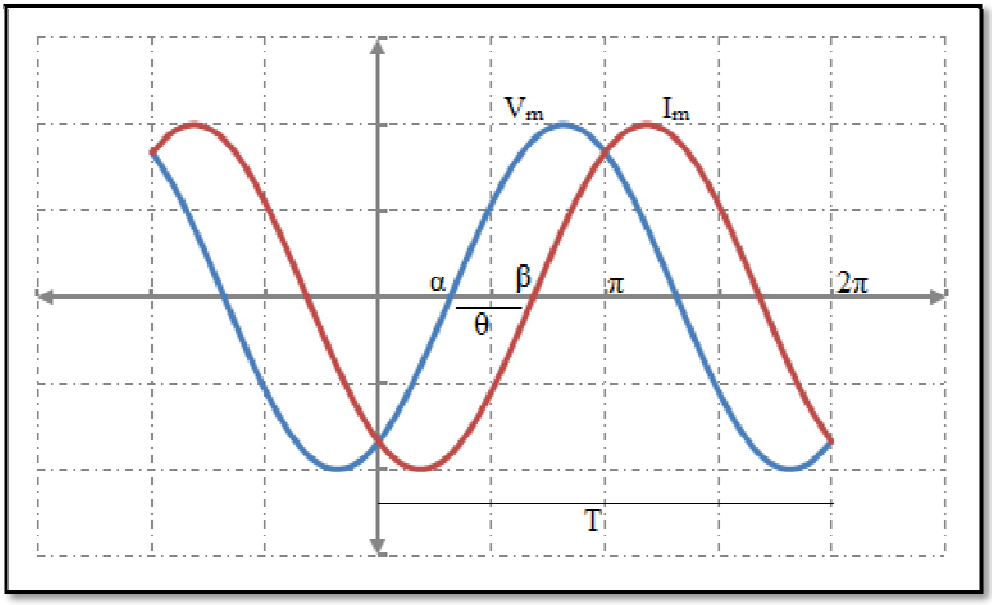

Figure 2.1. Pure sinusoidal waveforms [11]**.**

Using Euler's identity, the instantaneous voltage and current can be given by

$$\boldsymbol{v}(t) = \mathrm{Re}\left[V_{\max} e^{j(\omega t+\alpha)}\right] \tag{2.6}$$

and

$$\boldsymbol{i}(t) = \mathrm{Re}\left[I_{\max} e^{j(\omega t+\beta)}\right]. \tag{2.7}$$

Where Re denotes to the real part of the voltage (or current) phasor.

The RMS values can be presented in terms of exponential values as

$$\boldsymbol{V} = \mathrm{V} e^{j\alpha} \tag{2.8}$$

and

$$\boldsymbol{I} = Ie^{j\beta} \tag{2.9}$$

2.1.2 Single-phase power definitions

The power absorbed in an electrical network can be divided into two groups namely active and reactive. The instantaneous power absorbed by a load in a network can be defined by the following:

$$\begin{aligned} \boldsymbol{p}(t) &= \boldsymbol{v}(t)\boldsymbol{i}(t) \\ &= VI\cos(\alpha-\beta)\left\{1+\cos\left[2(\omega t+\alpha)\right]\right\}+ \\ &\quad VI\sin(\alpha-\beta)\left\{1+\sin\left[2(\omega t+\alpha)\right]\right\} \end{aligned} \tag{2.10}$$

where

$$\boldsymbol{p}_r(t) = VI\cos(\alpha-\beta)\left\{1+\cos\left[2(\omega t+\alpha)\right]\right\} \tag{2.11}$$

$$\boldsymbol{p}_{\text{var}}(t) = VI\sin(\alpha-\beta)\left\{1+\sin\left[2(\omega t+\alpha)\right]\right\} \tag{2.12}$$

equation (2.11) is the instantaneous active (real) power absorbed by the resistive component of the load and equation (2.12) is the instantaneous reactive power absorbed by the reactive components of the load [**12**]. The phase angle between the voltage and the current waveform

$$\theta = (\alpha-\beta) \tag{2.13}$$

is generally known as the power factor angle.

$$pf = \cos(\alpha-\beta) \tag{2.14}$$

The power factor, equation (2.14), is always positive. If the load is inductive the current phasor lags the voltage phasor, $\alpha > \beta$, and the load is said to have a lagging power factor. On the other hand if the load is capacitive the current phasor leads the voltage phasor, $\alpha < \beta$, resulting in a leading power factor.

From (2.11) and (2.14) the average real power can given by

$$P = VI\cos(\alpha - \beta) \tag{2.15}$$

and is measured in Watt (W). The reactive power is represented by

$$Q = VI\sin(\alpha - \beta) \tag{2.16}$$

and is measured in VAR. The apparent power absorbed by the load is given by

$$S = VI \tag{2.17}$$

and is measured in Volt Ampere (VA). The apparent power can also be given in the rectangular form (figure 2.2) as

$$\boldsymbol{S} = \boldsymbol{VI}^{*} = VI\cos(\theta) + jVI\sin(\theta) = P + jQ \tag{2.18}$$

where $\boldsymbol{I}^{*}$ is the conjugate of $\boldsymbol{I}$.

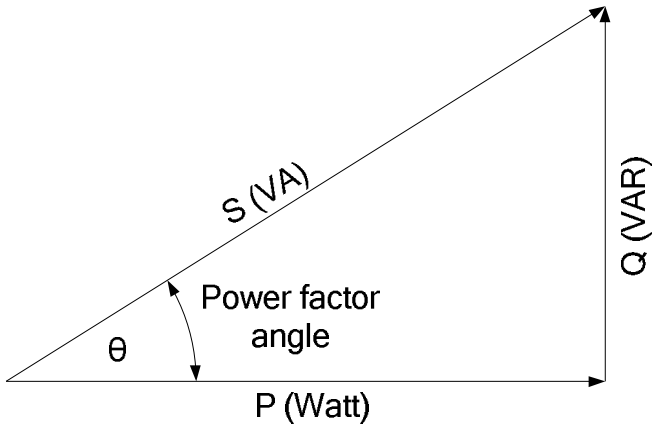

Figure 2.2. Power triangle

2.1.3 Three-phase voltage and current definition

Three-phase networks are comparable to single-phase systems regarding voltage and current definitions. Three-phase networks consists of three phases which are generally represented by phase a, b and c. The angle between each phase is equal

to $120°$. If a positive phase sequence[1] system is assumed, the voltage and current phasors are given by the following equations:

$$\boldsymbol{v}_a(t) = V_{a\max}\cos(\omega t) \tag{2.19}$$

$$\boldsymbol{v}_b(t) = V_{b\max}\cos(\omega t - 120°) \tag{2.20}$$

$$\boldsymbol{v}_c(t) = V_{c\max}\cos(\omega t + 120°) \tag{2.21}$$

Where $V_{a\max}$, $V_{b\max}$ and $V_{c\max}$ are the maximum value of the phase voltages measured from line to neutral.

$$\boldsymbol{i}_a(t) = I_{a\max}\cos(\omega t + \theta_a) \tag{2.22}$$

$$\boldsymbol{i}_b(t) = I_{b\max}\cos(\omega t + \theta_b - 120°) \tag{2.23}$$

$$\boldsymbol{i}_c(t) = I_{c\max}\cos(\omega t + \theta_c + 120°) \tag{2.24}$$

Where $I_{a\max}$, $I_{b\max}$ and $I_{c\max}$ are the maximum value of the phase currents in each phase. The phase difference (power factor angle) between each phase voltage and its resulting current are represented by θ_a, θ_b and θ_c (figure 2.3).

2.1.4 Three-phase power definitions

The total power dissipated in a three-phase network is equal to the sum of the powers in each phase. From equations (2.17), (2.15) and (2.16).

$$S_{total} = S_a + S_b + P_c \tag{2.25}$$

$$P_{total} = P_a + P_b + P_c \tag{2.26}$$

$$Q_{total} = Q_a + Q_b + Q_c \tag{2.27}$$

[1] A positive phase sequence is the term used if phase c leads phase a with 120°.and phase b lags phase a with 120°.

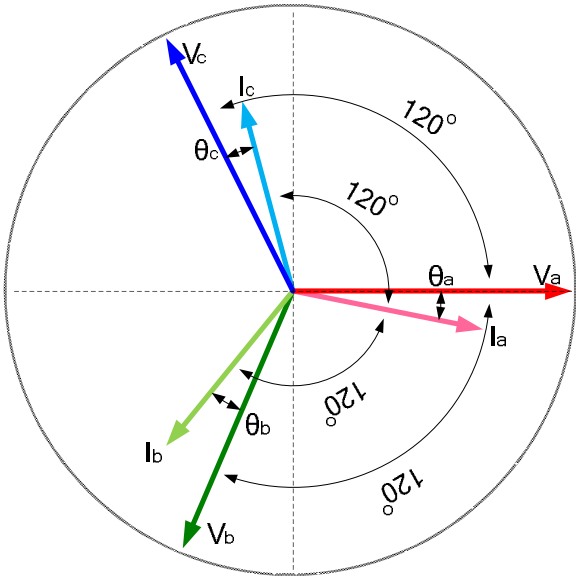

Figure 2.3. Phasor diagram of voltages and currents in a three-phase network

In a balanced three-phase network, the voltages across each phase and the currents in each phase are equal. Therefore the powers in each phase are equal.

$$S_a = S_b = S_c \tag{2.28}$$

$$P_a = P_b = P_c \tag{2.29}$$

$$Q_a = Q_b = Q_c \tag{2.30}$$

Equations (2.25), (2.26) and (2.27) can be simplified to:

$$\boldsymbol{S}_{total} = 3\boldsymbol{V}_a\boldsymbol{I}_a^* \tag{2.31}$$

$$P_{total} = 3V_aI_a\cos(\phi_a) \tag{2.32}$$

$$Q_{total} = 3V_aI_a\sin(\phi_a) \tag{2.33}$$

All of the definitions given in this section are applicable to symmetrical and sinusoidal waveforms. In systems with asymmetrical and non-sinusoidal waveform conditions, the definitions are not applicable [**8**].

2.2 Harmonic emission

The amount of power electronics utilized by the industry and loads are increasing due to their ability to be energy efficient. The non-linear load characteristics of power electronics increase the quantity of harmonics present in a network. As the effects of an increase in harmonics are detrimental, the need for better power quality (harmonic distortion) management have increased. Therefore, it is important to fully understand the characteristics of harmonics and to be able to accurately locate and quantify the existence of harmonics.

2.2.1 Defining harmonics

Harmonics in a power system are commonly defined as frequencies that are integer multiples of the fundamental frequency (50Hz in South Africa).

$$f_h = nf \tag{2.34}$$

where f_h is the harmonic frequency, h and n are integers and f is the fundamental frequency. In equation (2.34) h is defined as the harmonic order e.g. for the 5th harmonic order h and n are equal to 5, resulting in a frequency of 250 Hz represented by f_5.

If the voltage and current waveforms of a network contain harmonics, which is mostly the case in a practical environment, the waveforms will be distorted. Different methods exist which can be used to identify the different harmonics present in a waveform, a reliable and commonly used technique is the Fourier transform [**13**], [**14**], [**15**], [**16**], [**17**], [**18**], [**19**]. Fourier transform decomposes a nonsinusoidal waveform into sinusoidal waveforms of different frequencies. This is accomplished by transforming the nonsinusoidal waveform from the time domain to the frequency domain. The nonsinusoidal waveform is the sum of these individual sinusoidal waveforms and can be presented by equation (2.35).

$$\boldsymbol{v}(t) = V_0 + V_1\cos(\omega t) + V_2\cos(2\omega t) + ... + V_n\cos(n\omega t)\,. \tag{2.35}$$

In this expression V_0 is the DC component in the waveform, V_1 is the peak magnitude of the fundamental frequency and $V_{2,3...n}$ are the peak magnitudes of the

harmonic frequencies present in the waveform. Because of the waveform symmetry of even harmonics ($h = 2,4,6,...$) their effect on the fundamental waveform can be neglected as they cancel themselves out[2]. Therefore they are generally ignored in harmonic analysis.

An example of the effect that the 3rd and 5th uneven harmonics have on the fundamental frequency (50Hz) waveform are shown in figure 2.4. As seen from this figure the distorted waveform consists of the fundamental and the harmonic frequencies.

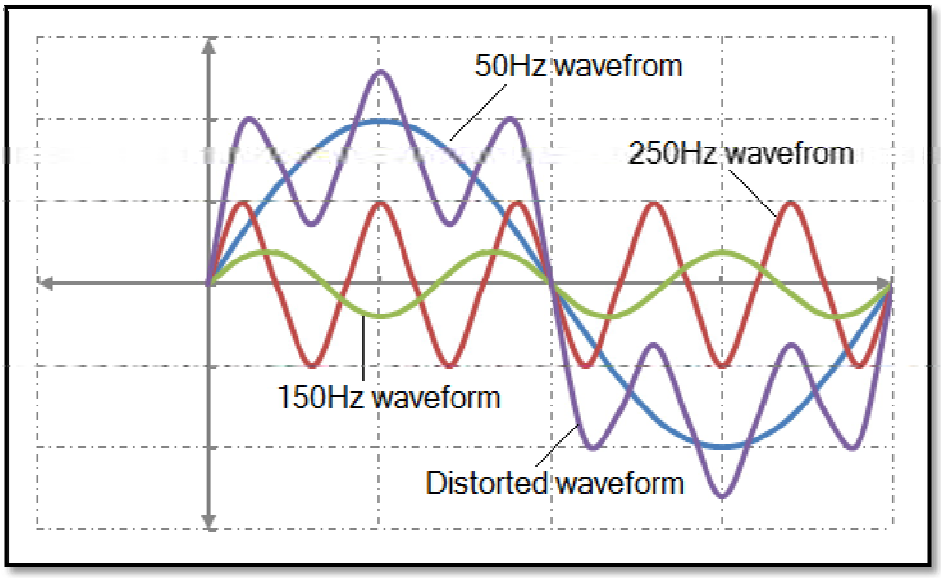

Figure 2.4. Nonsinusoidal (purple waveform) and harmonic waveforms.

The frequency spectrum of the distorted waveform in figure 2.4, is given in figure 2.5. From this, it is easy to obtain the information of the different frequencies that are present in the distorted waveform.

[2] Even harmonics have an equal amount of positive and negative maximums within halve a period of the fundamental waveform.

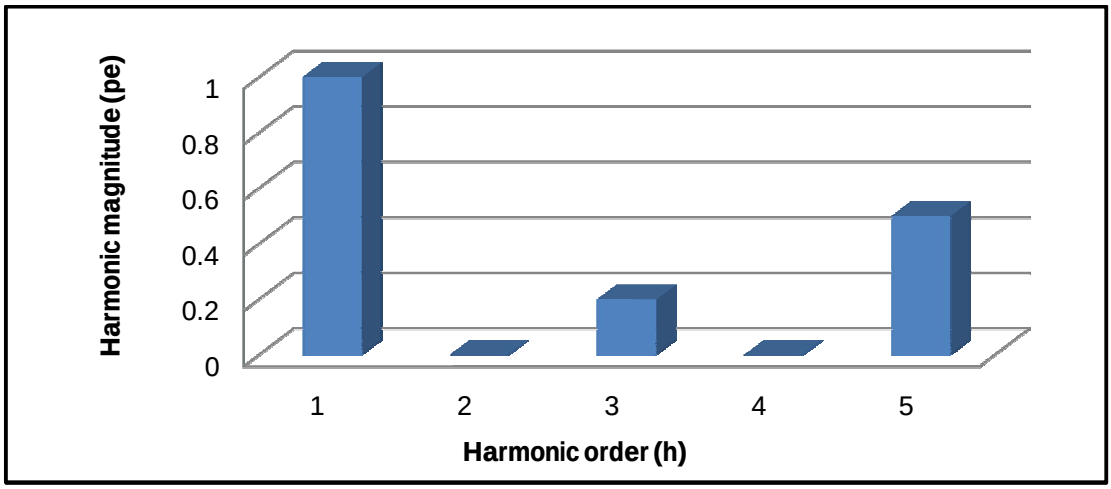

Figure 2.5. Fourier Transform of the distorted waveform in figure 2.4 .

2.2.2 Harmonic generation

The harmonics present in an electrical network can be from different sources e.g. electric power generators can generate harmonics due to non-linear magnetic flux coupling or vibrations. The most common sources of harmonics in an electrical network are non-linear loads.

If a load is linear then the current drawn by such load is in phase with the voltage supplied to the load. In other words, the power factor of this load is 1. A load is said to be non-linear if the current drawn by the load is out of phase with the voltage supplied to the load resulting in a power factor less than 1. The harmonic currents generated by non-linear loads then generate harmonic voltages due to the non-zero supply impedances.

It can also happen that linear loads generate harmonic currents, but this can only happen if the supply voltage is distorted.

The use of non linear loads in electric power networks is increasing, leading to an increased amount of harmonic distortion in waveforms. Non-linear loads that are known for their ability to generate harmonics are: Arc furnaces, Switch-mode Power Supplies (SMPS), rectifiers and variable speed drives etc. [**20**], [**21**].

2.2.3 Harmonic parameters

This section focuses on how to use the information in section 2.2.1 and 2.2.2 to advance the information on harmonic distortion.

The RMS value of a non-sinusoidal current waveform can be represented by the following equation;

$$I_{rms} = \sqrt{I_{1\_rms}^2 + I_{3\_rms}^2 + ... + I_{n\_rms}^2} \tag{2.36}$$

The same principle can be used for the RMS value of the voltage waveform.

The amount of current distortion due to a harmonic frequency can be represented as a percentage of the current's fundamental frequency value (with $\%f$ as the unit of measurement), or as a percentage of the current's total RMS value (with $\%r$ as the unit of measurement). The amount of current distortion present in a waveform is given by equation (2.37).

$$I_n = \frac{I_h}{I} 100 \tag{2.37}$$

Where I is either the value of the fundamental current or the RMS value of the total current.

The Quality of Supply (QoS) management requires amongst others, management of the quality of the voltage waveform. Waveform distortion is one aspect of QoS and generally referred to as Voltage Total Harmonic Distortion. The total harmonic distortion of a current waveform is given by the following formula:

$$THD_I = 100 \sqrt{\sum_{h=2}^{\infty} \left(\frac{I_h}{I_1} \right)^2} \tag{2.38}$$

THD_V and THD_I are used to symbolize the total harmonic distortion in the voltage and current waveform respectively. The concept of compatibility between loading and supply conditions sets an upper level to THD_V (such as 8%) [**22**].

2.2.4 Effect of harmonics

The presence of harmonics in a network can have very negative and detrimental effects on electrical equipment, causing them to malfunction or even fail.

Harmonics can cause capacitor banks (used for power factor correction) to fail because of reactive power overload, resonance frequencies and harmonic amplification. Other effects of harmonics include the increase of power losses in transformers and rotating machines that generates unwanted heat, which deteriorate the live expectancy of the equipment.

High order harmonics can generate electromagnetic frequencies (EMF), which can introduce electromagnetic interference (EMI) in sensitive equipment. The presence of EMI in a network can cause signal interferences which can affect control, protection and safety signals.

A more in-depth discussion on the effects of harmonics in a network is presented in [**20**], [**21**], [**23**].

2.3 Harmonic emission assessment techniques

Customers of a supply utility should comply with power quality harmonic standards to avoid costly penalties as a result of the damage that harmonics cause to electrical equipment. Therefore, with the increase of waveform distortion, comes the demand for better power quality management.

To exercise good power quality management, it is important to accurately assess the harmonic emissions in the network. Methods used for harmonic emission techniques can be divided into two groups; multi-point [**8**], [**7**], [**6**], [**9**], [**24**] and single-point [**1**], [**2**], [**4**], [**5**] measurement techniques.

Multi-point measurement techniques, utilize multiple, synchronized measurements commonly taken at the point of common coupling (PCC) and in each line connected to a load (feeders). One such method is the Joint Harmonic Active Power (JHAP) method, which utilizes the direction of HAP to determine the source of voltage distortion. The JHAP is recommended by IEEE 1459-2010 standards [**8**], as a

method that can be used to successfully determine the amount and the location of harmonic distortion.

2.3.1 Joint Harmonic Active Power (JHAP)

It is agreed that the classical power theory can be applied on per harmonic basis when voltage and current waveform distortion exists [**8**]. Various approaches exist when these powers have to aggregate in order to further information on all the energy phenomena in a power system.

From equations (2.8) and (2.35) it can be shown that, a distorted voltage and current waveform in the time domain can be presented in the synthetic frequency domain by a finite range of complex nth order harmonic phasors $\boldsymbol{V}_n$ and $\boldsymbol{I}_n$ defined as:

$$\boldsymbol{V}_n = U_n e^{j\alpha_n} \tag{2.39}$$

and

$$\boldsymbol{I}_n = I_n e^{j\beta_n} \tag{2.40}$$

The phase angles of the voltage and current phasor are represented by α_n and β_n respectively. The fundamental and harmonic real powers can then be calculated as:

$$P_1 = \mathrm{Re}\left\{\boldsymbol{V}_1 \boldsymbol{I}_1^*\right\} \tag{2.41}$$

and

$$P_h = \sum_n \mathrm{Re}\left\{\boldsymbol{V}_n \boldsymbol{I}_n^*\right\} \tag{2.42}$$

$\boldsymbol{I}_n^*$ denotes the complex conjugate of the harmonic phasor current, the product of $\boldsymbol{V}_n$ and $\boldsymbol{I}_n^*$ denotes the complex power.

The JHAP in all the harmonic components “flowing” through a node is then:

$$JHAP = \sum_{h\neq 1}^{N} V_h I_h \cos\left(\phi_h\right) \tag{2.43}$$

with:

$$\phi_h = \alpha_n - \beta_n \tag{2.44}$$

in which $h = 2,3,...,N$ with N the highest harmonic order considered.

A network diagram (figure 2.6), can be used to get a better understanding of how the direction of JHAP is utilized for harmonic emission assessment. If the direction of active power in the fundamental frequency component is being taken as positive (a positive value) when delivered to the PCC from the supply network (feeder into PCC) and positive when delivered from the PCC to the loads, then a negative value in JHAP (or in HAP at a harmonic) indicates that such load is the source thereof as it is opposite to the direction of the fundamental frequency active power.

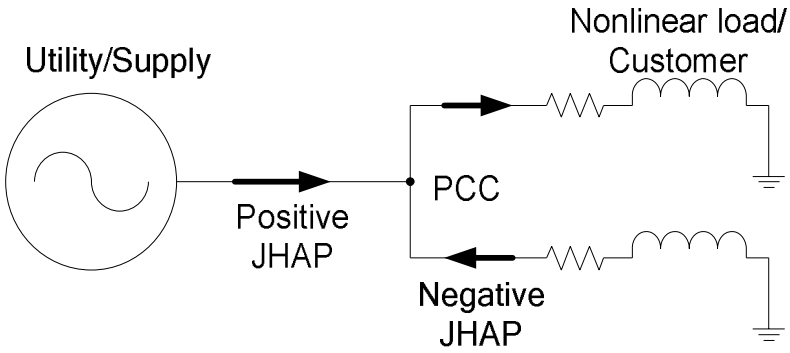

Figure 2.6. Single line network diagram for JHAP

It has been proven that multiple synchronized measurements should be taken, when using JHAP [**6**], [**7**], to further the information regarding power quality in a network. These laboratory and simulation experiment results proved that single-point methods utilizing the direction of JHAP cannot be used to evaluate harmonic emission in a network where multiple sources exist [**7**].

To assurance accurate results the period over which measurements are taken must be representative of the network's normal work cycle, this is normally a minimum period of seven days.

2.3.2 Harmonic Vector Method

Unlike multi-point measurement methods, single-point measurement methods only take measurements at a single point in a network. This is normally a point of common coupling (PCC).

A method claiming to locate and quantify the existence of harmonic distortion using only single-point measurements is the Harmonic Vector method [**1**], [**4**], [**5**].

To introduce the harmonic voltage emission level from a source of distortion, an equivalent network as shown in figure 2.7, is used. $\boldsymbol{E}_{h0}$ is the harmonic voltage phasor of the supply network as modelled and $\boldsymbol{V}_h$ is the harmonic voltage phasor across the load as measured at the point of supply (Source) to the load. $\boldsymbol{I}_h$ is the harmonic current phasor flowing through the source connection backwards to the supply network. $\boldsymbol{Z}_h$ represents the complex supply network impedance and $\boldsymbol{Z}_{hc}$ the complex load impedance. $\boldsymbol{I}_{hc}$ is the harmonic current phasor as generated by the source of distortion.

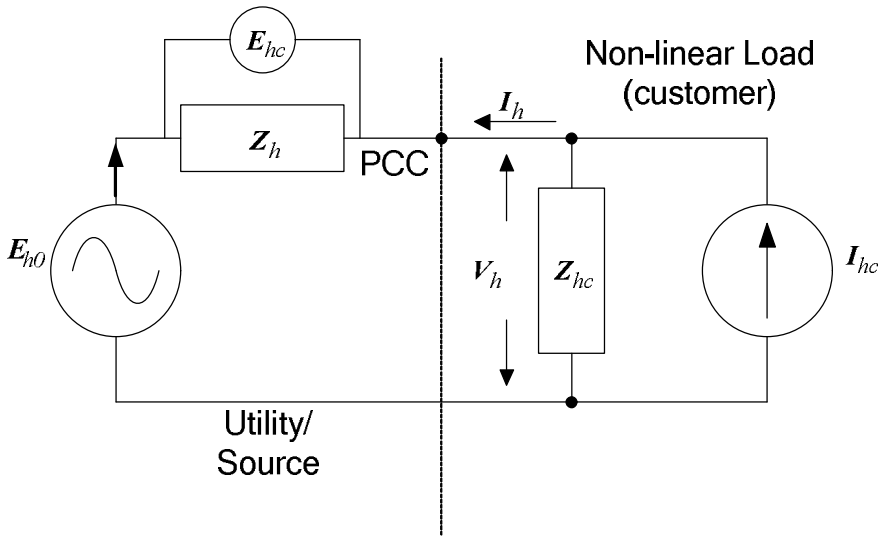

Figure 2.7. Equivalent network diagram

Application of this method requires that the magnitude of the harmonic voltage phasor $\boldsymbol{V}_h$ be larger than harmonic voltage phasor $\boldsymbol{E}_{h0}$ when the source of distortion is connected [**2**], [**4**].

The harmonic voltage emission from the distorting load into the supply network is defined as the magnitude of the harmonic voltage phasor $\boldsymbol{E}_{hc}$ and shown in figure 2.8.

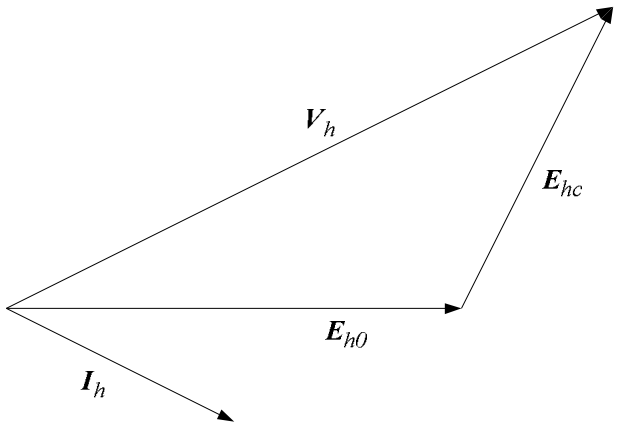

Figure 2.8. Phasor representation of harmonic emission.

The emission of harmonic current $\boldsymbol{I}_h$ is defined as the current that flows upstream through impedance $\boldsymbol{Z}_h$ when the distorting load is connected to the network. Equation (2.45) is used to determine $\boldsymbol{I}_h$:

$$\boldsymbol{I}_h = \boldsymbol{I}_{hc}\frac{\boldsymbol{Z}_{hc}}{\boldsymbol{Z}_h + \boldsymbol{Z}_{hc}} - \frac{\boldsymbol{E}_{h0}}{\boldsymbol{Z}_h + \boldsymbol{Z}_{hc}}. \tag{2.45}$$

The harmonic voltage phasor due to this emission is then determined as:

$$\boldsymbol{E}_{hc} = \boldsymbol{Z}_h\boldsymbol{I}_h = \boldsymbol{V}_h - \boldsymbol{E}_{h0}. \tag{2.46}$$

It is evident from equation (2.46) that the supply network impedance $\boldsymbol{Z}_h$ dictates the contribution made by the non-linear load to the harmonic voltage distortion at the PCC.

Obtaining the actual value of the supply impedance is not always practical [**25**], [**26**]. A reference network impedance $\boldsymbol{Z}_{h-ref}$ is used to represent the network impedance. Substituting $\boldsymbol{Z}_h$ in equation (2.46) with the reference impedance $\boldsymbol{Z}_{h-ref}$ enables the calculation of the harmonic voltage phasor, due to the emission of harmonics currents:

$$\boldsymbol{E}_{hc} = \boldsymbol{Z}_{h-ref}\boldsymbol{I}_h = \boldsymbol{V}_h - \boldsymbol{E}_{h0}\,. \tag{2.47}$$

The harmonic voltage emission is then defined as the magnitude of the harmonic voltage phasor $\left|\boldsymbol{E}_{hc}\right|$. Take note that this method is only valid if

$$\boldsymbol{V}_h > \boldsymbol{E}_{h0}\,. \tag{2.48}$$

otherwise the harmonic emission is taken as zero [**1**], [**2**].

2.4 Instruments and measurements

To successfully utilize any harmonic emission assessment techniques, it is necessary to obtain accurate measurements. For measurements to be valid for comparing results from two different methods a class A instrument must be used [**22**].

For both the JHAP and the harmonic vector method, harmonic voltages and currents must be measured. This requires accurate voltage and current transducers which are sensitive to the fundamental as well as the harmonic frequencies.

However in practice, it is not always possible to choose the right transducer for the application, as most companies have their own transducers designed specifically for their conditions. This is troublesome since most of the transducers available in practical environments are designed for the fundamental frequency and are not always accurate when measuring harmonic frequencies.

2.4.1 Sampling frequency

To correctly decompose the measured waveforms into their individual harmonic frequencies, measurements should be taken at a certain sampling frequency to avoid aliasing. This frequency is called the Nyquist frequency. To avoid aliasing of the reconstructed waveform the sampling frequency of an instrument should not be less than twice the frequency of the analysed harmonic i.e:

$$f_s \geq 2 f_N \tag{2.49}$$

f_s is the sampling frequency and f_N is the frequency of the highest harmonic order under evaluation [**21**], [**19**].

The IEEE 1459-2010 oblige that up to the 49th harmonic or the 25th, if the 49th is of no concern, should be measured for valid harmonic emission evaluations. Thus, the minimum sampling frequency of an instrument should be at least 4900Hz or 2500Hz for a fundamental frequency of 50Hz [**8**].

2.4.2 Synchronisation

The synchronisation of time allows for the comparing of data obtained at different locations in a network. Without synchronisation, comparing the data of distributed instruments can be very time consuming or even impossible, as experienced with the post event analysis of the major blackout that effected South Canada and the northern parts of the United States [**27**].

Synchronisation of instruments is achieved with time synchronised signal sources. The most familiar signal source is that of satellites used by Global Positioning System (GPS). Other sources of synchronised time signals include, earth-based radio signals and time-setting signals via the internet [**27**].

Earth-based radio signals such as the WWV, WWVH and WWVB are the cheapest methods of synchronisation but have practical limitations. Radio signals are very vulnerable to interferences such as EMI found at high-voltage power networks. Radio signals are also locally bound to certain regions and cannot be used for global scale

synchronisation. Due to these limitations this method of synchronisation is inaccurate and therefore less preferable than the other methods.

Time-setting signals are commonly used over the internet to set the time of computers. This method is normally fast and easy and all that is required is a network connection and the appropriate software. It is therefore recommended that computers and servers use this method for time synchronisation.

Satellite time synchronisation sources are the most reliable and accurate method of synchronisation. The advantages of the satellite signals are:

- They are not that susceptible to interferences.
- They are globally available.
- Not expensive to utilize.
- Are always up to standard.

GPS satellites were originally used by the U.S. Military for navigation purposes and were later made available to the public. The operation of a GPS depends on 24 GPS satellites each having four atomic onboard clocks kept current by atomic clocks at the U.S. Naval Observatory. The time of each GPS satellite is within a few nanoseconds from each other providing high accuracy synchronisation signals.

A GPS unit is at all times connected to at least four satellites. This enables the GPS to position itself in a three dimensional coordinate space; latitude, longitude and height above sea level. This enables the GPS to correct the delay in the time signals send from the satellites.

Some GPS units provide a pulse per second (pps). The pps is a signal sent from the satellites in the beginning of each second and can be used as a trigger signal for more accurate synchronisation. The amplitude of the pps is determined by the GPS unit while the length of the pulse can be adjusted, by changing the GPS's settings.

By utilizing any of the above methods for synchronisation it is possible to compare the JHAP measured at different locations. Therefore it increases the accuracy of harmonic emission assessment.

Chapter 3
Measurement techniques and development of a data model

Rens and *et al* [**7**] proved that the use of single-point measurements for the localisation of harmonic sources are not suitable, when the direction of JHAP is used. The reason for this, is that from computer simulations and laboratory experiments it was shown that loads have the ability to exchange harmonic active power between each other.

Due to the demand for practical, easy and effective harmonic emission assessment techniques, single-point methods are continuously being published claiming to be able to assess the source of harmonic distortion only using single point measurements. The harmonic vector method [**1**], [**2**] is one of these methods and although it does not use the direction of JHAP, this project will investigate its practical limitations due to the use of single point measurements.

This chapter discuss the development of the practical models, to investigate the exchange of HAP between loads and the evaluation of the Harmonic Vector Method.

3.1 Synchronization of multiple recorders

The NRS048-2 [**22**], proposes that class A measurement requirements must be met when comparing the measurement performance and results to standards. Therefore if the measurements taken during both the practical and the laboratory experiments are to be valid, a class A instrument must be used to take measurements. The instruments used for all the measurements are Power Quality recorders called Impedograph and is designed and manufactured by CtLab.

3.1.1 Instrument specifications

The ImpedoGraph is a SABS certified, class A Power Quality recorder designed to monitor Power Quality and other parameters according to international standards

and regulation. It is highly accurate and versatile and provides among others four voltages and currents inputs. Therefore the instrument used for the measurements during both experiments comply with the NRS048-2 and can be used for comparing different methods meant for harmonic emission evaluation.

3.1.1.1 Analogue to digital conversion

The waveforms recorded by the instrument are digitized at a 16 bits resolution at a sampling rate of 128 times the fundamental frequency with 4 times over sampling. Therefore waveforms with a fundamental frequency of 50 Hz are sampled at a frequency of 25.6 kHz.

By continuously adjusting the sampling frequency to 128 times that of the fundamental frequency, the instrument offers waveform data that can be converted to the frequency domain without any skewing and spectral leakage.

3.2 Measurements techniques

The same measurement technique were utilized for both the single point and multipoint measurements. During both the laboratory and practical experiments ImpedoGraphs were used to measure the voltage and current at the PCC and in each line supplying a load. All the measurements were synchronized to assure reliable and accurate data.

The measurements obtained from the instrument that captured data at the PCC were used for the single point measurement method. While the synchronized measurements from all the instruments were used for the multipoint measurement method.

This technique will ensure that the same data are used for both the methods and that the network's conditions will not change with the implementation of the different methods. Therefore it can be assumed that the results obtained from the different methods can be compared since they represent the same network conditions.

3.3 Practical investigation on the exchange of JHAP

To investigate the exchange of harmonic active power in a practical power network, measurements are recorded in a substation comprising two 400/66kV incomers supplying two local mines. One mine (load 1) use 12-pulse rectifiers to supply arc

furnaces a load well-known for producing large characteristic harmonics. Load 1 also has capacitor filter banks designed to filter out characteristic harmonics. Load 2 is a mine with electrical equipment vulnerable to harmonics. Load 1 is fed by two feeders and load 2 by a single feeder (figure 3.1).

3.3.1 Measurement setup

For this investigation, multiple synchronized measurements are taken by two groups of instruments with an accuracy of 0.1% up to the 30th harmonic. One group consists of three instruments and are positioned at each line connecting a load. The other group consisted of two instruments and are placed at the two incomers (figure 3.1).

Each instrument measures three-phase voltage and current waveforms. Voltage and current waveforms consists of 11 periods and are simultaneously digitized at a Nyquist frequency of 12.8 kHz. This data acquisition setup enables synchronous A/D conversion of 30 channels (15 voltages and 15 currents). Each measurement made by an instrument consists of 9856 data points[3].

Due to practical limitations and rules and regulations of the substation, it is not possible to install private VTs and CTs. Therefore voltages and currents are measured from the VTs and CTs, installed by the utility, assuming that they are accurate especially for the fundamental frequency.

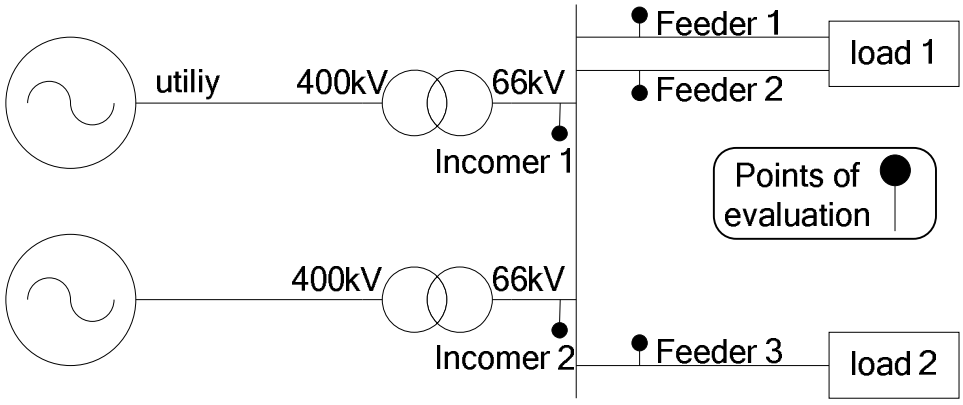

Figure 3.1. Practical network for the evaluation of the exchange of JHAP between loads.

[3] 11 waveforms each represented by 128 data points for 3 voltages and currents plus the time representing each data entry (11*128*7).

Measurements are taken every 10 minutes over a 6 hour period to avoid filling the instruments' memory and to secure a load profile representing different operating conditions.

3.3.2 GPS synchronisation

To achieve synchronisation between all instruments, two Garmin 18-LVC GPSs (figure 3.2) are used (one for each group of instruments). The GPSs provide the accurate pulse per second (pps) used for synchronising instruments with an accuracy of 1µs. Both the GPSs have internal antennas and are positioned outside the substation building to assure maximum accuracy.

Figure 3.2. Garmin GPS 18-LVC

3.3.2.1 Triggering problem

The Garmin 18-LVC provides a pps signal with a magnitude of 5 V and a duration set to 500 ms. The instruments used to record the measurements has a trigger threshold voltage of 12 V and is triggered by both the rising and falling edge of a trigger pulse (figure 3.3). In addition the instruments only have a fixed amount of memory space.

Therefore the pps signal received from the GPS will not be able to trigger the instrument as its voltage magnitude is below the required threshold voltage. Furthermore the pps has a period of 1 second and triggering the instrument twice

every second will result in filling the instrument's memory before the investigation is complete.

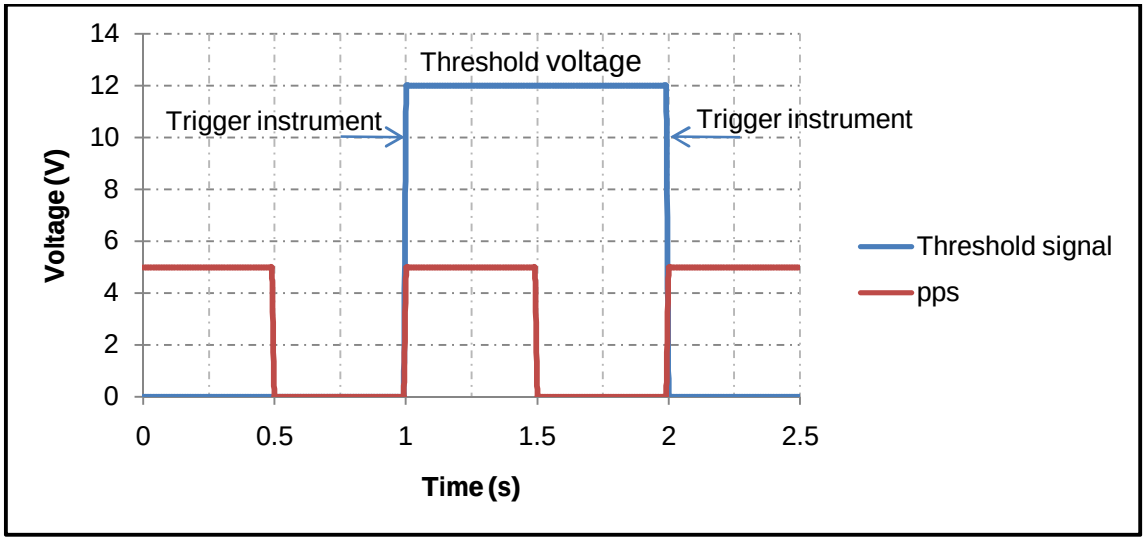

Figure 3.3. Pulse per second signal compared to threshold signal.

3.3.2.2 Synchronisation circuit board

To overcome these problems a circuit board is developed. The main function of the board is to receive the actual time from a GPS, compare the time to a pre set time and if necessary trigger an instrument.

The power quality instruments offers a 15 V DC (Direct Current) source. Using this source as an input and the pps from a GPS to switch a transistor the necessary threshold voltage is obtained and can be used to trigger an instrument (Figure 3.4).

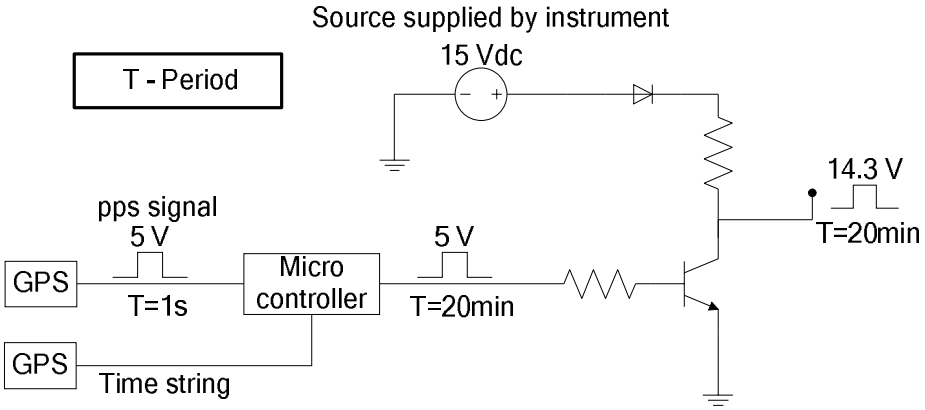

Figure 3.4. Circuit diagram

To avoid filling the memory of an instrument and still use the pps for synchronisation, a PIC16F886 microcontroller is used. The procedures of the microcontroller and the circuit board are as follows:

The microcontroller reads the time string (actual time), sent from a GPS. The time received by the microcontroller is then compared to a pre set time (trigger time), which the microcontroller is programmed with.

The microcontroller's external interrupt function is enabled if the two times match. The rising edge of a pps signal can then trigger the interrupt and in response the interrupt function switches the transistor into a new status (from off to on and vice versa).

After the transistor is switched the pre set time gets incremented with 10 minutes and the external interrupt function is disabled. The transistor then remains in its current status until the GPS's time concurs with the new trigger time and the external interrupt function is enabled. The Unified Modelling Language (UML) of the code used to program PIC is available in appendix A.

This process is repeated and thus generates a triggering signal with a period of 20 minutes and a 50% duty cycle. This ensures that the instruments will be triggered every 10 minutes.

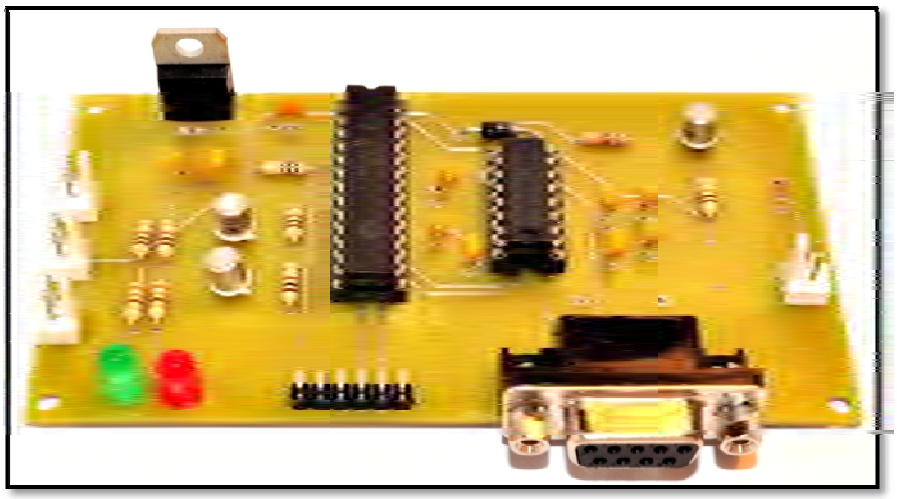

Figure 3.5. Circuit board used to synchronize the instruments.

To evaluate the accuracy of the synchronisation circuit board, two circuit boards, each with their own GPS, are setup and left for 24 hours. During which the trigger pulse of each circuit are measured and compared. A maximum error of 8 µs (0.04% of a 50 Hz waveform) is recorded (figure 3.6). There are also instances where the trigger signals achieved synchronisation with an error of less than 2 µs (figure 3.7). The inconsistency of the error is due to the error in the pps that differs from time to time depending on the position of the GPS satellites. Also the computing time of the microcontrollers are not exactly the same as they are fabricated from different pieces of silicon causing their clock frequencies to slightly differ.

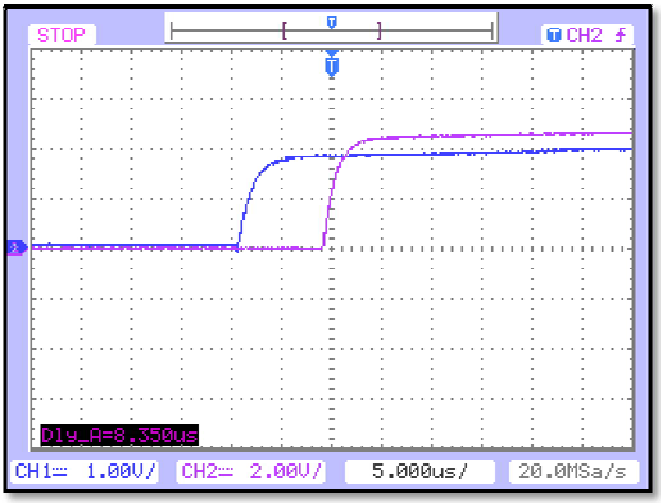

Figure 3.6. Trigger signals with maximum error. Signals with different magnitudes were used for illustration purposes.

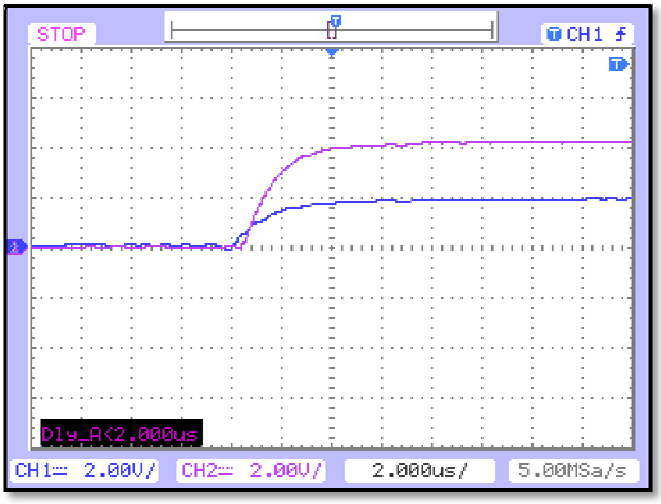

Figure 3.7. Trigger signals with maximum accuracy.

3.3.3 Processing the data

Using the circuit boards allows for accurate synchronisation of the five instruments that are used during the investigation. One of the circuit boards is used to trigger the three instruments situated at each line connecting a load and the other board triggers the remaining two instruments situated at the two incomers (figure 3.1). This assured accurate and synchronized measurements (waveform data).

The waveforms data measured at each location are saved as Microsoft Excel files and sorted according to time and location. A total of 85 excel files each containing 9856 entries are saved. Because of the amount of data and the time it takes to calculate the JHAP at each location using equation (2.43), a MathCAD^{TM} program is written to process the data (chapter 3.5).

The MathCAD^{TM} program imports all the data saved from each location and calculates the JHAP, for each measurement. After processing the data, MathCAD^{TM} saves the results in a Microsoft Excel format. Microsoft Excel will then be used to plot the results.

3.4 Evaluation of the Harmonic Vector Method

A 400 V and 5 kVA laboratory three-phase four-wire power system feeding two non-linear loads is constructed as shown in figure 3.8. The two loads are identical RL loads with 6-pulse controlled rectifiers.

Transformers are used to represent Line impedance and has a winding ratio of 1:1. The transformers are connected in star configuration to avoid blocking the 3rd order harmonics.

The amount of harmonics injected into the network can be controlled by the firing angle of each rectifier. As a result, the harmonics injected by the loads are changed by changing the firing angle of the rectifiers. This gives control over the harmonic emission in the network.

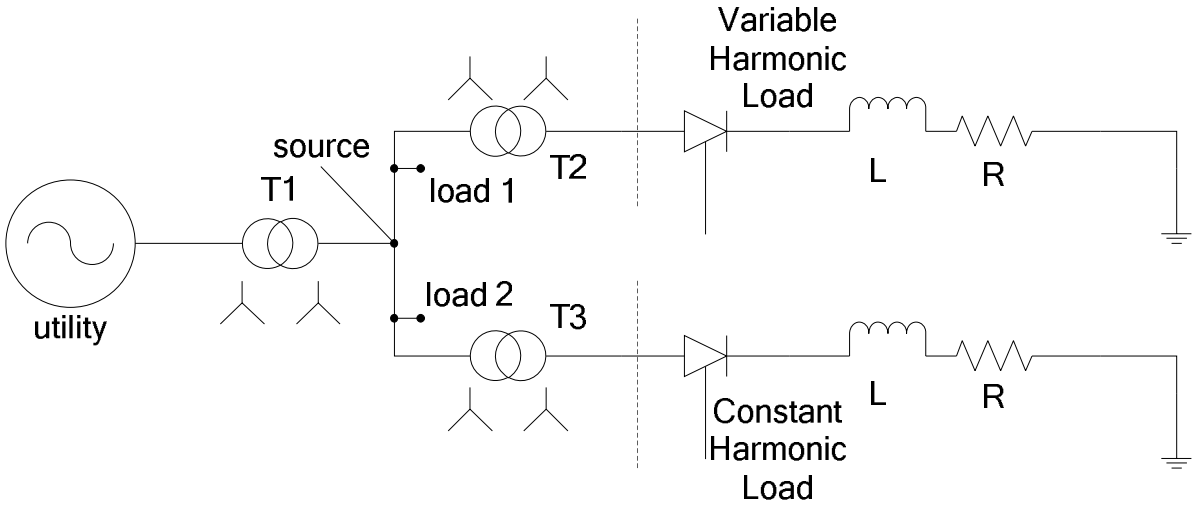

Figure 3.8. Controlled network for the evaluation of the Harmonic Vector Method.

To obtain different operating conditions, the loading and firing angle of load 2 is kept fixed (Constant Harmonic Load) whilst the firing angle of load 1 (Variable Harmonic Load) is adjusted from minimum to maximum value possible for a 6-pulse rectifier. The variable load is operated at nine different conditions for every condition the constant load is operated at. The constant load was operated at two different conditions. Therefore 18 different operating conditions were obtained by changing the firing angles of the rectifiers.

To evaluate the practical capabilities of the Harmonic Vector method, the harmonic emissions due to load 1 are evaluated, using both the Harmonic Vector and the JHAP method. The results will be compared and analysed in chapter 5.

3.4.1 Measurement setup

Voltage and current waveforms at each of the three measuring points (source, load 1, load 2) are digitized by instruments with an accuracy of 0.1% up to the 30th harmonic. Voltage and current waveforms are measured with the same power quality instruments that were used for the practical experiment.

After changing the firing angle of load 1, the system is left to reach steady-state conditions before another set of measurements are taken. This reduces the risk of

measuring transient currents that can cause erroneous results. Due to the voltage and current levels (400 V and 5 A) the instruments' internal transducers are used. Therefore improving the accuracy of the measurements, as these transducers have a larger bandwidth than transducers manufactured for the fundamental frequency.

The use of GPSs for synchronisation are not necessary because of the short distances between the instruments. Therefore to obtain synchronization between the instruments a 15 V DC signal is used to trigger the instruments. The signal is common to all the instruments and is controlled with a hand held switch.

3.4.2 Reference Impedance

Utilizing the Harmonic Vector method to assess the harmonic emission due to load 1 requires the reference impedance of the supply network as seen from Transformer 2 (equation (2.47)). Because the emission due to load 1 is under investigation the supply network is taken as the network from Transformer 2 upstream. Therefore the supply network as seen from Transformer 2 consists of load 2 and the Source.

Steady-state calculations are used to calculate the reference impedance of the supply network [**26**]. The following steps are followed:

1. The steady state voltages and currents waveforms are measured at Transformer 2 without load 1 connected (pre-disturbance).
2. Load 1 is then connected and the firing angle of load 1 is changed to the desired operating condition.
3. The steady-state voltages and currents waveforms are then measured (post-disturbance).
4. MathCAD^{TM} is used to calculate the CFFT of the pre- and post-disturbance waveforms.
5. $\boldsymbol{V}_h$ and $\boldsymbol{E}_{h0}$ are calculated and compared.
6. If $\boldsymbol{V}_h > \boldsymbol{E}_{h0}$ (a condition for the Harmonic Vector method) then the following equation is used to calculate the harmonic reference impedance.

$$Z_h = \frac{V_{h\_pre} - V_{h\_post}}{I_{h\_pre} - I_{h\_post}} \tag{3.1}$$

Where V_{h_pre} and I_{h_pre} are the harmonic voltages and currents before load 1 is connected and V_{h_post} and I_{h_post} the harmonic voltages and currents measured after load 1 is connected.

These steps are carried out on each phase and for each operating condition of load 2.

Step 6 is the condition that must be true, according to the harmonic vector method, before load 1 is considered as a source of harmonic distortion. If the condition in step 6 is not true, the harmonic impedance for that specific operating condition is taken as zero thus from equation (2.47), the harmonic emission due to load 1 is also zero.

3.4.3 Processing the data

The measurements taken at each location are saved as Microsoft Excel files and processed with a MathCAD™ program using equation (2.47) and (2.43). Microsoft Excel is then used to plot the results.

3.5 MathCAD™ program

To calculate the results for each measurement a MathCAD™ program is written that can process all the measured data. This program saves a lot of time and avoids tedious calculations by importing all the measurements and calculating all the results within a minute.

The MathCAD™ program is divided into six sections:

1. Declare
2. Import Data
3. Calculate CFFT
4. Calculate Results
5. Validate Results
6. Save Results

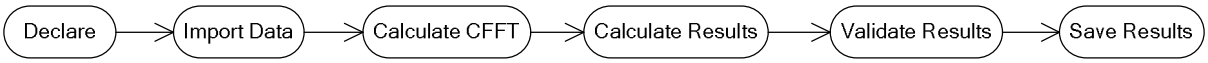

Figure 3.9.Simplified UML of MathCAD sections.

3.5.1 Declaration section

The location of an instrument determines the folder's, where the data files are saved, name and the time of the measurement are used as the name of the file e.g. if measurements are taken at the point of common coupling (PCC) at 13:50:03. The location of the Excel file will be saved in a folder named "PCC" and the name of the file will be "135003".

In the Declare section of the program the following variables must be declared:

1. Location: This is the name of the file where the data is saved. If three instruments were used, three locations must be declared.
2. Date: This is the name of the folder that contains the location folder of each instrument. The date the measurements were taken is normally used for this.
3. Start Time: This is the time of the first measurements taken.
4. End Time: This is the time of the last measurements taken.
5. Time Interval: This is the time period between each measurement and must be given in seconds.

All but the "Time Interval" data are given as string values.

This information is then used by the "import Data" section to import all the Excel files from a location into an array.

3.5.2 Import measured data

This section imports all the data from a location into a single array. To do this a function is written that receives parameters and returns an array.

After all the variables are declared the amount of files from each location are calculated using the start time, end time and the time interval (files). Variables (Data Arrays) are then declared one for each measurement location. Each variable then calls a function named "Batch_File" and sends the "Location", "Date", number of files,

"Start Time" and the "Time Interval" as parameters. The function then returns an array containing all the measurements of that location.

3.5.2.1 Batch_File function

The Batch_File function is loop function that loops trough the amount of data files saved for each measurement location. During each loop the function performs the following operations (Appendix B):

- Increment the for-loop condition counter. This counter counts from 0 to the amount of excel files, minus one. The reason for this, is because MathCAD™ starts counting from zero and not one.
- Convert the "Start Time" from a string value to an integer value so that it can be manipulated, mathematically.
- Calculate the time of the next file to be imported using the counter's value and the "Time Interval" value to manipulate the "Start Time" variable.
- Convert the new time into a string value. This is done in order for the time to be used as a file name.
- Create the address of the file to be imported. This is done by using the "Location", "Date", new time string and the file extension (.xls) of the file.
- Read the Excel file into an array entry. The entry of the array will contain a matrix the size of the imported excel file.

When the condition counter is greater than the amount of files that needs to be imported the function returns the array with N entries. Where N is the number of Excel files imported. Therefore by using this function an array, containing all the measured data, can be generated for each location. A simplified UML diagram of this section is available in Appendix B.

3.5.3 Calculate the Complex Fast Fourier Transform (CFFT)

To analyse the harmonics present in a waveform it must first be decomposed into individual harmonic components. This section of the program uses the waveforms data from each location and decomposes them into the harmonic components under investigation using the Complex Fast Fourier Transform. As with the data importing

section this section also uses a loop function (Calc_Harm) where within all the calculations are done.

Variables that must be declared for this function are:

- Dbegin: This is the number of the data entry, in the excel file, that represents the beginning of a waveform.
- Periods: This is the number of waveforms that must fit into the window used for the CFFT. The window size was chosen as 10 periods (5Hz) to increase accuracy of harmonic calculations.
- Sample: This is the amount of data points that represents one period of a waveform e.g. one period of a 50 Hz waveform sampled at 6400 Hz will be represented by 128 data points.
- Harm: This is an array with the harmonic orders that must be calculated as entries.

Using a 5 Hz (200 ms) window for the CFFT means that the fundamental frequency will be at the 10^{th} harmonic order and not at the 1^{st} as when using a 50 Hz (20 ms) window. This allows for the harmonic to be grouped in subgroups when calculating them (figure 3.10).

3.5.3.1 Calc_Harm function

The Calc_Harm function is a loop function that receives the waveforms data (Data Array), “Dbegin”, “Periods”, “Sample” and “Harm” as parameters and returns a matrix. The matrix returned by the function contains the complex harmonic information of each harmonic declared in “Harm”, for each measurement taken at a specific location. Therefore all the Excel files of a location will be grouped in a single matrix containing the harmonic information of that location. An example of a matrix returned by this function, if measurements are taken at 12:40 and 12:50 and the harmonic frequencies under investigation are the 3^{rd} and 5^{th} order harmonics, is shown in table 3.1.

Table 3.1. Results returned by Calc_Harm

Time	Va		Vb		Vc		Ia		Ib		Ic	
	3	5	3	5	3	5	3	5	3	5	3	5
12:40	-9.4+2.8i	-3.7+1.3i	…	…	…	…	…	…	…	…	…	…
12:50	-9.5+2.9i	-3.9+1.6i	…	…	…	…	…	…	…	…	…	…

The loop function loops trough all the entries in the data array it receives. The following operations are performed during each loop.

- Increment the for-loop condition counter. This counter counts from 0 to the amount of entries in the data array that the function receives.
- Create a sub matrix: The sub matrix is the window that will be used for the CFFT calculations. A sub matrix is created for each unit of each phase.
- Calculate the CFFT: The Complex Fast Fourier Transform is calculated for each sub matrix using a MathCAD^{TM} function. The results from this CFFT is similar to figure 3.10.
- Collect harmonic information: After the CFFT of a waveform is taken the data are collected and stored in an array. An array is created for each unit of each phase.
- Create matrix: The arrays of each unit are grouped together to form a matrix containing the complex harmonic information of each unit and phase (table 3.1).

When the condition counter is greater than the amount of entries in the Data Array the function returns the matrix. After this section is completed all the harmonic information needed to calculate the JHAP and the Harmonic Vector are stored in matrices representing the measurement locations. A simplified UML diagram of this section is available in Appendix B.

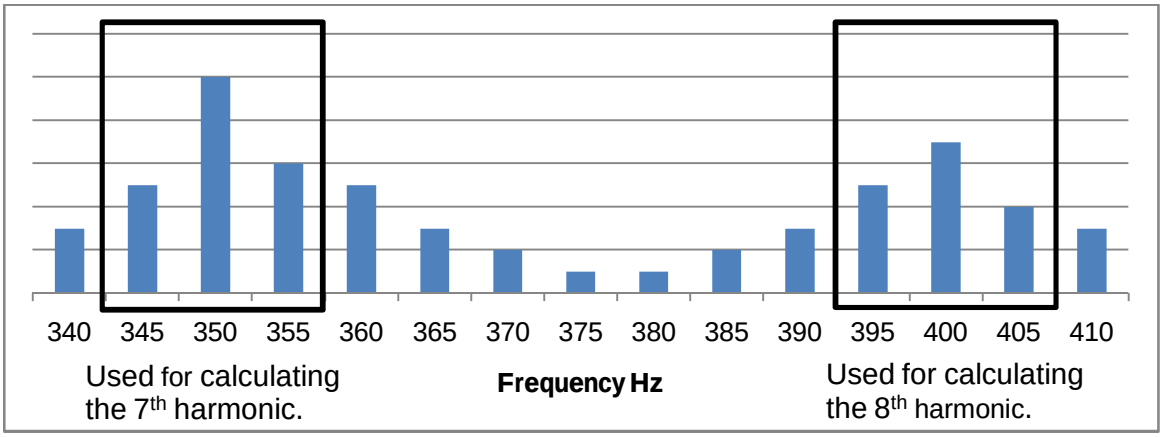

Figure 3.10. Harmonic spectrum with time window of 200 ms.

3.5.4 Calculate results

After all the harmonic frequency information is stored in matrices (one for each location) this section of the program calculates the HAP and the harmonic vector magnitudes for each measurement taken.

For both the JHAP and the Harmonic Vector method loop functions are used to gather the harmonic information stored in matrices and calculate the results.

3.5.4.1 Calculating the JHAP

This section of the program is used by both the practical and lab experiment.

To calculate the JHAP, of the harmonics under investigation, the matrix containing all the harmonic information is send to a function (Calc_hactpwr) as a parameter. The function then uses the harmonic information stored in the matrix in conjunction with equation (2.42) to calculate the JHAP at a certain point in a network. The function calculates the JHAP for each phase and the total JHAP. The results are stored in a matrix. After the JAHP is calculated for every measurement taken at a location, the matrix is return and assigned to a variable. A simplified UML diagram of this function is available in Appendix B.

3.5.4.2 Calculating harmonic emission utilizing the harmonic vector method

Since the practical experiment just focuses on the exchange of HAP between loads, this section is only utilized by the laboratory experiment. The operating conditions

used in this section are the different operating conditions achieved from changing the firing angels of the thyristor rectifiers.

This section of the program is divided into two parts. The first part calculates the harmonic impedances of the network and the second part calculates the harmonic vector magnitudes. In both parts the condition for this method is checked ($\boldsymbol{V}_h > \boldsymbol{E}_{h0}$) and if not met the value of the reference impedance as well as the value of the harmonic voltage vector are taken as zero.

The harmonic impedance of the network is calculated with equation (3.1) and the pre- and post distortion conditions are selected from a list of operating conditions. To calculate the network's harmonic impedance for every harmonic frequency under investigation a for loop is used. The loop function uses the pre- and post conditions selected in conjunction with a harmonic order, defined earlier in the program, to form an index. This information is then used to collect the harmonic's information from the harmonic matrix created in the program. The processes during each loop are as follows:

- Calculate pre- and pos tdistortion voltages, $\boldsymbol{V}_h$ and $\boldsymbol{E}_{h0}$ of each phase.
- Check condition $\boldsymbol{V}_h > \boldsymbol{E}_{h0}$.
- If the condition is true then the network harmonic impedance is calculated otherwise it is taken as zero.
- The results are stored in a matrix.

The selection of the operating conditions determines the network's harmonic impedance. Therefore different pre and post conditions must be selected for each firing angle setting which the rectifier at load 2 was set at.

The second part of this section then uses the matrix created by the first part to calculate the harmonic emission. A loop function is used to loop through all the different operating conditions of load 1. The harmonic emission in each phase due to load 1 is then calculated for every operating condition provided that $\boldsymbol{V}_h > \boldsymbol{E}_{h0}$, otherwise the emission is taken as zero. The results are then stored in a matrix. Simplified UML diagrams of this section is available in Appendix B.

3.5.5 Validate and save results

Before the results are saved the data imported and the results are checked to make sure that they are accurate. To do this a program is written in MathCAD™ where basic information are calculated and compared with results obtained with the power quality recorders.

It's been mentioned that the results calculated by the different sections of the program are stored in matrices. To validate the results obtained with the MathCAD™ program the HAP, waveforms and the magnitudes of the frequencies under investigation are plotted and compared with the results given by a power quality recorder. If the results obtained by the program for single harmonic components concur with the results given by the recorder it can be assumed that the results calculated by the program is also accurate.

To evaluate the measurements imported by the program, this section of the program calculates some basic and fundamental information of a single imported file. After selecting an arbitrary imported file the following data are calculated:

- Waveforms. The waveforms of each phase are plotted.
- CFFT. The Complex Fast Fourier Transforms of each phase is calculated and plotted.
- Unit magnitudes: The voltages, currents and powers of the fundamental and harmonic frequencies are calculated.
- Phasor diagrams. The phasor diagrams are plotted.

All these results are evaluated and compared to the results measured by an ImpedoGraph. After the results are validated and is agreed that they are accurate the results are saved as Microsoft excel files.

This MathCAD™ program makes it possible to calculate all the necessary results in a very short period of time and avoids error prone, time consuming calculations.

figure 3.11 shows the different stages of the data throughout the MathCAD™ program.

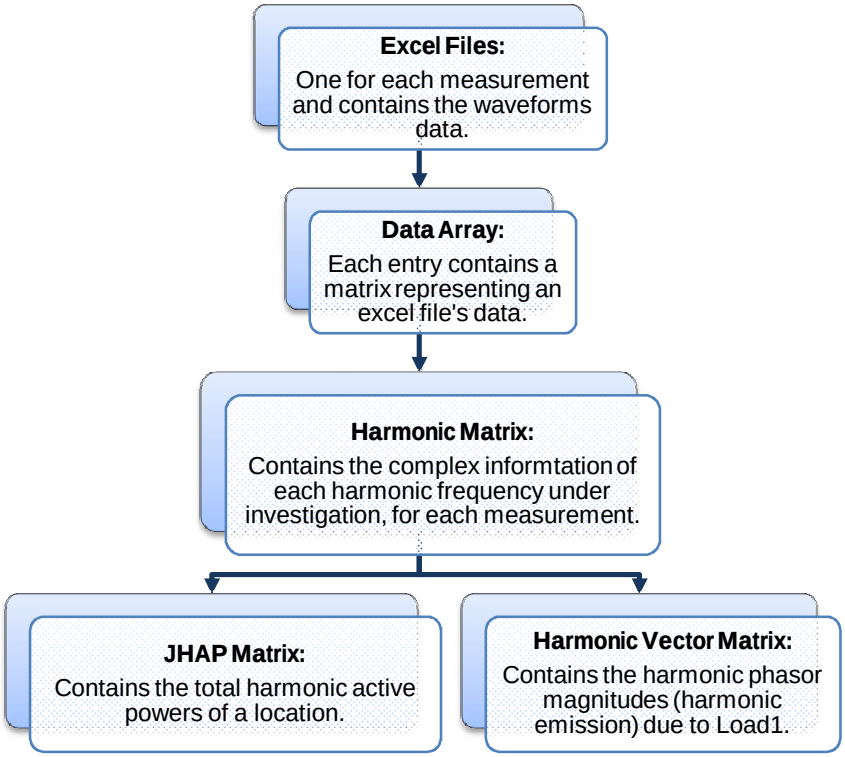

Figure 3.11. Different stages of the data in the MathCAD™ program.

Chapter 4
Investigating the exchange of harmonic active power

Previous chapters discussed the setup of the practical experiment and how the measurements are converted to results. This chapter will look at the results obtained during this experiment and analyse it. Typical results discussed in this chapter are the fundamental active powers, harmonic active powers and phasor diagrams at each point of evaluation.

To ensure accurate and reliable measurements that will be able to represent the network's power quality status, measurements were taken at five different locations in the network. Measurements were taken at the PCC and in each line that supplies a load. The five locations are divided into three groups as discussed in section 3.2 (figure 3.1):

1. PCC: Measurements taken at Incomer 1 and Incomer 2.
2. Load 1: Measurements taken at Feeder 1 and Feeder 2.
3. Load2: Measurements taken at Feeder 3.

All the measurements were synchronized, with the aid of GPSs, which enabled the investigation of the exchange of harmonic active powers between loads in a practical environment.

4.1 Fundamental frequency results

Since the VTs and CTs used for this experiment were specifically manufactured for the fundamental frequency, it can be assumed that the results calculated for this frequency are accurate. Therefore by analysing the fundamental frequency (undistorted 50Hz frequency) one can determine the load profile of the network during the investigation. Also from these results it is possible to see if the instruments were setup correctly and what the accuracy of the measurements was.

The direction of fundamental active power was taken as positive when delivered from the utility to the PCC, (through each incomer) and positive if delivered from the PCC to each load (through the feeders). Figure 4.1 supports this as the inflow of power at the PCC is positive as is the power measured at the loads. By using equation (4.1), Kirchhoff's[4] law is used to calculate the error made in the measurements.

$$Error = \frac{P_{PCC\_in} - P_{PCC\_out}}{P_{PCC\_in}} \times 100 \tag{4.1}$$

Where P_{PCC_in} is the total power delivered to the PCC and P_{PCC_out} is the power flowing out of the PCC. From equation (4.1) it can be illustrated that the average error made with the fundamental frequency is smaller than 0.01%

$$Error = \frac{(P_{PCC} - P_{Load\,1} - P_{Load\,2})}{P_{PCC}} \times 100$$
$$= \frac{(129.67 - 120.51 - 9.17)}{129.67} \times 100$$
$$\approx 0.00\%$$

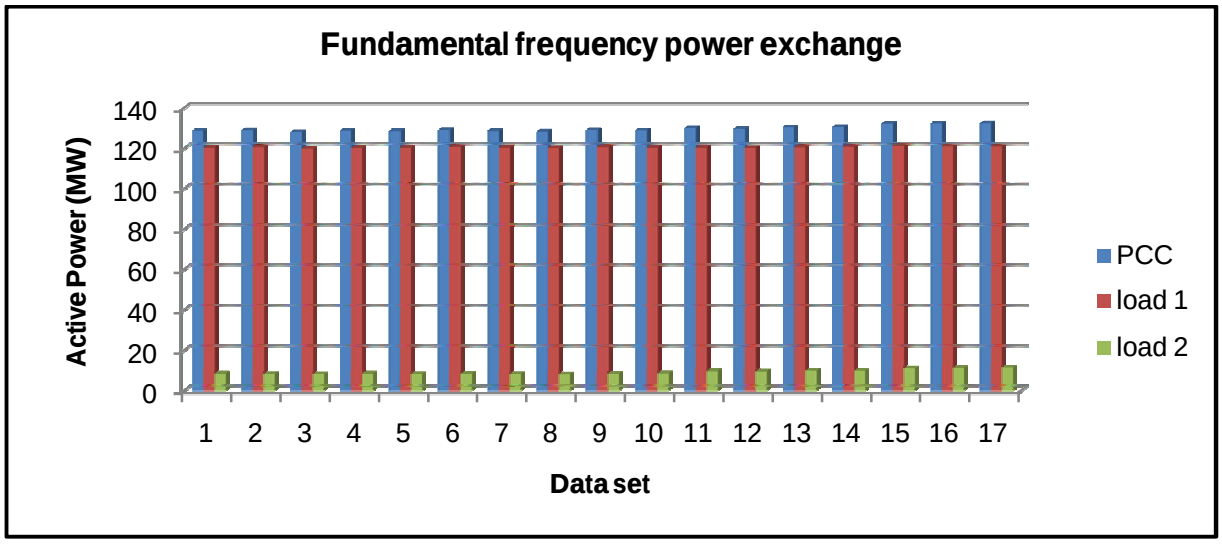

Figure 4.1. Fundamental frequency active power.

[4] Kirchhoff's current and voltage laws state that: The algebraic sum of the currents into a node at any instant is zero and the algebraic sum of the voltages around a loop at any instant is zero. Therefore the total power flowing into the PCC must be equal to the total power flowing out of the PCC.

Note that in figure 4.1 none of the loads are a source of harmonics which in this case in the 50Hz component. This is expected as the only supply of power in this system was the utility and this is indicated by the positive value of the active power. The positive values in the active powers measured at the loads indicate that that loads are currently withdrawing power from the utility.

To validate the setup of the power quality instruments, the fundamental voltages and currents phasor diagrams at each location are plotted (figure 4.1 to 4.4) and analysed.

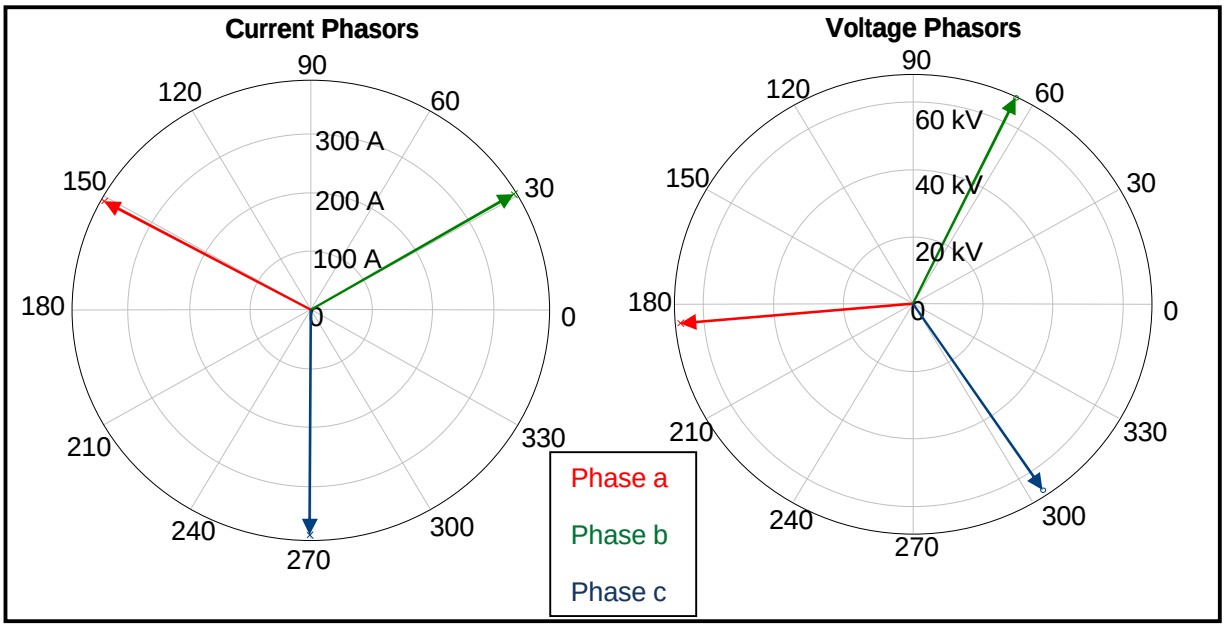

Figure 4.2. Fundamental voltage (right) and current (left) phasor diagrams at Incomer 1.

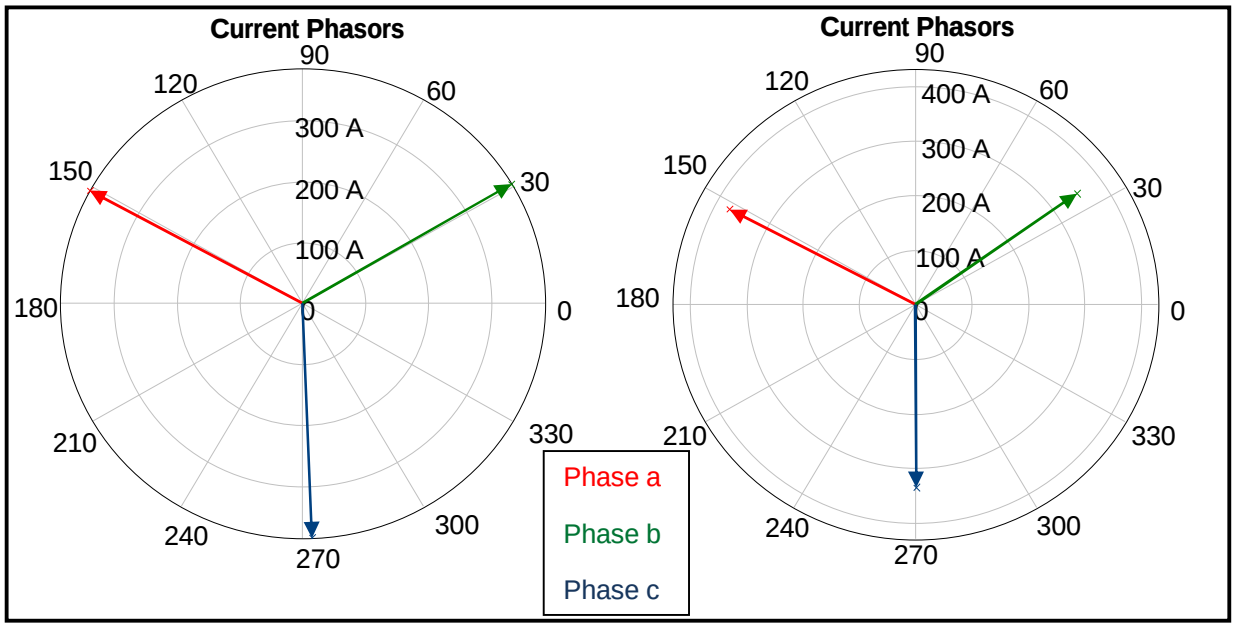

Figure 4.3. Fundamental current phasor diagrams at Incomer 2 (left) and Feeder 1 (right).

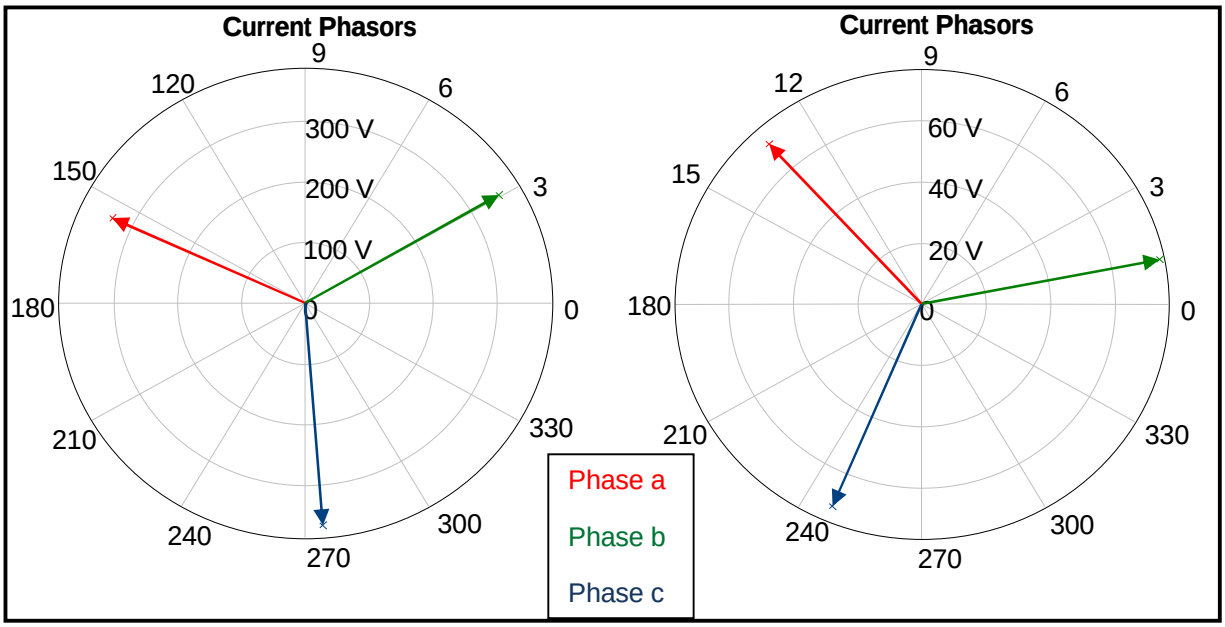

Figure 4.4. Fundamental current phasor diagrams at Feeder 2 (left) and Feeder 3 (right).

The voltage at the PCC (Incomer 1) is common at all the locations, as a result only one voltage phasor diagram is needed (figure 4.2). From the phasor diagrams it can be seen that a positive phase rotation is measured at each location. Furthermore the voltages and currents magnitudes concur with those from the instruments and the given network information.

Therefore from the results obtained for the fundamental frequency it can be said that:

- The instruments are accurately synchronized with an average error of 0.01% in the fundamental frequency power.
- The direction of power flow is taken as positive if it flows from the utility to the PCC and from the PCC to the loads.
- The transducers are correctly connected to the instruments.
- The instruments are correctly setup.
- The measured data are correctly imported into the MathCAD™ program.

4.2 Joint Harmonic Active Power (JHAP)

From the literature study it was found that the direction of the JHAP can be utilized to investigate and locate the source of harmonic distortion. Previous studies proved that loads have the ability to exchange harmonic active powers between each other.

To prove that loads exchange HAP in a practical environment the JHAP results obtained in this experiment are analysed.

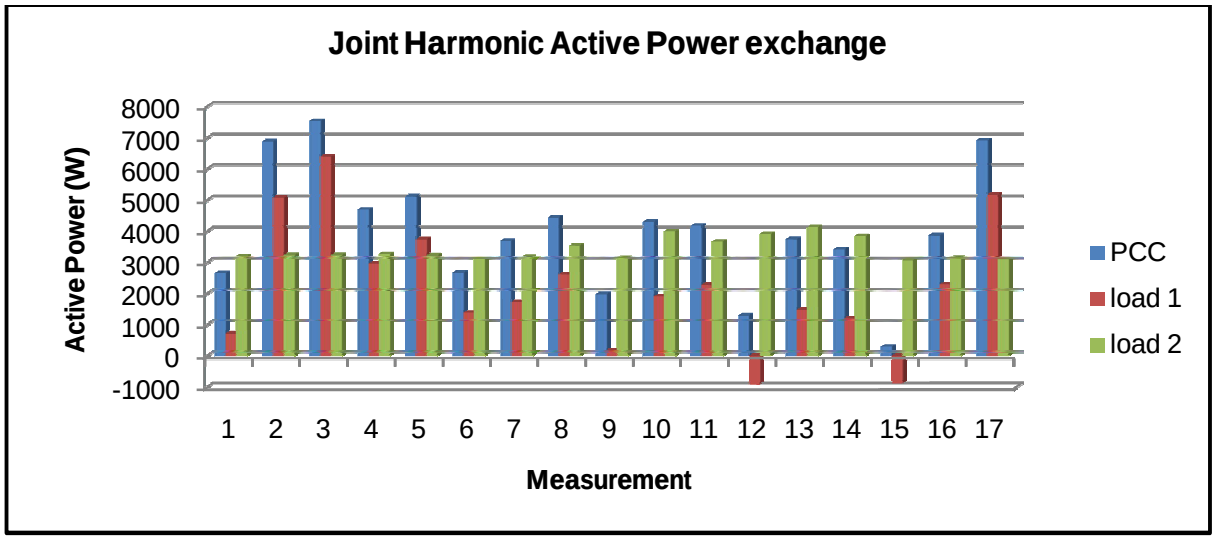

Figure 4.5. Joint Harmonic Active Power with h=3,5,7,...,49.

The JHAP measured at each location is plotted in figure 4.5. The results show that load 1 can be a source of harmonic distortion (data sets 12 and 15) and at a different operating condition absorb harmonic distortion e.g. data set 2. Applying equation (4.1) to the JHAP results reveals that there is an average error of 41% which is far too great for the results to be valid.

$$Error = \frac{(JHAP_{PCC} - JHAP_{Load\,1} - JHAP_{Load\,2})}{JHAP_{PCC}} \times 100$$
$$= \frac{(3987.7 - 2203.4 - 3416.9)}{3987.7} \times 100$$
$$= 41\%$$

The reason for this large error can be a result of the transducers' accuracy at high harmonic frequencies with small magnitudes e.g. the 30th harmonic. Another reason for the error may be to due to instruments that are not synchronised. Since the results from the fundamental frequency showed that the instruments were synchronized the reason for the error are due to the accuracy of the transducers at high frequencies. Therefore low accuracy levels are expected at high frequencies with smaller harmonic magnitudes since the transducers used, are manufactured for the fundamental frequency.

To achieve a better accuracy, the dominant harmonics were analysed which had larger magnitudes that the VTs and CTs could measure. To find these dominant harmonics the frequency spectrums of the voltages and currents at the PCC were analysed.

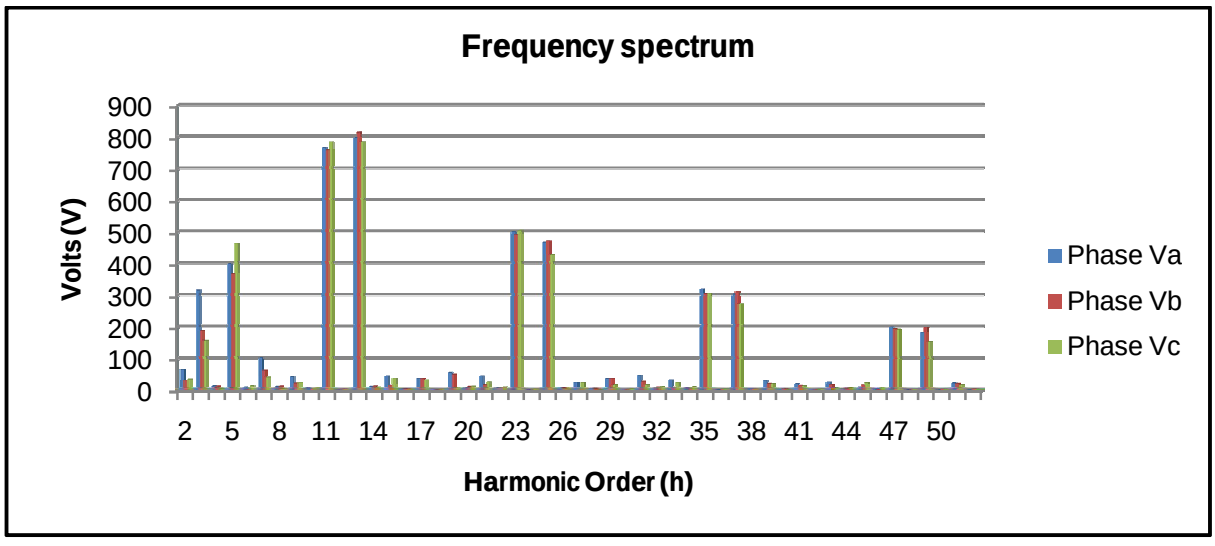

Figure 4.6. The frequency spectrum of the voltages at the PCC (Incomer 1).

Looking at the frequency spectrum of the voltages at the PCC (figure 4.6), it can be seen that the 11th and 13th are the dominant harmonics. This result was excepted as a 12-pulse rectifier produces waveform distortion at harmonic orders equal $h = 12n \pm 1$ where n is an integer. The 3th and 5rd order harmonics are not characteristic of the 12-pulse rectifier and may be due to distortion caused by load 2 or the utility. Similar results are obtained with the frequency spectrum of the currents at the PCC (figure 4.7). The difference in the voltage and current harmonic dominance is due to different harmonic impedances.

Therefore to achieve more accurate results the dominant characteristic harmonics (11th and 13th harmonic) and the dominant non-characteristic harmonic (5th harmonic) are evaluated.

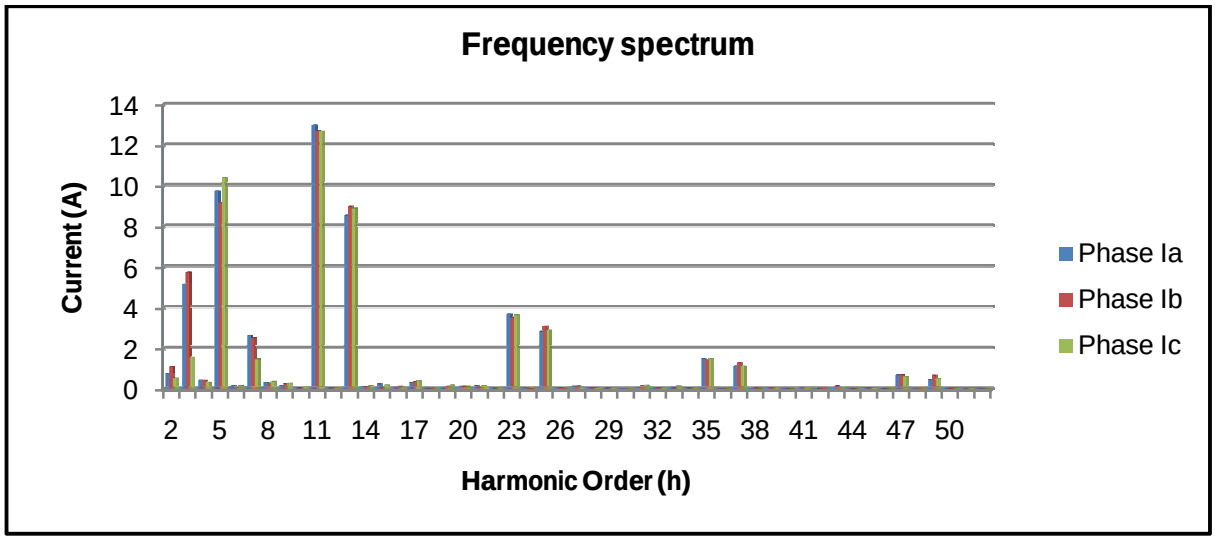

Figure 4.7. The frequency spectrum of the current at the PCC (Incomer 1).

4.3 Evaluating dominant harmonics

To evaluate the exchange of HAP the active power of the dominant harmonics are calculated and plotted.

From figure 4.8, it is clear that the only source of the 5th harmonic distortion is, as expected, the utility (positive HAP). Furthermore the harmonic distortion generated is absorbed by both the loads. Applying equation (4.1) to this results shows that an average error of 3.91% is made with these measurements. Therefore by analysing

the harmonics with greater magnitudes results in a higher accuracy since they are easier to measure.

If the direction of the 11th HAP (figure 4.9) is analysed, it is easy to see that the source of 11th harmonic distortion is load 1 (negative HAP). This distortion is then absorbed by the utility and load 2. As with the measurements of the 5th harmonics order the error made with these measurements are very small and is calculated with equation (4.1) as 1.8%.

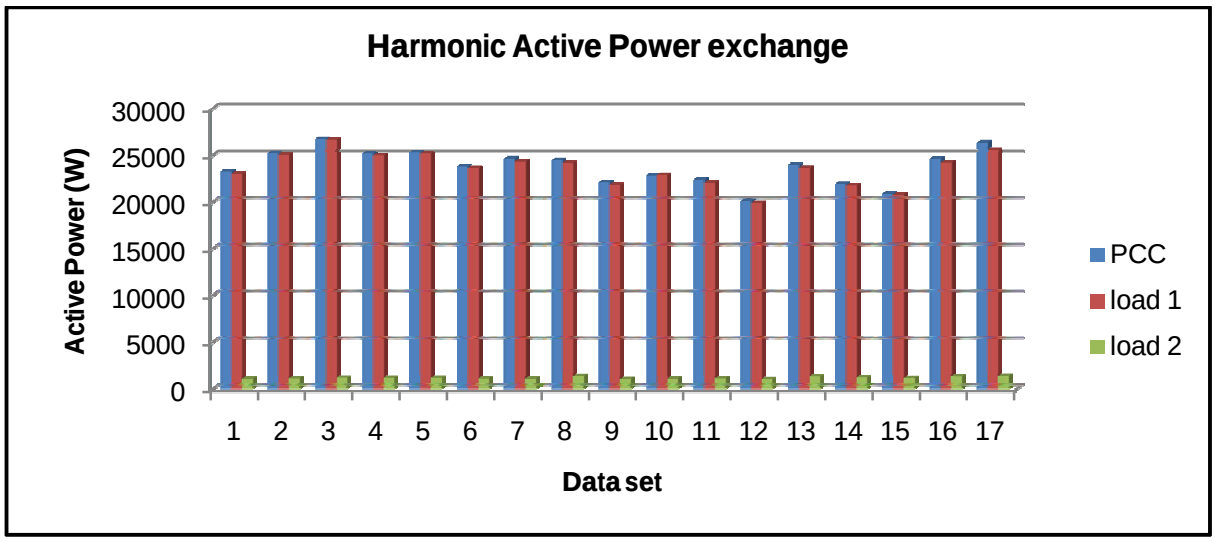

Figure 4.8. 5th harmonic order active power.

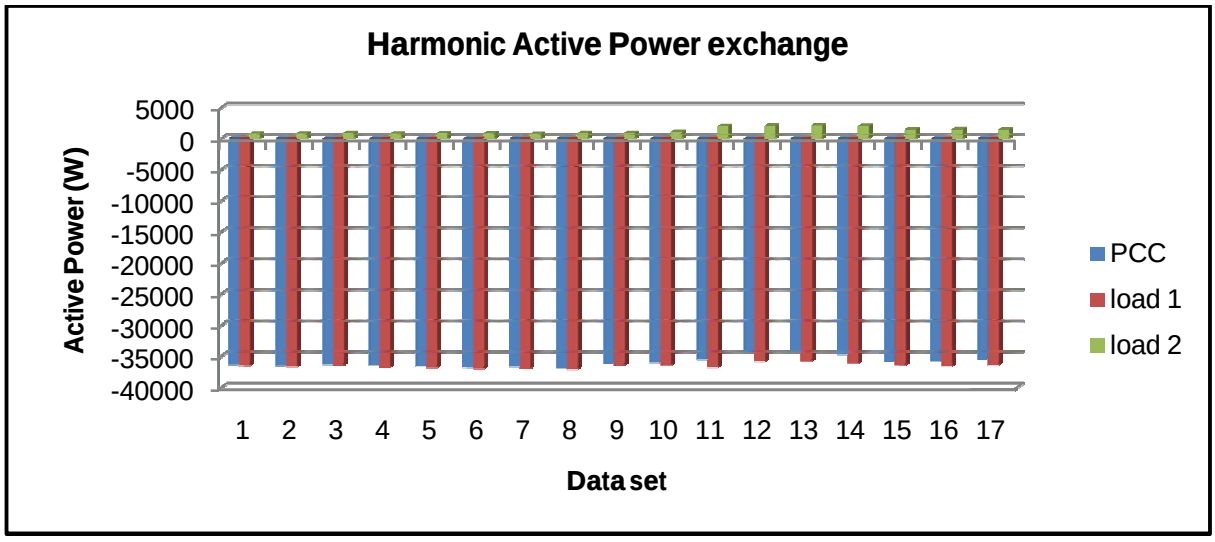

Figure 4.9. 11th harmonic order active power.

Figure 4.10 shows the HAP results for the 13th harmonic order. When applying equation (4.1) to the 13th HAP, the average error is calculated as 0.45%. Analysing the results shows that the main source of the 13th harmonic order distortion is the utility (positive HAP). This is not expected as the 13th harmonic order is a characteristic harmonic produced by the 12-pulse rectifier at load 1. Therefore a reason for this result may be, filter banks (at load 1) absorbing this harmonic distortion.

Load 2 also absorbs the 13th harmonic order distortion (data sets 1 - 8 has a positive HAP value), but at a different operating condition it is a source of the 13th harmonic order distortion (data sets 11 - 17 has a negative JHAP value). To get a better perspective of this results, figure 4.11 and 4.12, are used.

From figure 4.11 it can be seen that load 2 absorbs the harmonic distortion at data sets 1 - 10, but is a source at data sets 11 - 17. A comparison of figure 4.11 and 4.12 shows a relation between the fundamental active power and the 13th HAP. It can be seen that load 2 changed from absorbing to supplying harmonic distortion as its power demand changed. A reason for this can be that a big non-linear load was operated (increase in the fundamental active power) when data sets 11 - 17 were measured.

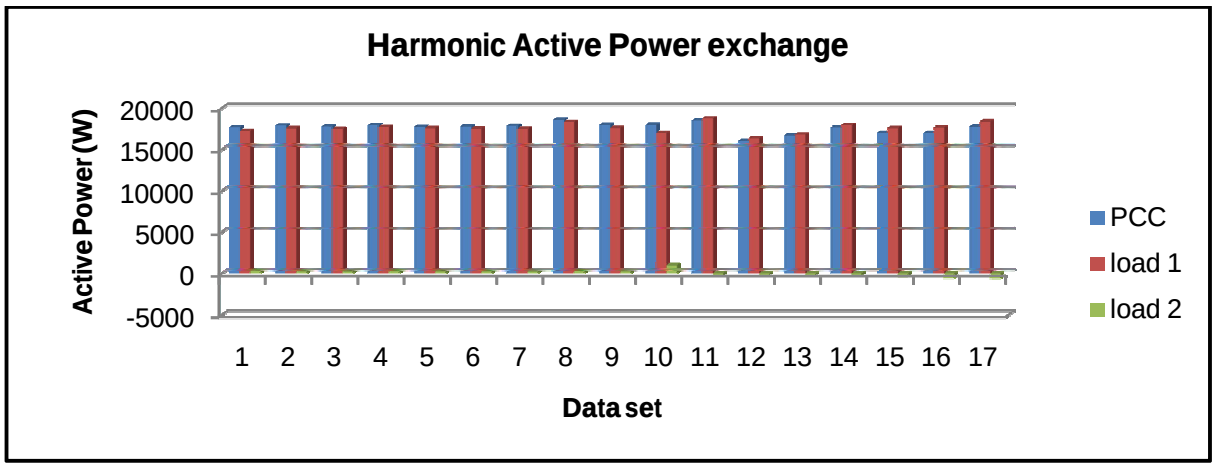

Figure 4.10. 13th harmonic order active power.

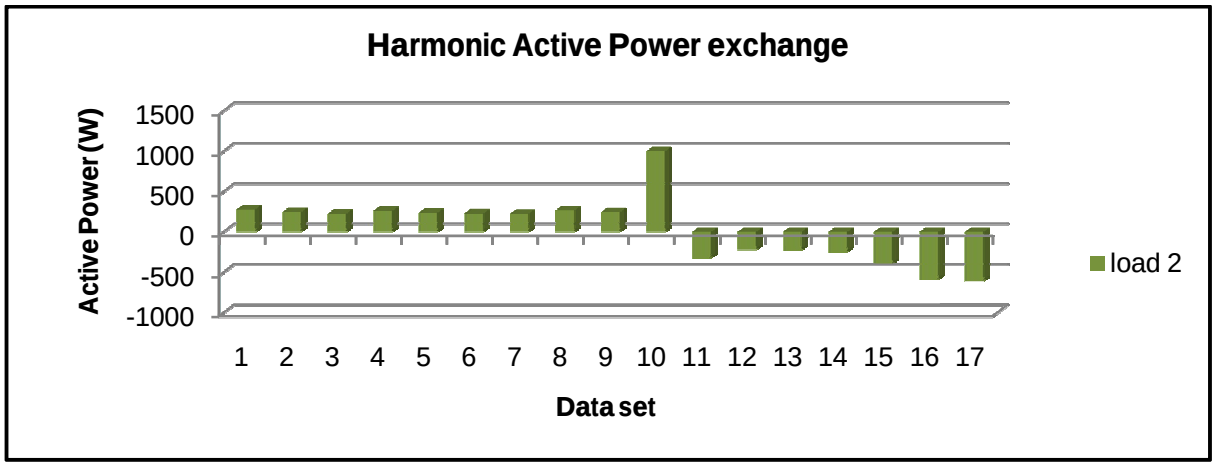

Figure 4.11. 13th harmonic order active power at load 2 with suitable range.

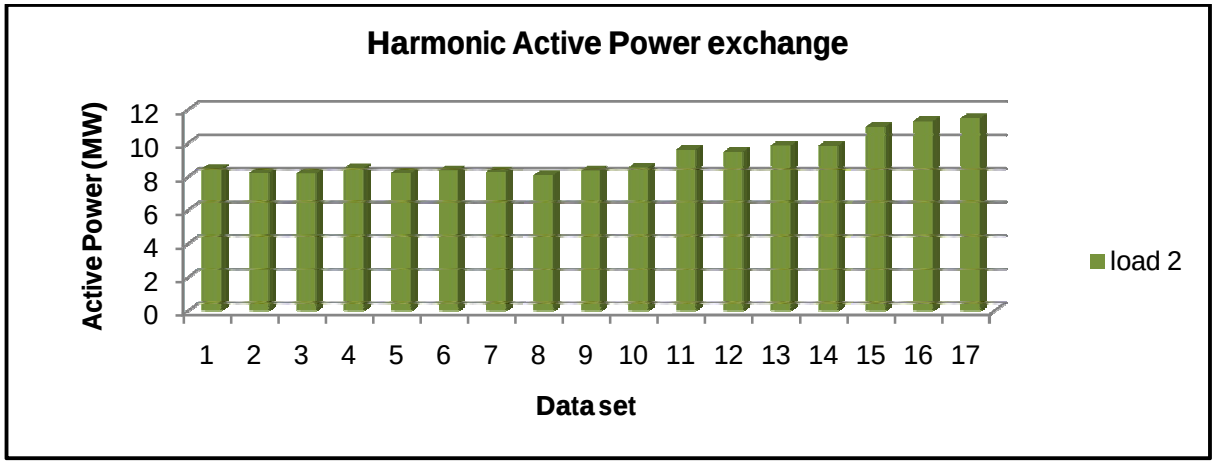

Figure 4.12. The fundamental active power at load 2.

This proves that loads have the ability to exchange harmonic active power and can either be a source of distortion or absorb distortion depending on their operating conditions.

A negative HAP will be measured at a load if the direction of the current is opposite the direction taken as positive. However for load 2 to be a source of distortion not only do the harmonic currents have to flow away from load 2 but they must also flow in the same directions as the currents flowing towards the absorbing entities, which in this case is load 1.

To further the information on the exchange of HAP by load 2, the current phasor diagrams are plotted for the 15th data set. Figure 4.2, 4.3 and 4.4 verified that the currents at Incomer 1 and Incomer 2 are equal in magnitude and phase angle, the same can be said about the currents at Feeder 1 and Feeder 2. Therefore it is only necessary to plot the phasor diagrams of Incomer 1, Feeder 1 and Feeder 3 (figure 4.13 and 4.14).

From the phasor diagrams, it can be seen that the currents at the PCC (Incomer 1) and the currents at load 1 (Feeder 1) are flowing in the same direction, which is towards load 1 as indicated by the positive HAP. Therefore if load 2 is a source of harmonic distortion, the current generated by this load must also flow towards load 1.

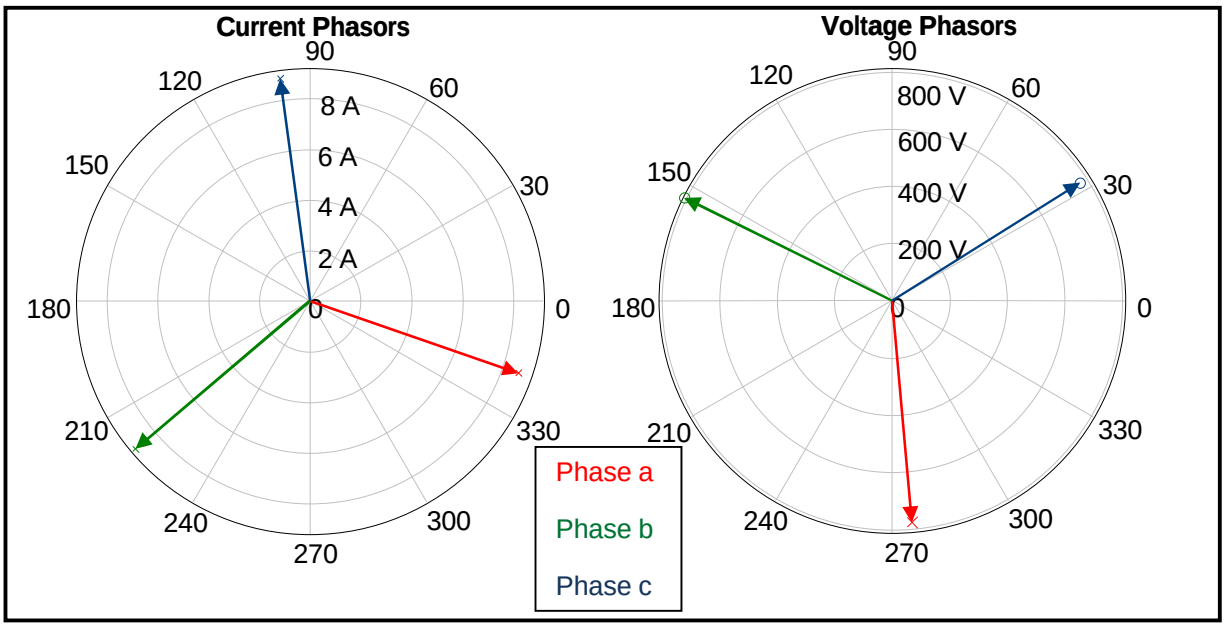

Figure 4.13. 13th harmonic voltages (right) and currents (left) phasor diagrams (Incomer 1)

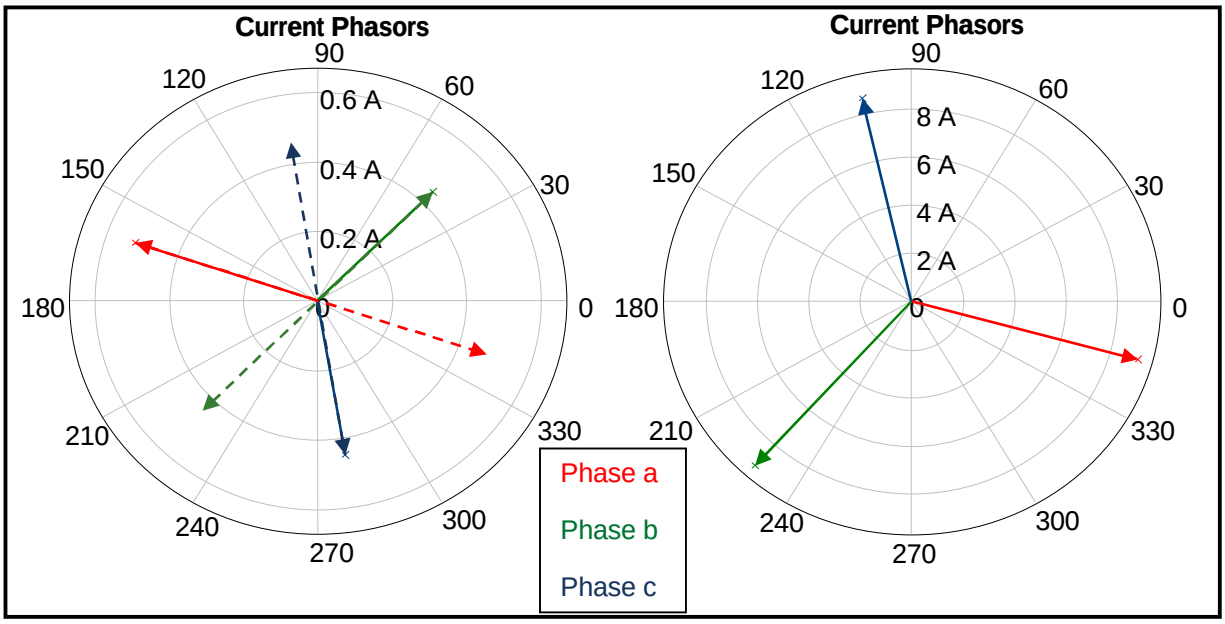

Figure 4.14. 13th harmonic current phasor diagrams of Loads 1 (right) and Load 2 (left).

Taking the direction of power flow as positive, if it is delivered from load 2 to the PCC, hence sifting the currents at load 2 with 180° degrees. From figure 4.14 it can be seen that the currents generated by load 2 flow in the same direction as the currents at load 1. Therefore, it is concluded that the 13th harmonic order distortion generated by load 2 is absorbed by load 1.

Results obtained indicate that loads in a practical network can be a source of harmonic distortion or absorb harmonic distortion depending on their operating conditions. Furthermore it is indicated that loads have the ability to exchange HAP between each other. This concurs with the simulation and laboratory results previously obtained by Rens and *at al* [**6**], [**7**].

Chapter 5
Validating the Harmonic Vector method

To evaluate the Harmonic Vector method, a practical but controlled network was setup for experiments. This allowed control of the harmonic distortion due to a load, which is not feasible in a practical environment. This chapter analyse the results obtained during this experiment in an attempt to get a better understanding of practical restrictions when utilizing the Harmonic Vector method.

To evaluate the Harmonic Vector method the harmonic emissions due to load 1 were investigated with both the Harmonic Vector and the JHAP method and the results were compared.

The no-load supply voltages were not perfectly sinusoidal and the degree of distortion was confirmed as fairly constant over time.

5.1 Fundamental frequency results

Figure 5.1 indicates that a change in firing angle of the rectifier at load 1 controls the magnitude of the active power exchange at the fundamental frequency. Furthermore, the figure indicates that load 2 was kept fixed throughout the two parts of the experiment.

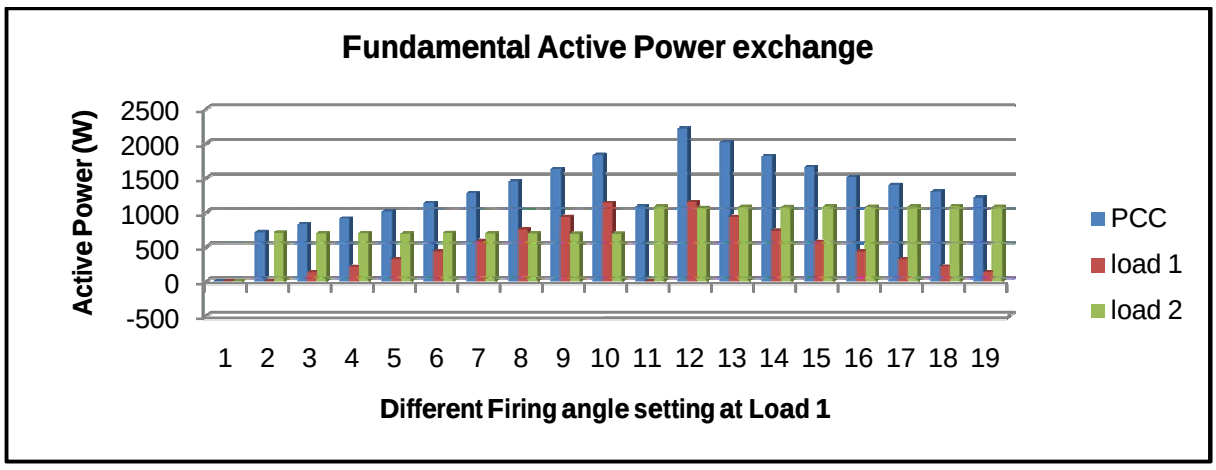

Figure 5.1. Fundamental frequency active power.

To validate the synchronisation of the instruments, the total input of power should match to the total output of power (Kirchhoff's law). Applying equation (4.1) to the fundamental frequency active power, the average error is 0.07%, hence the instruments were accurately synchronized.

The voltages and currents were measured using the instruments' internal transducers which provided high accuracy measurements. The voltages measured at the PCC is common to all the measurement points in the network. From figure 5.2 and 5.3, it can be seen that the supply voltages and the currents measured at each point in the network have a positive phase rotation. Furthermore the voltages and current magnitudes correspond to the network information.

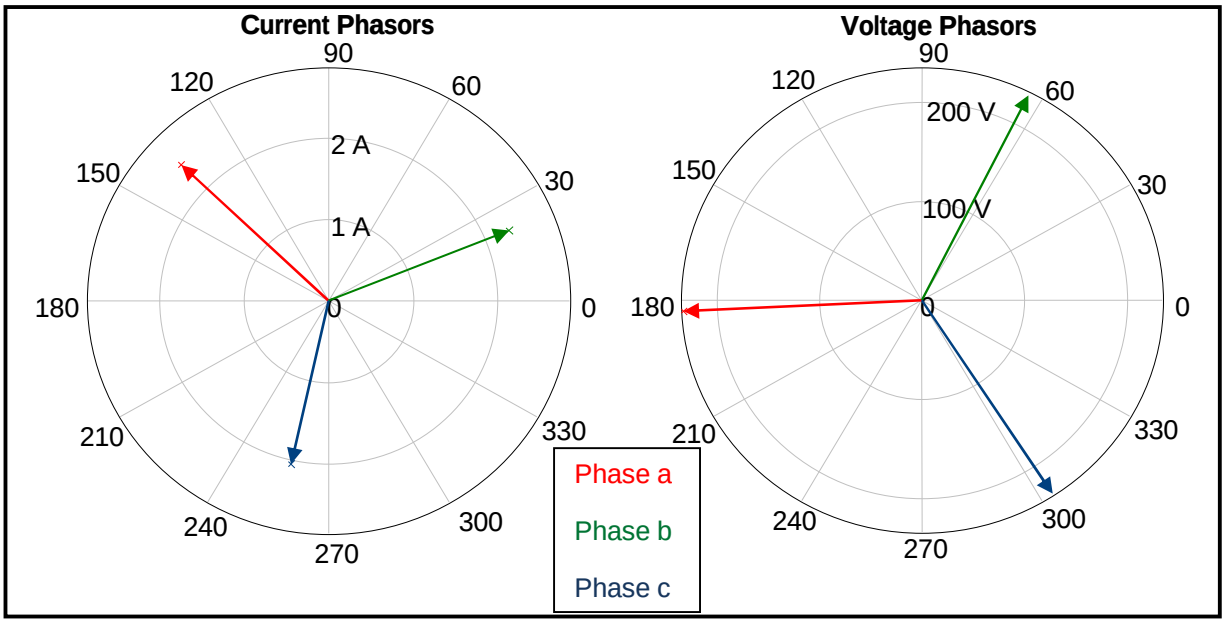

Figure 5.2. Fundamental phasor diagrams of the voltages (right) and currents (left) at the PCC

From the results obtained for the fundamental frequency it can be assumed that:

- The instruments were accurately synchronized.
- The saved data were accurately imported into MathCAD™.
- The instruments were correctly setup and connected to the network.

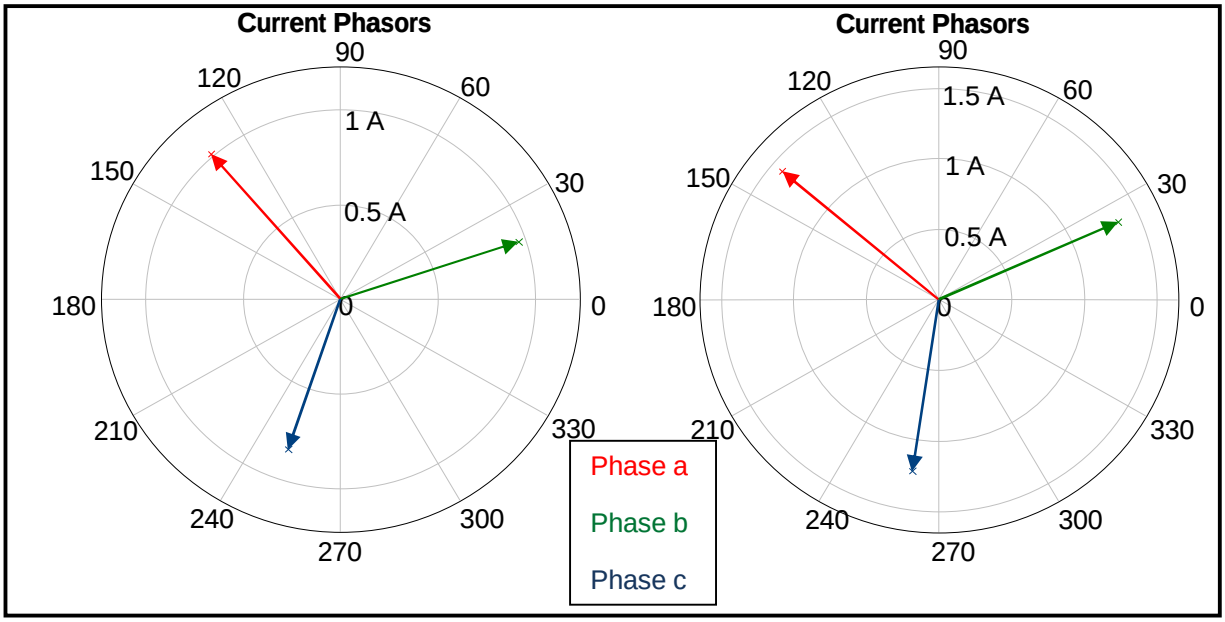

Figure 5.3. Fundamental current phasors of Load 1 (left) and Load 2 (right)

5.2 Joint Harmonic Active Power results.

To utilize the direction of HAP the direction of fundamental power flow is taken as positive when delivered by the supply to the PCC and positive if delivered from the PCC to the loads. Figure 5.4 contains the JHAP for harmonics up to the 49th harmonic order. The figure indicates that the harmonic distortion due to load 1 varies as the firing angle of the rectifier is changed. Furthermore load 1 (which is the load under investigation) is either a source of distortion or it absorbs harmonic distortion depending on the firing angle settings.

To evaluate the harmonic emission due to load 1 using the Harmonic Vector method, it is necessary to obtain the dominant harmonic information. Figure 5.5 and 5.6, indicates that the dominant harmonics measured at load 1 are the 6-pulse rectifier's characteristic harmonics where $h = 6n \pm 1$ (5th and 7th harmonics). The HAP and the Harmonic Vector method are utilized to assess the distortion caused by these dominant harmonic orders. Comparing the results of the two different methods gives an indication of the Harmonic Vector method's practical restrictions.

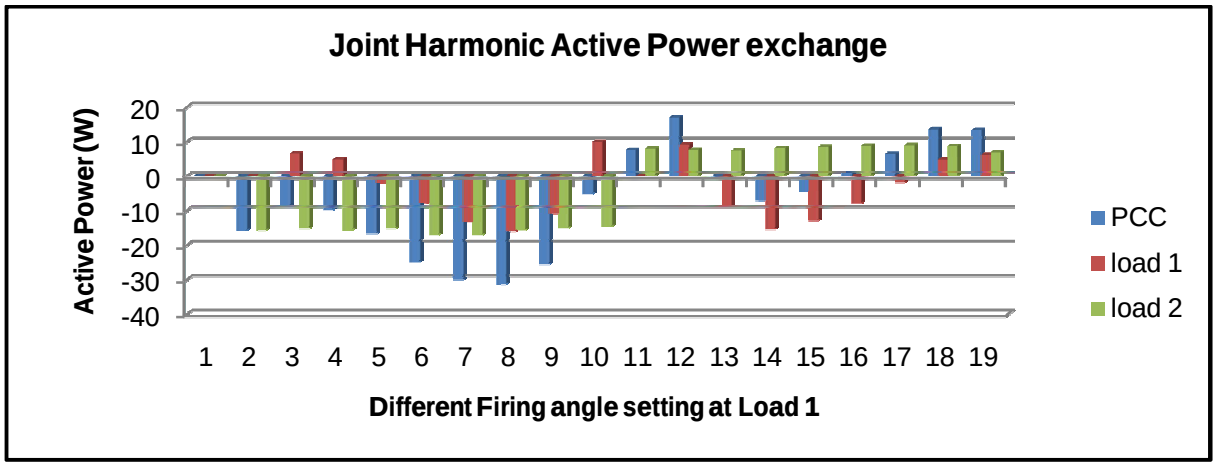

Figure 5.4. Joint Harmonic Active Power with h=3,5,7,...,49.

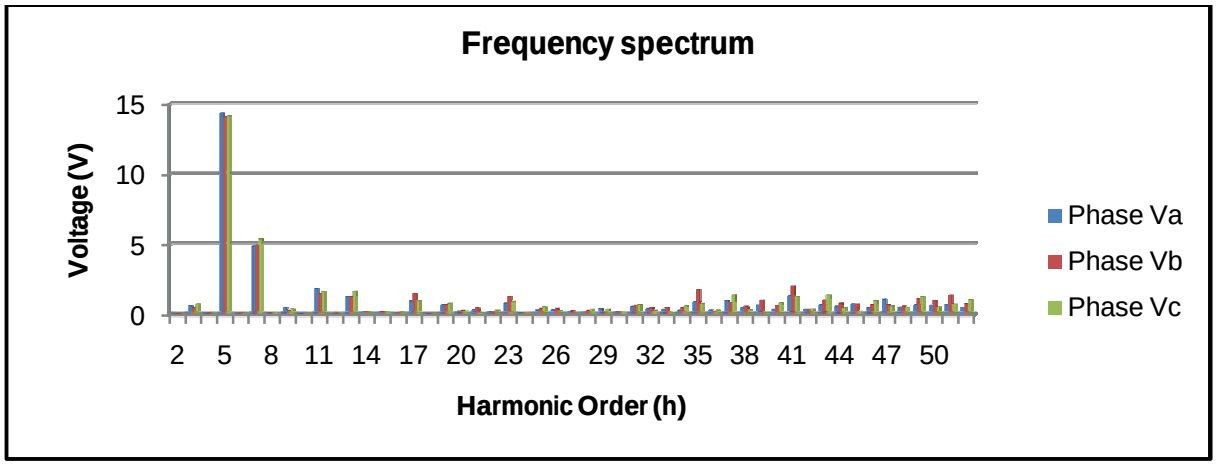

Figure 5.5. Frequency spectrum of the voltages at load 1.

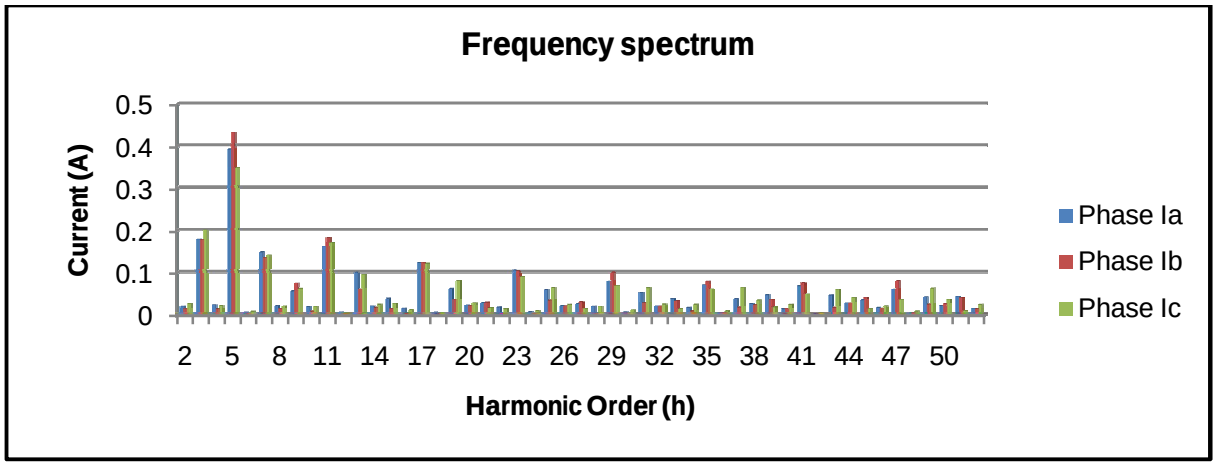

Figure 5.6. Frequency spectrum of the currents at load 1

5.3 Harmonic Vector method results

To utilize the Harmonic Vector method equation (2.47) requires a reference harmonic impedance of the supply network. For the laboratory experiment the harmonic emission due to load 1 was under investigation and load 2 together with the utility formed the supply network as seen from load 1. The firing angle of the rectifier at load 2 was set to one angle while the firing angle of the rectifier at load 1 was varied through settings 3 - 10. To create different supply networks (as seen from Transformer 2) the firing angle of the rectifier at load 2 was changed. Keeping the firing angle of the rectifier at load 2 fixed at the new value, the firing angle of the rectifier at load 1 was changed through settings 12 - 19. The network's impedance for the dominant harmonics are calculated using equation (3.1), the results are given in table 5.1, 5.2 and 5.3.

Table 5.1. Reference harmonic impedance phase a.

Supply Network	5th Harmonic impedance	7th Harmonic Impedance
Friring angle 2-10	$15.15 \angle 131.04°$	$60.483 \angle -20.91°$
Firing angle 11-19	$18.9 \angle -104.44°$	$41.86 \angle -21.56°$

Table 5.2. Reference harmonic impedance phase b

Supply Network	5th Harmonic impedance	7th Harmonic Impedance
Friring angle 2-10	$14.18 \angle 137.24°$	$50.32 \angle -18.94°$
Firing angle 11-19	$16.94 \angle -102.04°$	$39.87 \angle -30.46°$

Table 5.3. Reference harmonic impedance phase c

Supply Network	5th Harmonic impedance	7th Harmonic Impedance
Friring angle 2-10	$19.23 \angle 125.5°$	$45.722 \angle -28°$
Firing angle 11-19	$22.3 \angle -93.99°$	$36.49 \angle -20.39°$

The results for the 5^{th} and 7^{th} dominant harmonics are indicated in figure 5.7 and 5.8 respectively. Figure 5.7 indicates that if the firing angle of the rectifier is set at 5 - 9 or 13 - 16, load 1 is a source of the 5^{th} harmonic distortion (negative HAP). However if the firing angle is set at 3, 4, 10, 11, 18 or 19, load 1 absorbs the 5^{th} harmonic distortions (positive HAP). The reason for this change in distortion due to load 1 is because, changing the firing angle of the rectifier changes the shape and the magnitude of the current drawn by the load. Because of Ohm's law, the change in the

current waveform instigates a change in the voltage waveform. Load 1 was disconnected from the network during settings 1, 2 and 11, hence the zero active power values.

The Harmonic Vector method will indicate if load 1 is a source of distortion, by giving the magnitude of the distortion voltage due to load 1. If load 1 is not a source of distortion, the magnitude of the distortion voltage will be zero. Figure 5.7 indicates that load 1 contributes to the 5th harmonic distortion when the firing angle of the rectifier is set between 5 - 8, or 13 - 19. At the other instances load 1 was not detected as a source of distortion.

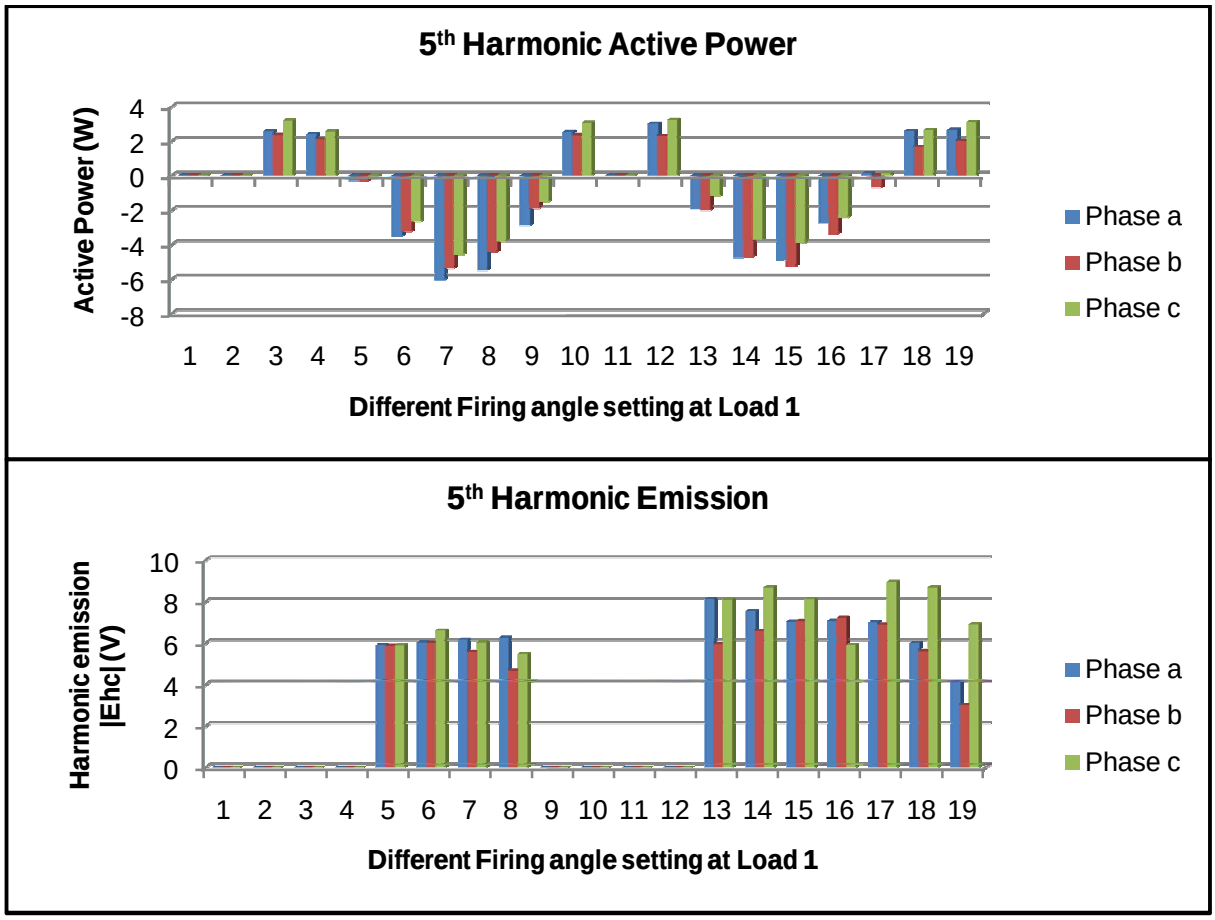

Figure 5.7. Active power exchange in 5th harmonic (top) and emission at 5th harmonic per Harmonic Vector Method (bottom) as calculated for load 1.

The same can be said when analysing the 7th harmonic order. Figure 5.8 indicates that when using the direction of HAP load 1 is a source of distortion at settings 3-5,8,9 and, 17-19 (negative HAP). While according to the Harmonic Vector method load 1 contributes to the distortion at settings 3,7-9,13-15,18 and 19.

If the results for the 5th and 7th harmonic orders, obtained by the two assessment techniques, are compared they respectively agree 84% and 74% of the time. Therefore the results of the HAP and the Harmonic Vector method for both the 5th and 7th harmonic order do not concur with each other. This enforces the findings in [**6**] and [**7**], that single point measurements cannot be used to assess the harmonic distortion due to a single load if such load is connected to a network where there exist multiple sources of distortion.

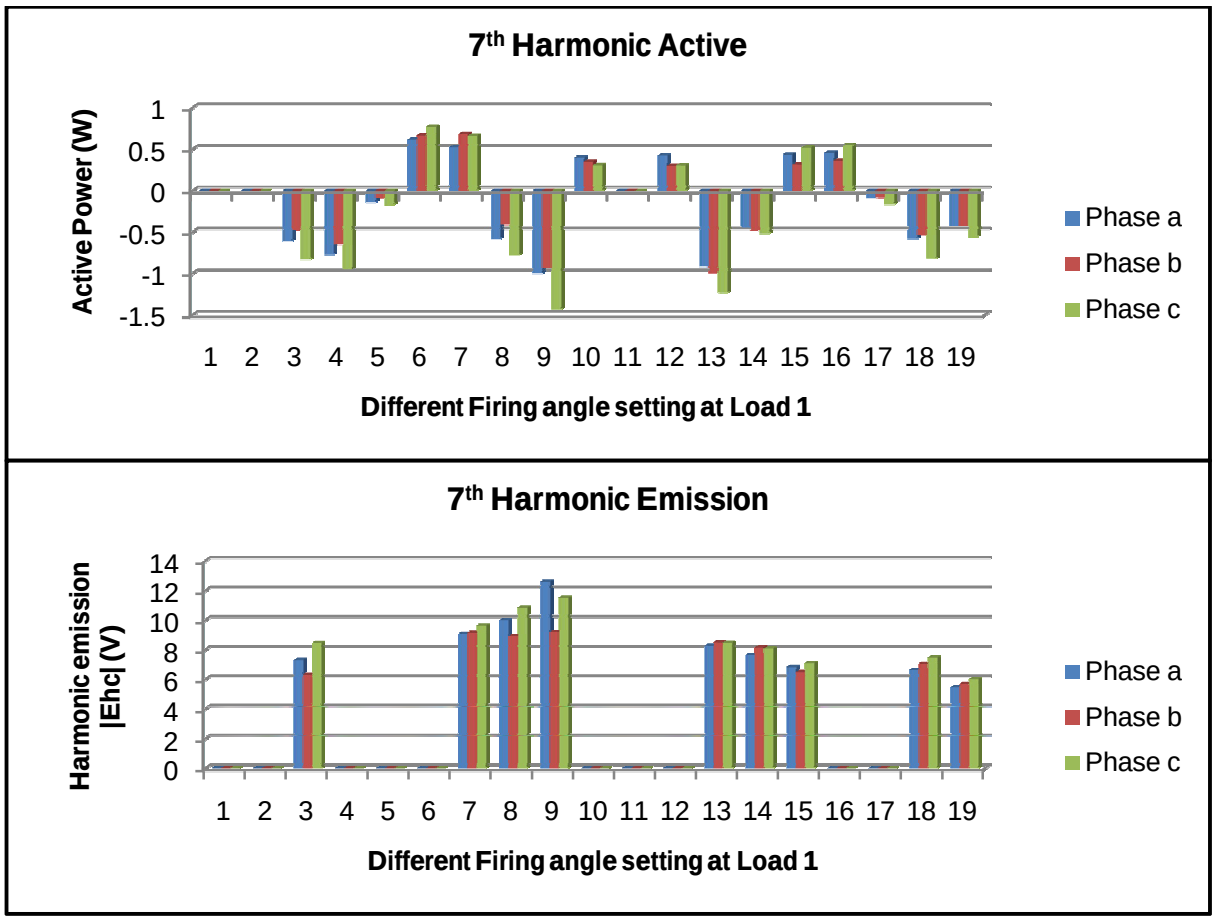

Figure 5.8. Active power exchange in 7th harmonic (top) and emission at 7th harmonic per Harmonic Vector Method (bottom) as calculated for load 1.

Chapter 6

Conclusion and recommendations

Previous chapters discussed the theory, methodology and results of this project. This chapter analyse the results obtained with both experiments and gives a conclusion on the exchange of HAP between loads and the practical limits of the Harmonic Vector method.

For this project, two experiments were conducted. The first experiment were carried out at a substation were two 400/66 kV incomers fed two loads. The goals of this experiment were to prove that loads, in a practical power network, have the ability to exchange HAP between each other. And to also demonstrate that a load can either be a source of distortion or it can absorb harmonic distortion depending on its operating condition.

The second experiment was carried out on a controlled network, where the distortion due to loads could be varied by changing the firing angles of 6-pulse thyristor rectifiers. In this project the harmonic emissions due to a load were investigated with both the Harmonic Vector method (single point measuring method) and by utilizing the direction of JHAP (multi-point measuring method). The results were then compared to analyse the validity of the Harmonic Vector method.

6.1 Exchange of harmonic active power

If the direction of active power in the fundamental frequency component is being taken as positive (a positive value) when delivered to the PCC from the supply network (feeder into PCC) and positive when delivered from the PCC to the loads, then a negative value in JHAP (or in HAP at a harmonic) indicates that such load is generating it, as it is opposite to the direction of the fundamental frequency active power.

6.1.1 Joint Harmonic Active Power (JHAP)

From figure 4.5 it was seen that if JHAP is used for the localisation of a harmonic source, then the utility remain a source of harmonics. The figure also indicated that load 1 and load 2 was mostly absorbing HAP without generating any although knowledge on the type of loads suggested that it should be generating HAP. The error made with the JHAP results could be due to the transducer's low accuracy at high harmonic orders, as the current transducers used for this experiment were designed for the fundamental frequency. Figure 4.6 and 4.7 indicate that the dominant harmonics were the 5^{th}, 11^{th} and the 13^{th} order harmonics. Furthermore with JHAP, the harmonics may cancel out resulting in the wrongfully identification of the source thereof. Therefore it is recommended that individual harmonic active power must be investigated for accurate results.

6.1.1 Harmonic Active Power (HAP)

Investigating the 5^{th}, 11^{th} and the 13^{th} harmonic orders produced results with very little error. Because the dominant harmonics had greater magnitudes the provided transducers could measure them with a higher degree of accuracy which lead to the accurate results.

The HAP at the 5^{th} harmonic was absorbed by both load 1 and load 2 for all of the time with the interpretation that the PCC (utility) has been producing it (figure 4.8). The HAP at the 11^{th} harmonic was delivered by load 1 to load 2 and the utility as they absorbed it all of the time (figure 4.9). This furthers the knowledge that the 11^{th} harmonic is characteristic of the operation of load 1.

The HAP from the 13^{th} harmonic was produced by the utility (PCC) and absorbed by load 1 for all of the time although this harmonic is also a characteristic harmonic of the load 1's operation (figure 4.10). Load 2 absorbed the HAP for measurements 1 to 10 and then started generating HAP for measurements 11 to 17 (figure 4.11). The change from consuming to generating the HAP corresponds to a change in the fundamental active power delivered to load 2 (figure 4.12). Note that the sum of HAP at load 2 and the utility (PCC) is the value consumed by load 1.

A non-linear load can therefore be a source of HAP and then consume HAP at a later stage depending on its operating conditions. HAP can also be exchanged between non-linear loads meaning that a value of HAP at the terminals of a load constitutes the interaction of different non-linear loads; hence the HAP, measured at a single point in a network were multiple sources of distortion exist, cannot be used to quantify the contribution of that load to THD_V.

6.2 Practical validation of the Harmonic Vector method

To utilize the direction of HAP, the direction of active power in the fundamental frequency component was taken as positive (a positive value) when delivered to the PCC from the supply network (feeder into PCC) and positive when delivered from the PCC to the loads. A negative value in JHAP (or in HAP at a harmonic) indicates that such load is the source thereof as it is opposite to the direction of the fundamental frequency active power.

Figure 5.1 indicates that a change in firing angle of the rectifier at load 1 controlled the active power exchange at the fundamental frequency. The inflow of power should match the total outflow over all harmonic components, but as non-linear loads have the ability to exchange energy between harmonic components, some difference in the reconciliation of energy per harmonic component could exist.

Figure 5.4 indicates that the JHAP (indicated by “PCC” values) was not always “flowing” back towards the supply network. Similar behaviour existed in the JHAP at load 1 and 2. It is clear that JHAP was exchanged between the loads and although both generated JHAP, the sum of the powers were not always flowing upstream as indicated by the PCC values. These results were obtained by synchronous measurements in all three lines.

The Harmonic Vector method was to be applied on a per-harmonic basis. It required comparison of the HAP in the 5^{th} and 7^{th} harmonic components as plotted in figure 5.7 and 5.8. When the 5^{th} harmonic (a dominant component) was evaluated and a comparison was made between the results found using the direction of HAP and the Harmonic Vector method it was found that both identified the source, and level of emission in the 5^{th} harmonic, but only for certain operating conditions.

Conditions existed where load 1 was a source of harmonic distortion (5th HAP being negative) but the Harmonic Vector method had a zero value as the condition $|V_h| > |E_{h0}|$ was not met. Also, positive values of 5th HAP existed indicating absorption of that component by load 1 whilst the Harmonic Vector method reported that load 1 contributed to the 5th harmonic component in voltage. Therefore there exists a contradiction in the results obtained with the two different methods.

Similar contradiction in the results were obtained for the 7th harmonic component where the Harmonic Vector method reported that load 1 contributed to this harmonic distortion while the results of the HAP indicated that load 1 absorbed the harmonic distortion (Figure 5.8).

6.3 Conclusion

By successfully synchronizing the instruments and measurements during the practical experiment, the project managed to effectively conduct such an experiment for the first time on such a large scale. The results obtained with practical measurements in a high voltage power system is in agreement with the results obtained in [**6**] and [**7**].

Therefore it is confirmed that in a network, where there exist multiple sources of distortion, loads have the ability to exchange HAP between each other. Furthermore a load can either be a source of distortion or consume harmonic distortion depending on its operating condition. Thus measurements at all nodes of interest in a power system will have to be acquired and synchronously to understand the energy phenomena dictating the voltage waveform distortion.

The results obtained with the laboratory experiment, indicate that the Harmonic Vector method contradicts the behaviour of HAP. If it is agreed that the direction (sign) of HAP can be used to label a load as a source of that HAP or a sink thereof [**8**], it is expected that the evaluation of the emission of that harmonic voltage through application of the Harmonic Vector method will yield similar results, but it did not.

It is thus concluded that the limitation in practical application of the Harmonic Vector method [**1**], [**2**], [**5**], [**4**] as demonstrated by the results, is due to single-point measurements in use to determine the level of emission.

6.4 Recommendations

Due to restricted access to large power substations, measurements were only taken for a day, while the practical experiment was carried out. It is therefore recommended that measurements should be taken for at least a week. This will allow for better load profiles and analysis of a load's different operating conditions and how it manipulates the distortion levels in the network. Furthermore to achieve more accurate results it is recommended that transducers with a large bandwidth should be used as the results indicated that failing to do so would result in erroneous JHAP results. An alternative that will also provide more accurate results will be to utilize the metering CT's, if installed in the substation, as they are more accurate than the CTs used for protection.

A practical solution to an accurate evaluation of the harmonic emission by a single distorting load when these distortion loads are distributed all over, such as in a real-world power system, need research and development. Fundamental network principles dictate the exchange of HAP between non-linear loads and any attempt to accurately quantify and qualify the harmonic emission of a distorting load has to acknowledge these principles. Therefore a single point method will be practically valid if its results comply with those of the JHAP method. Unfortunately current literature are misleading as it still claim that single point measurements can be used to assess the harmonic emission due to a load [**2**].

Bibliography

[1] E. D. Jaeger, "Disturbance emission level assessment techniques (CIGRE-CIRED joint working group C4.109)," pp. 1-2, 2009.

[2] E. D. Jaeger, "Review of Emission Assessment Techniques (CIGRE-CIRED joint working group C4.109)," 2011.

[3] W. Xu and Y. Liu, "A method for determining customer and utility harmonic contributions at the point of common coupling," *Power Delivery, IEEE Transactions on*, vol. 15, pp. 804-811, 2000.

[4] T. Pfajfar, B. Blazic, and I. Papic, "Harmonic Contributions Evaluation With the Harmonic Current Vector Method," *Power Delivery, IEEE Transactions on*, vol. 23, pp. 425-433, 2008.

[5] T. Pfajfar, B. Blazic, and I. Papic, "Methods for estimating customer voltage harmonic emission levels," in , 2008, pp. 1-6.

[6] P. H. Swart, J. D. van Wyk, and M. J. Case, "On the technique for localization of sources producing distortion in transmission networks.," *ETEP*, vol. 6, no. 5, Sep. 1996.

[7] A. P. J. Rens and P. H. Swart, "On Techiniques for the Localisation of Multiple Distortion Sources in Three-Phase Networks: Time Domain Verification.," *ETEP*, vol. 11, no. 5, Aug. 2001.

[8] "IEEE Standard Definitions for the Measurement of Electrical Power Quantities Under Sinusoidal, Nonsinusoidal, Balanced, or Unbalanced Conditions," vol. IEEE Std 1459-2010, Feb. 2010.

[9] L. Cristaldi and A. Ferrero, "Harmonic power flow analysis for the measurement of the electric power quality," *Instrumentation and Measurement, IEEE Transactions on*, vol. 44, pp. 683-685, 1995.

[10] T. Pyzalski and K. Wilkosz, "Identification of harmonic sources in a power system: A new method," pp. 1-6, 2005.

[11] S. G. Bhag and R. H. Hüseyin, *ELECTRIC MACHINERY AND TRANSFORMERS*, 3rd ed. New York: OXFORD UNIVERSITY PRESS, 2001.

[12] G. J. Duncan, S. Mulukutla S., and O. Thomas J., *POWER SYSTEM ANALYSIS AND DESIGN*, 4th ed., H. Gowans, Ed. Toronto, Canada: Thomson Learning, 2008.

[13] C. F. Drummond and D. Sutanto, "Classification of Power Quality disturbances using the iterative Hilbert Huang Transform," in , 2010, pp. 1-7.

[14] K. W. Louie, P. Wilson, R. W. Wachal, A. Wang, and P. Buchanan, "HVDC Power System Harmonic Analysis in the Time and Frequency Domains," in , 2006, pp. 1-8.

[15] J. Qiang, X. Jian, Z. Gao, and J. Wei, "Measurement of Harmonics and Inter-Harmonics Based on DWFFT," in , 2008, p. 453.

[16] M. Szmajda, K. G. andrecki, and J. Mroczka, "Gabor Transform, Gabor-Wigner Transform and SPWVD as a time-frequency analysis of power quality," in , 2010, pp. 1-8.

[17] R. Yacamini, "Power system harmonics. II. Measurements and calculations," *Power Engineering Journal*, vol. 9, pp. 51-56, 1995.

[18] E. Zheng, Z. Liu, and L. Ma, "Study on harmonic detection method based on FFT and wavelet transform," in , vol. 3, 2010, pp. V3-413-V3-416.

[19] S. K. MITRA, *Digital Signal Processing; A computer-based approach*, 3rd ed. New York, New York: McGraw-Hill , 2006.

[20] C. Sankaran, *Power Quality*. Boca Raton, Florida: CRC Press LLC, 2002.

[21] Z. Hanzelka, "Hanbook of Power Quality," in *Handbook of Power Quality*, A. B. Baggini, Ed. Chichester, England: John Wiley & Sons, Ltd, 2088, ch. 7, pp. 188-261.

[22] "Electricity Supply- Quality of SupplyVoltage characteristics: Compatibility levels, limits and assessment methods," NRS048-2, 2003.

[23] J. C. Das, *Power Systems Analysis Short-Circuit Load Flow and Harmonics*. New York, United States of America, 2002, ch. 17-20, pp. 554-689.

[24] L. Cristaldi, A. Ferrero, and S. Salicone, "A distributed system for electric power quality measurement," *Instrumentation and Measurement, IEEE Transactions on*, vol. 51, pp. 776-781, 2002.

[25] K. O. H. Pedersen, A. H. Nielsen, and N. K. Poulsen, "Short-circuit impedance measurement," *Generation, Transmission and Distribution, IEE Proceedings*-, vol. 150, pp. 169-174, 2003.

[26] W. Xu, E. E. Ahmed, X. Zhang, and X. Liu, "Measurement of network harmonic impedances: practical implementation issues and their solutions," *Power Delivery, IEEE Transactions on*, vol. 17, pp. 210-216, 2002.

[27] K. Behrendt and K. Fodero, "The Perfect Time: An Examination of Time Synchronization Techniques," *Schweitzer Engineering Laboratories*, pp. 1-17, 2005.

[28] F. M. Fernandez and P. S. C. Nair, "Estimation of supply side harmonics by using network impedance data," in , 2010, pp. 1-6.

[29] K. Wilkosz, "Harmonic Sources Localization: Comparison of methods utilizing the voltage rate or the current rate," pp. 1-6, 2007.

[30] W. Xu, X. Liu, and Y. Liu, "An investigation on the validity of power-direction method for harmonic source determination," *Power Delivery, IEEE Transactions on*, vol. 18, pp. 214-219, 2003.

[31] C. Muscas, L. Peretto, S. Sulis, and R. Tinarelli, "Implementation of multi-point measurement techniques for PQ monitoring," vol. 3, pp. 1626-1631Vol3, 2004.

[32] C. Muscas, L. Peretto, S. Sulis, and R. Tinarelli, "Investigation on Multipoint Measurement Techniques for PQ Monitoring," *Instrumentation and Measurement, IEEE Transactions on*, vol. 55, pp. 1684-1690, 2006.

Appendix A

PIC code UML

This chapter provides the UML diagram of the code used to program a microcontroller (figure a.1). The microcontroller was utilized on the circuit board that triggered the power quality instruments during the practical experiment.

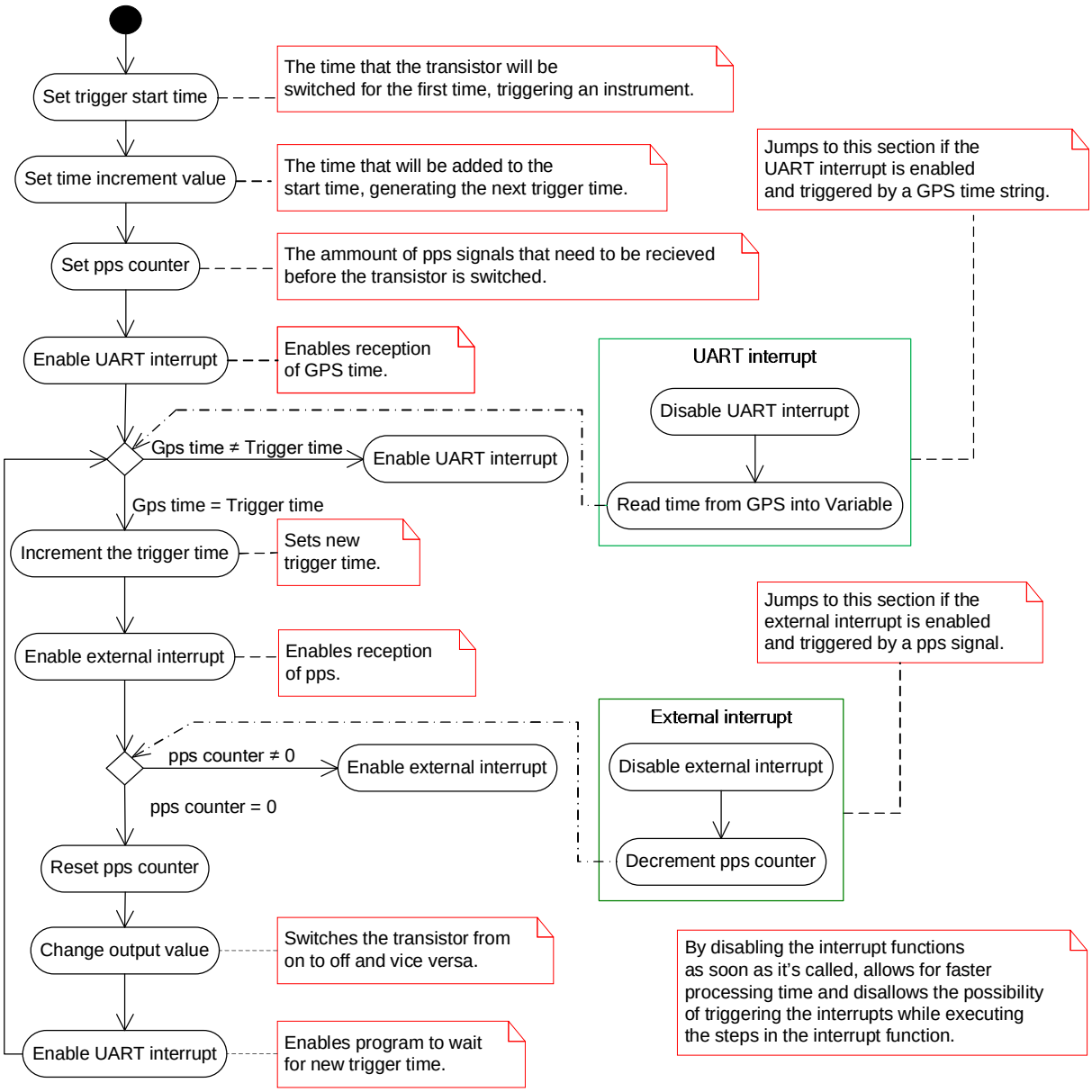

Figure A.1. Simplified UML of microcontroller code.

Appendix B

MathCAD code UML

This chapter provides the UML models for each section of the MathCAD™ program used to process the data.

B.1 Batch_File simplified UML

The Batch_File function importes all the data files saved by the power quality instruments.

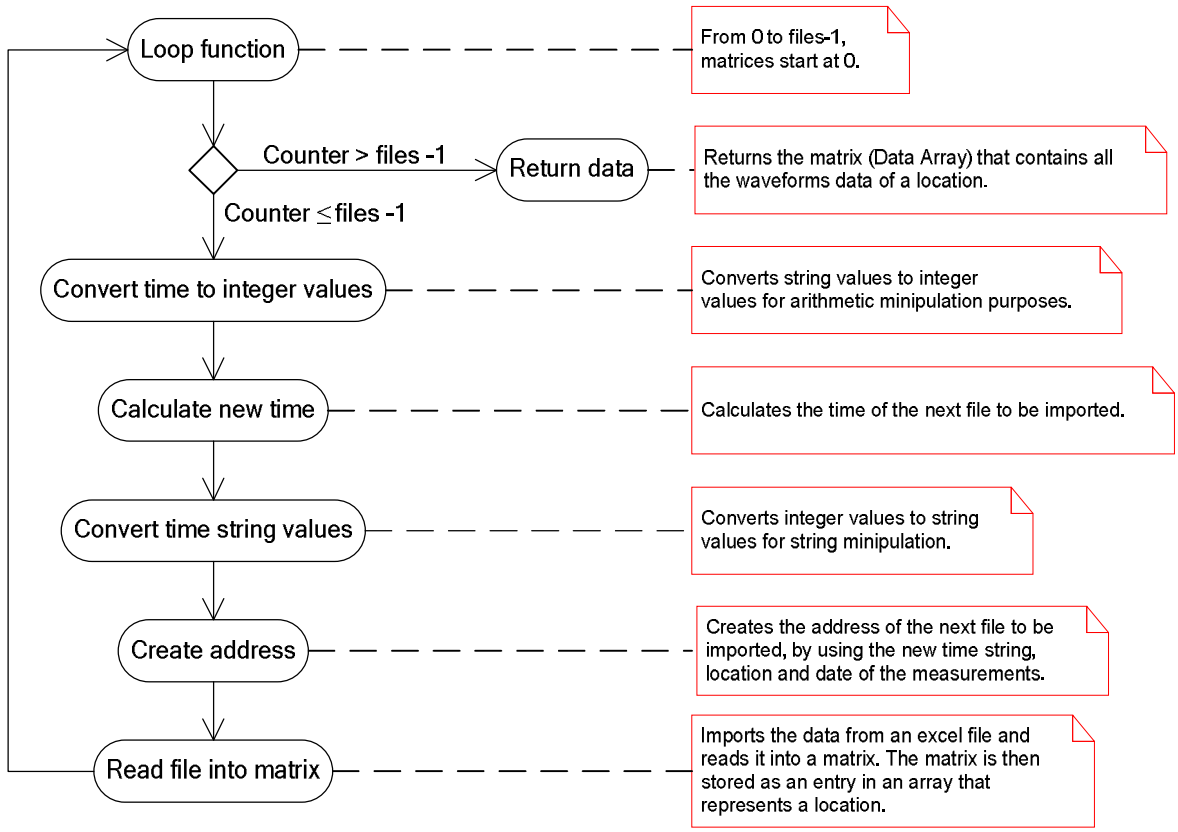

Figure B.1. Simplified UML of the Batch_File UML.

B.2 Calc_Harm simplified UML

The Calc_Harm function calculates the CFFT of the waveforms measured.

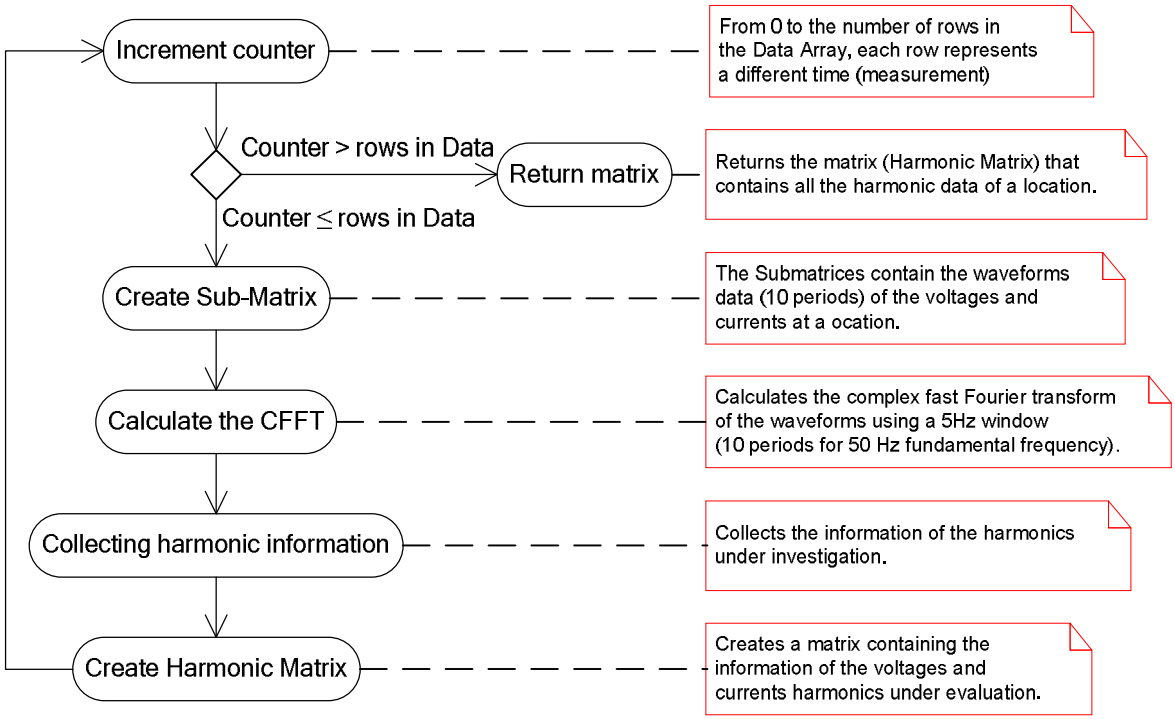

Figure B.2. Simplified UML of the Calc_Harm function.

B.3 Clac_hactpwr simplified UML

The Calc_hactpwr function calculates the HAP of the harmonics under investigation.

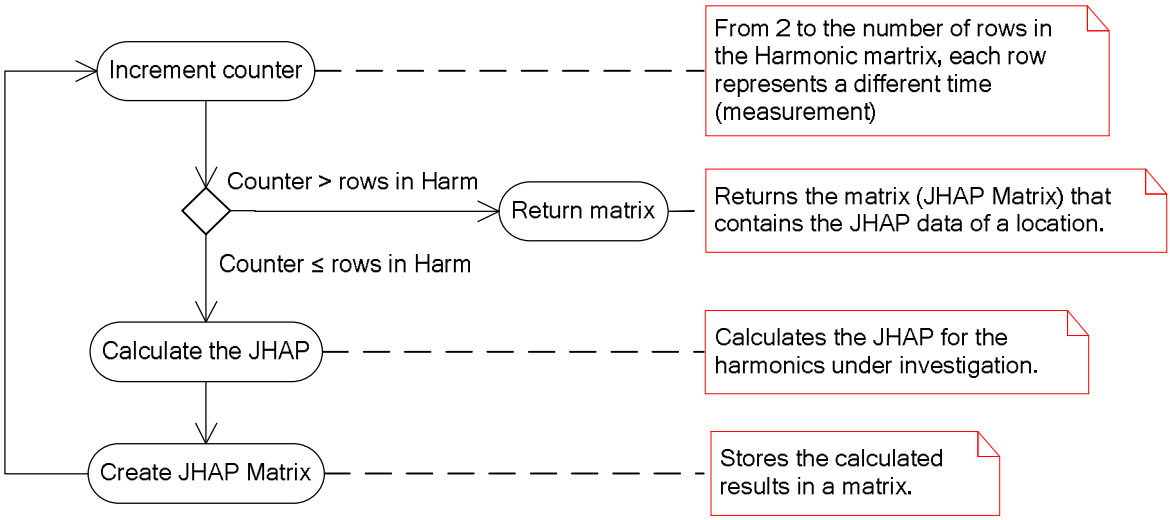

Figure B.3. Simplified UML of the Calc_hactpwr function.

B.4 A simplified UML diagram for calculating the network harmonic impedance.

Figure B. shows the UML diagram of the section in the MathCAD™ that calculates a network's reference harmonic impedance.

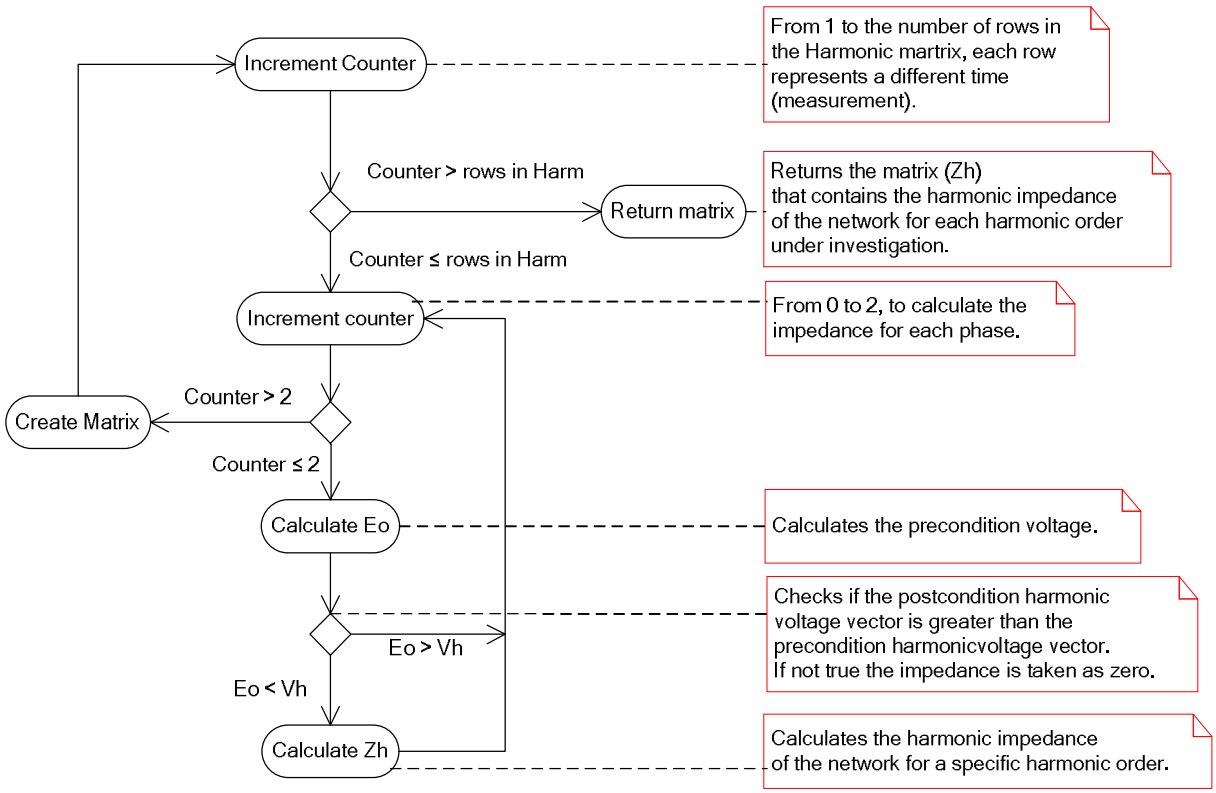

Figure B.4. Simplified UML of the section that calculates the network harmonic impedance.

B.5 A simplified UML diagram for calculating the Harmonic Vector due to the load under investigation.

Figure B.5. shows the UML diagram of the section in the MathCAD™ that calculates the Voltage Harmonic Vector of the load under investigation.

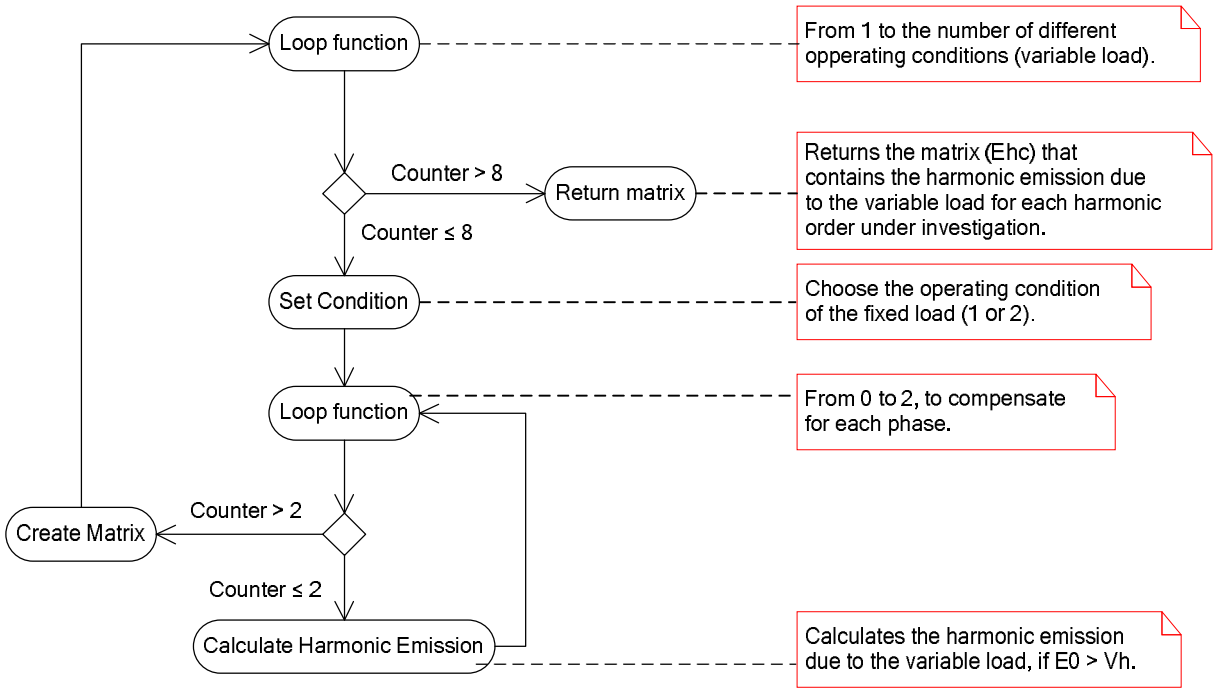

Figure B.5. Simplified UML of the section that calculates the Voltage Harmonic Vector.

Appendix C
Publications arising from research

During the period of this project two conference papers were written and accepted by international and IEEE accredited conferences. This chapter gives a brief overview of the conferences and provides the paper for each conference.

C.1 International Conference on Harmonics and Quality of Power

The ICHQP is an international IEEE technical conference established 27 years ago and is one of the leading conferences in the field of power quality. The paper written for this conference focused on the validity of single point measurements used for the localisation of harmonic sources (pages 76 - 81).

C.1.1 The Validation of single point Measurements for the localization of Multiple Harmonic Sources

Power quality management requires inexpensive and simple methods for electric power quality monitoring. This paper investigates the validity of single point measurements for the localisation of sources of waveform distortion as methods claiming the possibility thereof based on the direction of the HAP are continuously being published.

C.2 IEEE Africon

The Africon conference focused on sustainable energy and communications development for Africa and was held in Zambia. The paper written for this conference investigated the Harmonic Vector method and its practical restrictions due to the use of single point measurements (pages 82 - 87).

C.2.1 A Practical Evaluation of Harmonic Emission

This paper reports an evaluation of harmonic emission assessment. The results obtained by the Harmonic Vector method are correlated to the behaviour of HAP by means of synchronized measurements in a three-phase power system.

The Validation of Single point Measurements for the Localization of Multiple Harmonic Sources

D. Serfontein and A.P.J. Rens

***Abstract*— Power quality management requires inexpensive and simple methods for electric power quality monitoring. This paper investigates the validity of single point measurements for the localization of sources of waveform distortion as methods claiming the possibility thereof based on the direction of the harmonic active power are continuously being published.**

***Index Terms*— Harmonic analysis, harmonic distortion, power quality, power system measurements, power System monitoring**

I. Introduction

The portion of energy converted by non-linear loads in the modern power system is increasing due to the energy-efficiency and the sophistication possible with power electronics. Higher voltage and energy ratings are continuously forthcoming. These devices withdraw non-linear load currents resulting in voltage waveform distortion at the Point of Common Coupling (PCC) due to non-zero supply impedances between voltage source and the PCC.

Quality of Supply (QoS) management requires amongst others, management of the quality of the voltage waveform. Waveform distortion is one aspect of QoS and generally referred to as Voltage Total Harmonic Distortion (VTHD). The concept of compatibility between loading and supply conditions sets an upper level to VTHD (such as 8%).

Single-point measurements are still claimed in literature (for example [6]) to be able to qualify and quantify the extent by which a specific load contributes to the VTHD at a PCC. It is generally agreed that the direction of harmonic active power commensurate with the location of the source [8] if a single source of distortion exists. The concept of Total (Joint) Harmonic Active Power (JHAP) summates all the active powers in all the harmonic components at the node under investigation.

It was shown in [8], [9] that when more than one source of waveform distortion exist in an interconnected power system, all nodes connecting a load or a source have to be studied by means of synchronous measurements as non-linear loads have the ability to exchange harmonic active power between each other and not only between load and source.

It was shown by means of laboratory measurements and simulation [8], [9] that a single-point measurement and harmonic active power cannot be used to further reliable information on the contribution of a specific non-linear load to the VTHD at the PCC if non-linear loads are distributed all over the power system. If this is indeed a valid conclusion, then, application of JHAP is useless in the management of VTHD.

Methods based on the direction of the harmonic active power are still being published claiming to further information on VTHD based on single-point measurements. The validity of single-point measurements methods are evaluated in this paper by analysis of synchronized measurements obtained in a practical power system.

II. Theoretical Considerations

A brief overview on the fundamental aspects of power theory pertaining to this investigation is listed below [9].

A. Joint harmonic active power

It is agreed that the classical power theory can be applied on per harmonic basis when voltage and current waveform distortion exists. Various approaches exist when these powers have to aggregate in order to further information on all the energy phenomena in a power system but the goal of this paper focus only on power theory aspects on which general agreement exists.

The complex Fourier series allow for defining time-domain based distorted voltages and currents shown in (1) and (2):

$$u(t) = \sum_n u_n(t) \tag{1}$$

and

$$i(t) = \sum_n i_n(t) \tag{2}$$

These quantities is obtained by summing the constituent n^{th} order time-dependent complex quantities:

D. Serfontein is with the School for Electrical, Electronic and Computer Engineering, North-West University, Potchefstroom, South-Africa (e-mail: duan.serfontein@nwu.ac.za

A.P.J. Rens is with the School for Electrical, Electronic and Computer Engineering, North-West University, Potchefstroom, South-Africa (e-mail: johan.rens@nwu.ac.za)

$$u_n(t) = U_n e^{jn\omega t} \tag{3}$$

and

$$i_n(t) = I_n e^{jn\omega t} \tag{4}$$

over the harmonic order range.

Where $\boldsymbol{U}^*_n$ and $\boldsymbol{I}^*_n$ are defined as:

$$\boldsymbol{U}_n = U_n e^{j\alpha_n} \tag{5}$$

and

$$\boldsymbol{I}_n = I_n e^{j\beta_n} \tag{6}$$

represent the n^{th} order harmonic phasors of voltage and current respectively. In (5) and (6), α_n and β_n respectively represent the phase angles of the voltage and current. The scalar, time-dependent voltage and current, represented in a more general form by (1) and (2) , follows from:

$$u(t) = \sqrt{2}\,\mathrm{Re}\left\{\sum \underline{u}_n(t)\right\} \tag{7}$$

and

$$i(t) = \sqrt{2}\,\mathrm{Re}\left\{\sum_n \underline{i}_n(t)\right\} \tag{8}$$

The total time-dependent real power that is physically measurable in a distorted network can be defined as:

$$p(t) = \sum_n \sqrt{2}\,\mathrm{Re}\left\{\underline{u}_n(t)\right\}\sqrt{2}\,\mathrm{Re}\left\{\underline{i}_n(t)\right\} \tag{9}$$

From which it can be shown that the Total Average Real Power (or Joint Harmonic Active Power) is:

$$P = \sum_n U_n I_n \cos\phi_n \tag{10}$$

with:

$$\phi_n = \alpha_n - \beta_n \tag{11}$$

The rms value of the voltage and current can be shown to be:

$$U = \sqrt{\sum_n |U_n|^2} \tag{12}$$

and

$$I = \sqrt{\sum_n |I_n|^2} \tag{13}$$

In accordance with the classic approach the average harmonic real power at the harmonic order n can also be calculated directly from the harmonic phasor values of the voltage and current as:

$$P_n = \mathrm{Re}\left\{\underline{U}_n \underline{I}^*_n\right\} \tag{14}$$

Where I^*_n denotes the complex conjugate of the harmonic phasor current and the product of U^*_n and I^*_n denotes the complex power.

The fundamental and harmonic real powers can be respectively calculated as:

$$P_1 = \mathrm{Re}\left\{\underline{U}_1 \underline{I}^*_1\right\} \tag{15}$$

and

$$P_h = \sum_n \mathrm{Re}\left\{\underline{U}_n \underline{I}^*_n\right\} \tag{16}$$

in which n=2, 3,…, k with k the highest harmonic order.

III. Measurements And Results

Measurements were taken at the PCC of a 400 V network. The supply source is constituted by a 11/0,4 kV 400kVA transformer. Two non-linear loads are connected to the PCC as shown in Fig. 1. Load 1 mainly consists of solid-state drives and Load 2 of a data center withdrawing about 60 kVA and 40 kVA respectively.

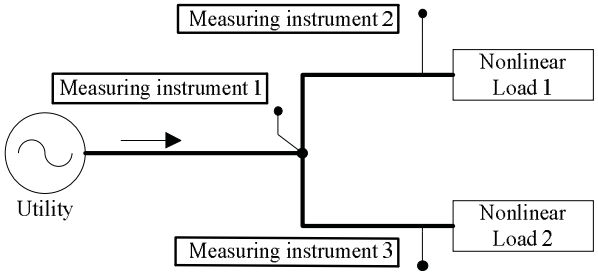

Fig. 1. Single-line diagram of the network

The phase voltages at the PCC are common to the three measurement points. Currents were measured in each line connecting a load and the source to the PCC. Power Quality (PQ) instruments of Class A were used at each measurement points. Voltages and currents were simultaneously digitized at a 16 bits resolution and at a Nyquist frequency of 12.8 kHz. Each instrument adjusts the sampling frequency cycle-by-cycle to ensure that 2^n data points fits exactly into a fundamental frequency wavelength. Without skewing, a reliable result can be expected from the Fourier analysis of the digitized, time-domain data.

Synchronization between the instruments was done by a timing pulse derived from a GPS device to ensure that all

18 channels (9 voltages and 9 currents) were digitized synchronously. Data was collected for 24 hours, as it is a representative duty cycle for these loads. Typical waveforms of the network that were collected during the 24 hours are shown in Fig 2, 3, 4 and 5.

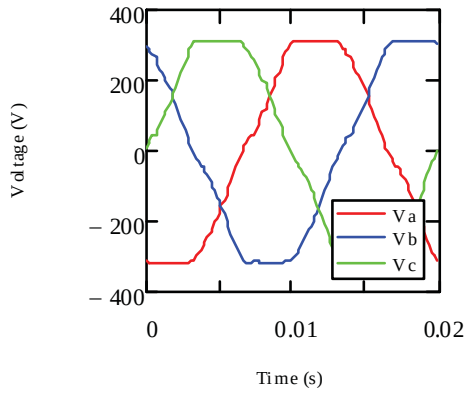

Fig. 2. Typical Voltage waveforms at the PCC

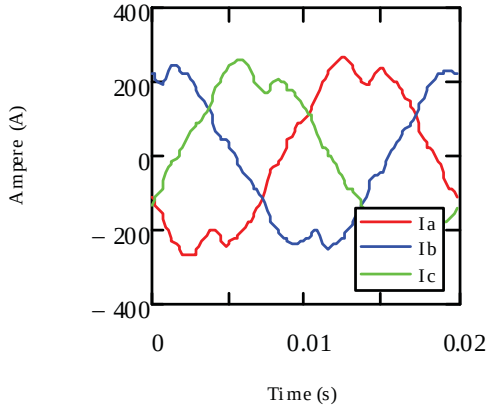

Fig. 3. Typical Current waveforms into the PCC

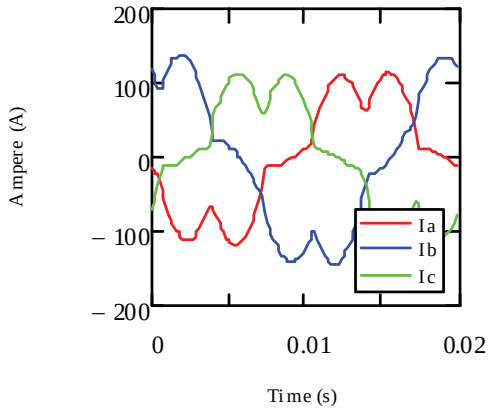

Fig. 4. Current waveforms into nonlinear load 1

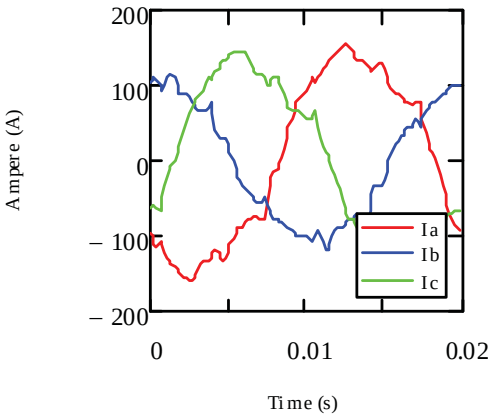

Fig. 5. Current waveforms into nonlinear load 2

The dominant harmonics are listed in terms of magnitude and phase angle in table I, II, III and IV. Some harmonics, expected to be characteristic, were found to be small enough to be ignored. The reason was not verified.

TABLE I.
DOMINANT HARMONIC VOLTAGE MAGNITUDES AND PHASE ANGLES AT PCC

(*h*)	$V_a(h)$	$\alpha_a(h)$	$V_b(h)$	$\alpha_b(h)$	$V_c(h)$	$\alpha_c(h)$
1	236.2	149.3	234.4	29.1	234.6	-90.4
5	12.4	-171.0	12.0	-53.7	12.6	68.4
7	5.1	-137.2	4.4	103.1	4.8	-12.1
11	1.7	-155.9	1.7	-38.3	1.76	87.3
17	0.6	77.3	1.1	-136.6	0.4	-30.6

TABLE II.
DOMINANT HARMONIC CURRENT MAGNITUDES AND PHASE ANGLES INTO PCC

(*h*)	$I_a(h)$	$\beta_a(h)$	$I_b(h)$	$\beta_b(h)$	$I_c(h)$	$\beta_c(h)$
1	179.4	117.9	171.6	-8.2	167.9	-119.2
5	15.9	-0.6	12.9	137.0	17.0	-114.9
7	7.2	-102.6	5.5	127.6	6.7	23.4
11	5.4	-62.2	5.3	55.3	5.5	-174.5
17	2.3	153.0	3.8	-51.6	1.3	32.8

TABLE III.
DOMINANT HARMONIC CURRENT MAGNITUDE AND PHASE ANGLES TOWARDS NONLINEAR LOAD 1

(*h*)	$I_a(h)$	$\beta_a(h)$	$I_b(h)$	$\beta_b(h)$	$I_c(h)$	$\beta_c(h)$
1	73.7	109.5	95.9	-8.2	71.8	-128.4
5	18.5	145	16.4	143.6	18.5	-106.6
7	3.5	-144.9	4.1	91.6	3.7	-18.1
11	3.8	-50.4	3.7	70.4	4.1	-169.4
17	1.8	-110.9	1.9	13.8	1.9	131.4

TABLE IV.
DOMINANT HARMONIC CURRENT MAGNITUDE AND PHASE ANGLES TOWARDS NONLINEAR LOAD 2

(*h*)	$I_a(h)$	$\beta_a(h)$	$I_b(h)$	$\beta_b(h)$	$I_c(h)$	$\beta_c(h)$
1	105.7	124.3	75.9	-8.7	97.2	-112.3
5	5.3	-110.7	3.8	-12.7	3.2	130.7
7	5.2	-75.9	3.2	175.9	4.5	54.9
11	1.9	-87.01	2.1	25.9	1.5	164.9
17	3.1	118.7	3.6	-79.7	2.6	-16.8

Phasor diagrams indicating the 7^{th} harmonic phase angles and magnitudes are given in Fig. 6, 7, 8 and 9 as demonstration of the relative phase relation.

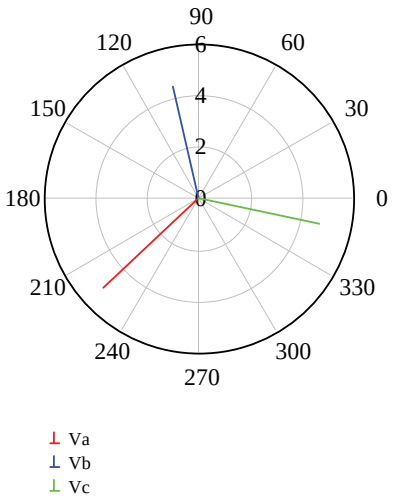

Fig. 6. Three phase 7th harmonic voltage phasors at PCC

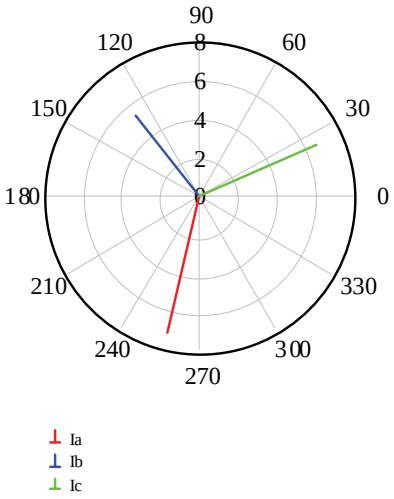

Fig. 7. Three phase 7th harmonic current phasors at PCC

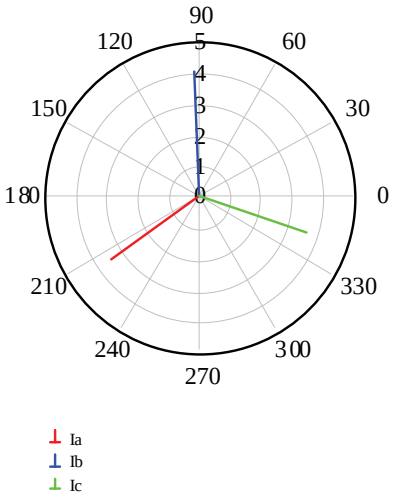

Fig. 8. Three phase 7th harmonic current phasors at Load 1

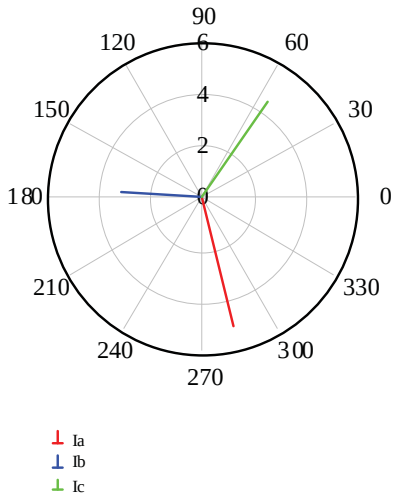

Fig. 9. Three phase 7th harmonic current phasors at load 2

From these results the JHAP (16) and the Harmonic Active Power (HAP) (14) was calculated at each measurement point every 15 min and the results are depicted in Fig.10, 11, 12, 13 and 14.

IV. Discussion

If the direction of active power in the fundamental frequency component is being taken as positive (a positive value) when delivered to the PCC from the utility (feeder into PCC) and positive when delivered from the PCC to the loads, then a negative value in JHAP (or in HAP at a harmonic) indicate that such load is generating it, as it is opposite to the direction of the fundamental frequency active power. From Fig. 14 it can be seen that if JHAP is used for the localization of a harmonic source, then load 1 remain a source of harmonics. Fig. 14 also indicate that load 2 was mostly absorbing harmonic active power without generating any although knowledge on the type of load suggested that it should be generating harmonic active power.

The HAP at the 5th harmonic was absorbed (Fig. 10) by the feeder for all of the time with the interpretation that the PCC has been producing it whilst load 2 absorbed HAP at the 5th harmonic. HAP at the 7th harmonic (Fig. 11) was delivered by the feeder to both loads as both loads absorbed it all of the time. This is against the knowledge that the 7th harmonic is characteristic of the operation of both loads.

The HAP at the 11th harmonic (Fig. 12) was mostly produced by load 1 and absorbed by load 2 and the feeder. Note that the sum of HAP at load 2 and the feeder is the value produced by load 1.

About all of the HAP at the 17th harmonic (Fig 13) produced by load 1 was absorbed by load 2.

A non-linear load can therefore be a source of HAP and then consume HAP at a later stage. HAP can also be exchanged between non-linear loads meaning that a value

of HAP at the terminals of a load constitutes the interaction of different non-linear loads; hence the value cannot be used to quantify the contribution of that load to VTHD.

V. Conclusion

Although the results discussed in this paper were obtained with practical measurements in a low voltage power system, it is in agreement with the results obtained in [8] and [9].

Single point measurements, which make use of harmonic active power, cannot be used to determine the location and contribution of a source of harmonics to the VTHD at a PCC in an interconnected power system, with sources of distortion located all over. Measurements at all nodes of interest in that power system will have to be acquired and synchronously to understand the energy phenomena dictating the voltage waveform distortion.

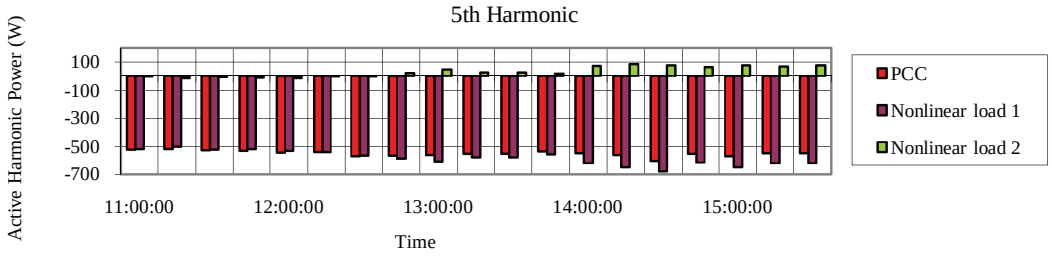

Fig. 10. 5th harmonic: Harmonic Active Power

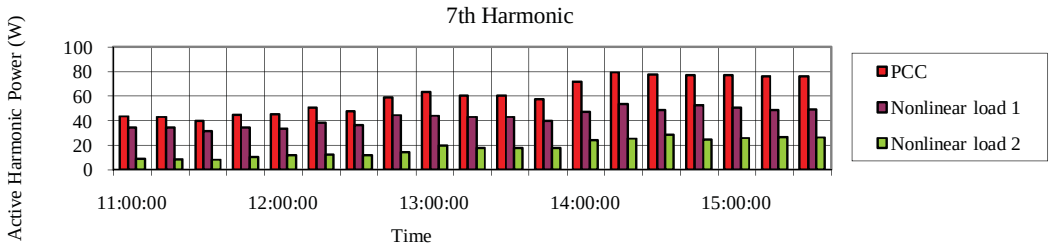

Fig. 11. 7th harmonic Harmonic Active Power

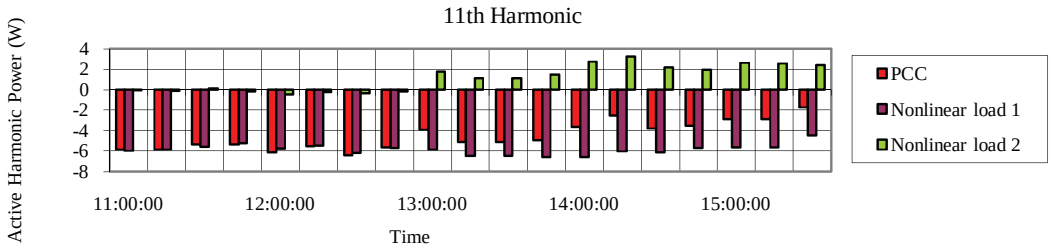

Fig. 12. 11th harmonic Harmonic Active Power

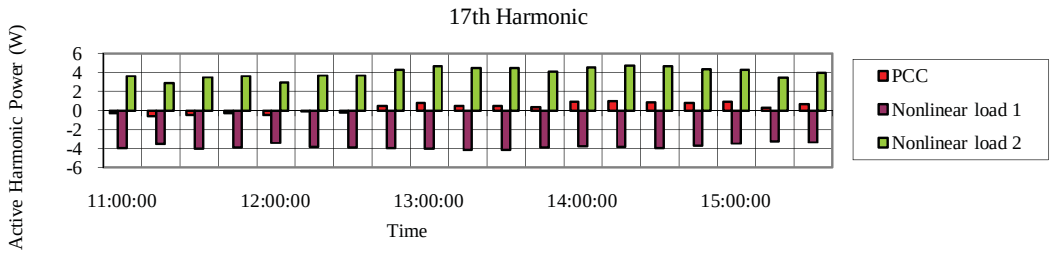

Fig. 13. 17th harmonic Harmonic Active Power

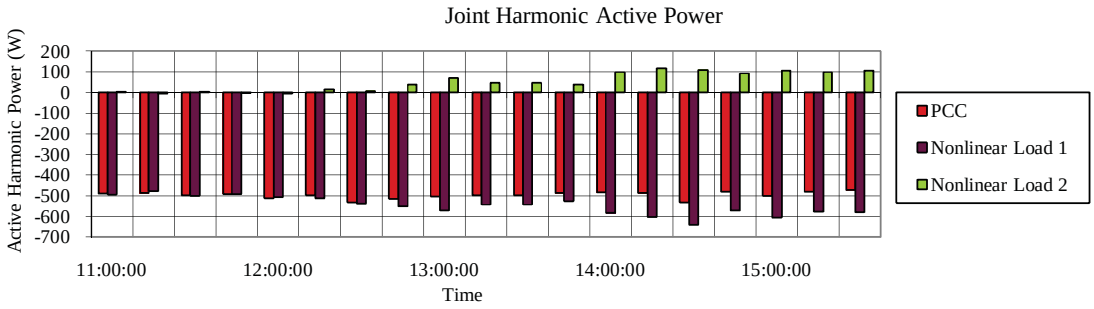

Fig. 14. The Joint Harmonic Active Power with k=20

VI. References

[1] W. Xu, X. Liu, and Y. Liu, "An investigation on the validity of power-direction method for harmonic source determination," *Power Delivery, IEEE Transactions on*, vol. 18, pp. 214-219, 2003.

[2] C. Muscas, L. Peretto, S. Sulis, and R. Tinarelli, "Implementation of multi-point measurement techniques for PQ monitoring," vol. 3, pp. 1626-1631Vol3, 2004.

[3] K. Wilkosz, "Harmonic Sources Localization: Comparison of methods utilizing the voltage rate or the current rate," pp. 1-6, 2007.

[4] L. Cristaldi, A. Ferrero, and S. Salicone, "A distributed system for electric power quality measurement," *Instrumentation and Measurement, IEEE Transactions on*, vol. 51, pp. 776-781, 2002.

[5] L. Cristaldi and A. Ferrero, "Harmonic power flow analysis for the measurement of the electric power quality," *Instrumentation and Measurement, IEEE Transactions on*, vol. 44, pp. 683-685, 1995.

[6] T. Pyzalski and K. Wilkosz, "Identification of harmonic sources in a power system: A new method," pp. 1-6, 2005.

[7] T. Pyzalski, R. Lukomski, and K. Wilkosz, "Utilization of the voltage rate to localization of harmonic sources in a power system," vol. 3, pp. 1091-1094Vol3, 2004.

[8] P. H. Swart, M. J. Case, and J. D. v. Wyk, "On Techniques for Localisation of Sources Producing Distorion in electric power networks," *ETEP*, no. 6, pp. 485-490, Nov. 1994.

[9] A. P. J. Rens and P. H. Swart, "On techniques for the Localisation of multiple Distortion Sources in Three-Phase Networks: Time Domain Verification," *ETEP*, vol. 11, no. 5, Jul. 2001.

VII. Biographies

Johan Rens (Ph.D) is employed at the North West University (NWU), Potchefstroom, South Africa, researching various aspects of quality in electrical energy.

Duan Serfontein (B.Eng) is working towards a M.Eng degree in electrical engineering at the North-West University (NWU) in Potchefstroom, South Africa.

A Practical Evaluation Of Harmonic Emission Assessment

Duan Serfontein and Johan Rens
School for Electrical, Electronic and Computer Engineering
North-West University of Potchefstroom
Potchefstroom, South Africa
20313810@nwu.ac.za, rens.johan@nwu.ac.za

Abstract—. **This paper reports an evaluation of harmonic emission assessment. The results obtained by the Harmonic Vector Method are correlated to the behavior of harmonic active power by means of synchronized measurements in a three-phase power system.**

Keywords-component; Harmonic Emission, Joint Harmonic Active Power, Harmonic Vector Method, Localization of harmonic sources

I. INTRODUCTION

Solid-state power electronics further high levels of sophistication and efficiency in energy conversion. The principle of operation is inherently non-linear and harmonic load currents have to be sustained by the supply impedances. Voltage waveform distortion result and as the energy levels at which these solid-state devices operate, remain on the increase, the assessment of the harmonic emission of a specific source thereof, remain an interesting academic problem. New academic and professional claiming to be able to assess how much a single source of waveform distortion is contributing in an interconnected power system are continuously forthcoming. A successful method is valuable as management of distortion levels overall, will benefit by such knowledge.

Most of these methods use measurements obtained at a single point in the network [1],[2], [3],[4], [5]. Some methods lack practical application and contribute at most at a scientific level. A method claiming practical application is the Harmonic Vector Method reviewed by the CIGRE-CIRED joint working group C4.109. This method requires a reference impedance from the supply source, and phasor information on harmonic voltages and currents phasor to assess the harmonic distortion contributed to the network by a single source of distortion [2],[4]. The method seems practical, as exact knowledge on the harmonic impedance at the source of distortion or the supply network is not needed. Synchronized measurements of voltage and current phasors are required but possible with modern instrumentation.

It is well known that the evaluation of distorting loads can be done by inspection of the direction of the Joint Harmonic Active Power (JHAP) [6], [7], [8], [9] if a single source of distortion exists. Practical application is a challenge, as all nodes in the power system under study have to be characterized by means of synchronized measurements. A single-point measurement in the localization of distortion sources in an interconnected power system is useless when harmonic active power is used in the assessment [6],[7].

This paper evaluates the harmonic emission assessment technique as reviewed by the CIGRE-CIRED working group C4.109 by application in a practical power system but with variables controlled and mostly known. If such single-point measurements can be used to further reliable information on the contribution of a specific non-linear load to the Total Harmonic Distortion (VTHD) at the point of common coupling (PCC) when non-linear loads are distributed all over the power system, it will find valuable application into practical engineering application in the management of harmonic waveform distortion.

II. THEORETICAL CONSIDERATIONS

A brief overview on the fundamental aspects of power theory relevant to this investigation is listed below [7], [8].

A. Joint harmonic active power

It is agreed that the classical power theory can be applied on per harmonic basis when voltage and current waveform distortion exists [8]. Various approaches exist when these powers have to aggregate in order to further information on all the energy phenomena in a power system, but this paper make use of power theory aspects on which general agreement exists.

A distorted voltage and current waveform in the time domain can be presented in the synthetic frequency domain by a finite range of complex harmonic phasors $\boldsymbol{V}_n$ and $\boldsymbol{I}_n$ defined as:

$$\boldsymbol{V}_n = V_n e^{j\alpha_n} \tag{1}$$

And

$$\boldsymbol{I}_n = I_n e^{j\beta_n} \tag{2}$$

represent the nth order harmonic phasor of voltage and current respectively with V_n and I_n the rms values. The phase angles of the voltage and current phasor are represented by α_n and β_n

respectively. The fundamental and harmonic real powers can then be calculated as:

$$P_1 = Re(\boldsymbol{V}_1 \boldsymbol{I}_1^*) \quad (3)$$

and

$$P_h = \sum_h Re(\boldsymbol{V}_h \boldsymbol{I}_h^*) \quad (4)$$

$\boldsymbol{I}^*_n$ denotes the complex conjugate of the harmonic phasor current, the product of $\boldsymbol{V}_n$ and $\boldsymbol{I}^*_n$ denotes the complex power.

The Joint Harmonic Active Power (JHAP) in all the harmonic components "flowing" through a node is then:

$$JHAP = \sum_{h\neq 1}^{N} V_h I_h \cos(\emptyset_h) \quad (5)$$

with:

$$\emptyset_h = \alpha_h - \beta_h \quad (6)$$

in which h=2,3,…, N with N the highest harmonic order considered.

B. Harmonic Vector Method

To introduce the harmonic voltage emission level from a source of distortion, an equivalent network as shown in Fig. 1, is used. $\boldsymbol{E}_{h0}$ is the harmonic voltage phasor of the supply network as modeled and $\boldsymbol{V}_h$ is the harmonic voltage phasor across the load as measured at the point of supply (Source) to this load. $\boldsymbol{I}_h$ is the harmonic current phasor flowing through the source connection backwards to the supply network. $\mathbf{Z}_h$ represents the complex supply network impedance and $\boldsymbol{Z}_{hc}$ the complex load impedance. $\boldsymbol{I}_{hc}$ is the harmonic current phasor as generated by the distortion source.

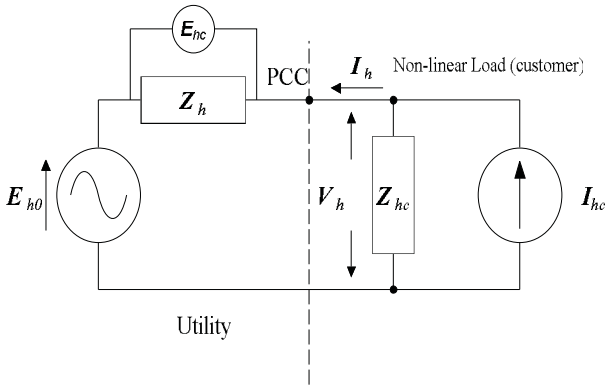

Fig. 1. Equivalent network diagram

Application of this method [2], [4], requires that the magnitude of the harmonic voltage phasors $\boldsymbol{V}_h$ to be larger than harmonic voltage phasor $\boldsymbol{E}_{h0}$ when the distortion source is connected. The harmonic voltage emission from the distorting load into the supply network is then defined as the magnitude of the harmonic voltage phasor $\boldsymbol{E}_{hc}$ and shown in Fig. 2.

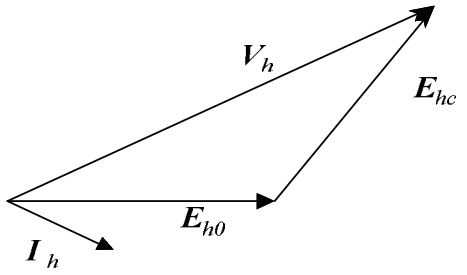

Fig. 2. Phasor presentation of harmonic emission of a source of distortion [2].

The emission of harmonic current $\boldsymbol{I}_h$ is defined as the current that flows upstream through impedance Z_h when the distorting load is connected to the network. Equation (6) is used to determine $\boldsymbol{I}_h$:

$$\boldsymbol{I}_h = \boldsymbol{I}_h \frac{\boldsymbol{Z}_{hc}}{\boldsymbol{Z}_h + \boldsymbol{Z}_{hc}} - \frac{\boldsymbol{E}_{h0}}{\boldsymbol{Z}_h + \boldsymbol{Z}_{hc}} \quad (6)$$

The harmonic voltage phasor due to this emission is then determined as:

$$\boldsymbol{E}_{hc} = \boldsymbol{Z}_h \boldsymbol{I}_h = \boldsymbol{V}_h - \boldsymbol{E}_{h0} \quad (7)$$

It is evident from (7) that the supply network impedance $\boldsymbol{Z}_h$ dictates the contribution of the distortion source to the harmonic voltage distortion at the PCC.

The practical measurement of the supply impedance is not straightforward and a reference network impedance $\boldsymbol{Z}_{h\text{-}ref}$ is used in [2], [10], [11], [12]. Substituting $\boldsymbol{Z}_h$ in (7) with the reference impedance $\boldsymbol{Z}_{h\text{-}ref}$ enable calculation of the harmonic voltage phasor due to the emission of current harmonics:

$$\boldsymbol{E}_{hc} = \boldsymbol{Z}_{h-ref} \boldsymbol{I}_h = \boldsymbol{V}_h - \boldsymbol{E}_{h0} \quad (8)$$

The harmonic voltage emission is then defined as the magnitude $|\boldsymbol{E}_{hc}|$ [2]. Take note that this is only valid when $\boldsymbol{V}_h > \boldsymbol{E}_{h0}$ [2].

III. PRACTICAL EVALUATION

A. Data Acquisition

A laboratory three-phase four-wire power system with base values of 400 V and 5 kVA was constructed as shown in Fig. 3. Transformers with a ratio of 1:1 represented line impedances. Adjustment of the firing angle of 6-pulse thyristor rectifiers enabled control of the two distortion sources. The no-load

supply voltages were not perfectly sinusoidal and the degree of distortion was confirmed as fairly constant over time.

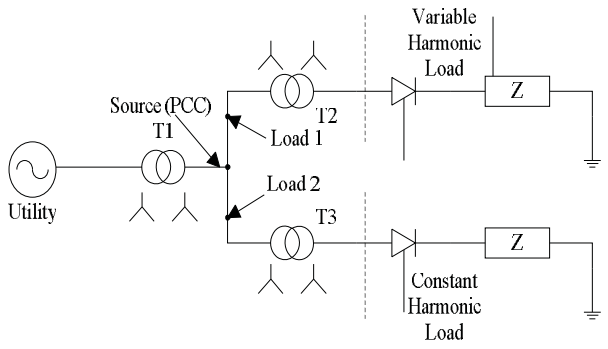

Fig. 3. Single line diagram of the network used.

Voltage and current waveforms at each of the three measuring points (Source, Load 1, Load 2) were digitized with instruments with claimed accuracy of 0.1% up to the 30th harmonic. Voltages and currents were simultaneously digitized at a 16-bit resolution and Nyquist frequency of 12.8 kHz. These instruments adjust the sampling frequency cycle-by-cycle to ensure 2^n data points fits into a fundamental frequency wavelength to avoid possible skewing and spectral leakage when converting to the frequency domain in MathCAD™. This data acquisition setup enabled synchronous A/D conversion of 18 channels (9 voltages and 9 currents).

The loading and firing angle of Load 2 was kept fixed whilst the firing angles of Load 1 was adjusted from the minimum to the maximum value possible for a 6-pulse rectifier. The supply network impedance and harmonics was fixed. This ensured a fixed contribution to the harmonic voltages ($\boldsymbol{E}_{h0}$) and a fixed supply network impedance ($\boldsymbol{Z}_h$). The variation in harmonic current and voltage phasors $\boldsymbol{I}_h$ and $\boldsymbol{E}_{hc}$ as emitted by the variable distortion load are then analyzed according to the methodology under investigation.

Measurements were processed in MathCAD™ to determine the harmonic voltage emission methodology (as reviewed by the Joint Working Group C4-109 of CIGRE-CIRED and discussed in section II-B above). The results obtained where then correlated/validated with the behavior of the Joint Harmonic Active Power (based on the discussion in section II-A above).

B. Results

A 10-cycle window was used in the Fourier transform to optimize the accuracy in phase angle between voltage and current [8] as the near orthogonal relation (impedance dominantly inductive) between higher order voltage and current harmonic phasors can result in a different sign in the active power calculation. The magnitude of harmonic voltage phasors in Fig. 4 indicate the 5th and 7th harmonic to be dominant at the Point of Common Coupling (PCC).

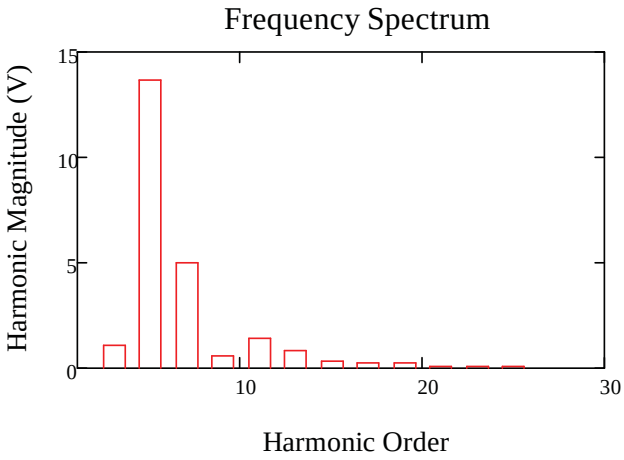

Fig. 4. Magnitude of harmonic voltage phasors at the PCC

The active power for the fundamental frequency and the non-fundamental frequencies are presented in Fig. 5, 6, 7 and 8.

The harmonic voltage emission at Load 1 was only considered valid if the magnitude of the harmonic voltage without the distorting load was less than the magnitude of the harmonic voltage with the distorting load i.e. $\boldsymbol{V}_h > \boldsymbol{E}_{h0}$ If this condition was not valid, the value of the harmonic emission at Load 1 was taken as zero.

IV. DISCUSSION

If the direction of active power in the fundamental frequency component is being taken as positive (a positive value) when delivered to the PCC from the supply network (feeder into PCC) and positive when delivered from the PCC to the loads, then a negative value in JHAP (or in harmonic active power at a harmonic) indicate that such load is the source thereof as it is opposite to the direction of the fundamental frequency active power.

Fig. 5 indicates that a change in firing angle of the rectifier at Load 1 control the active power exchange at the fundamental frequency. The inflow of power should match the total outflow over all harmonic components, but as non-linear loads have the ability to exchange energy between harmonic components, some difference in the reconciliation of energy per harmonic component could exist.

Fig. 5 also indicates that Joint Harmonic Active Power (indicated by "Source" values) is not always "flowing[1]" back towards the supply network. Similar behavior exists in the JHAP at Load 1 and 2. It is clear that JHAP is exchanged between the Loads and although both generate JHAP, the sum is not always flowing upstream as indicated by the Source values. These results were obtained by synchronous measurements in all three lines.

[1] Power "flow" is strictly speaking a misnomer, as energy should rather be assigned to the concept of "flow".

The Harmonic Vector Method is to be applied on a per-harmonic basis. It requires comparison of the harmonic active power in the 5th and 7th harmonic components as plotted in Fig. 6 and Fig. 7. If the 5th harmonic (a dominant component) is evaluated and a comparison is made between the results found using the direction of harmonic active power and the Harmonic Vector Method it can be seen that both identify the source, and level of emission in the 5th harmonic, but only for certain operating conditions.

Conditions exist where Load 1 is a source of harmonic distortion (5th harmonic active power being negative but the Harmonic Vector Method has a zero value zero as the condition $|\boldsymbol{V}_h| > |\boldsymbol{E}_{h0}|$ was not met. Also, positive values of 5th harmonic active power exist indicating absorption of that component by Load 1 whilst the Harmonic Vector Method reports that Load 1 contributed the 5th harmonic component in voltage. The latter observation is a contradiction in results.

Similar contradictory results are obtained for the 7th harmonic component where the Harmonic Vector Method reports contribution of that component whilst the harmonic active power was absorbed by Load 1 as indicated in comparing the results plotted in Fig. 7 for the different setting in firing angle.

V. CONCLUSION

The results obtained indicate that the Harmonic Vector Method contradicts the behavior of harmonic active power. If it is agreed that the direction (sign) of harmonic active power can be used to label a load as a source of that harmonic active power or a sink thereof, it was expected that evaluation of the emission of that harmonic voltage as found through application of the Harmonic Vector Method will yield similar results, but it did not.

It is thus concluded that the limitation in practical application of the Harmonic Vector Method [1], [2], [4] as demonstrated by the results reported in this paper, is due to single-point measurements in use to determine the level of emission. A practical solution to an accurate evaluation of the harmonic emission by a single distorting load when these distortion loads are distributed all over such as in a real-world power system, need research and development. Fundamental network principles dictate the exchange of harmonic active power between non-linear loads and any attempt to accurately quantify and qualify the harmonic emission of a distorting load has to acknowledge these principles.

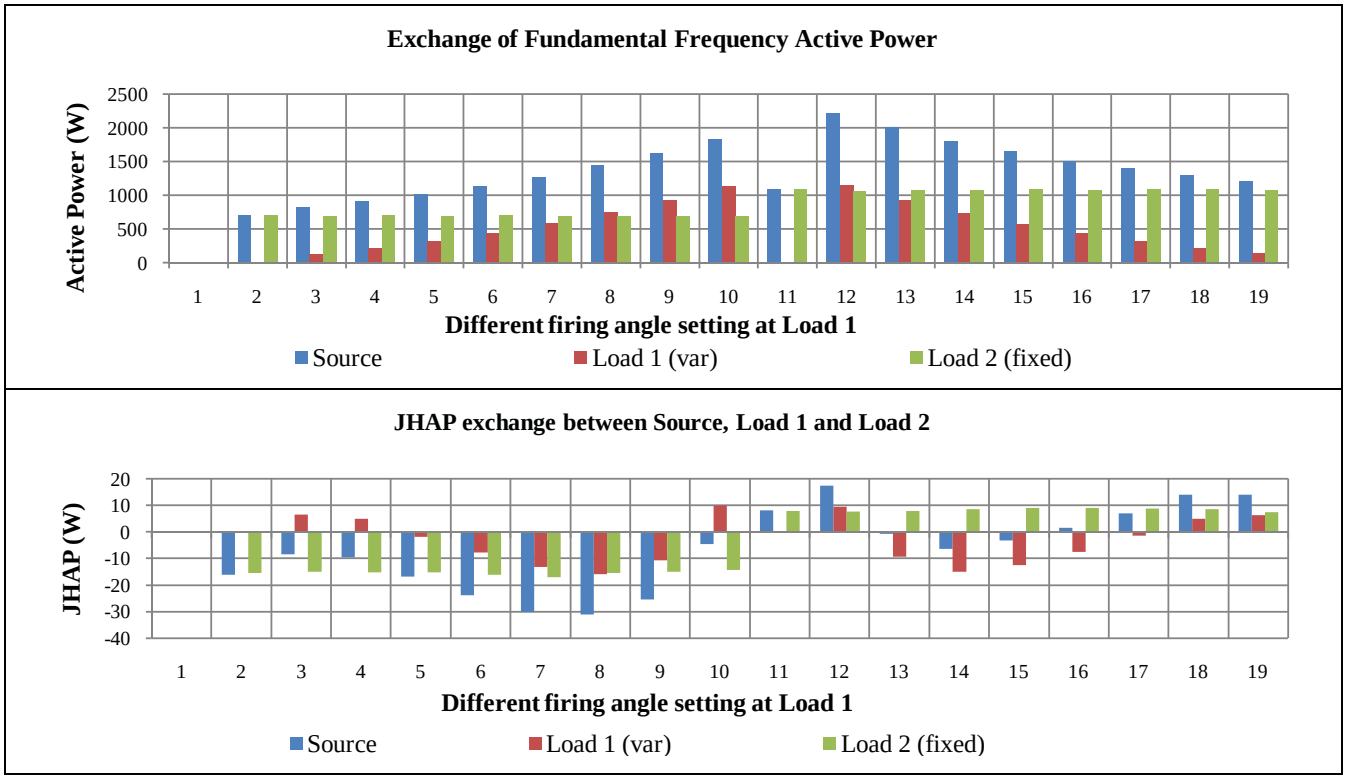

Fig. 5. Fundamental Frequency active power exchange (top) and JHAP exchange (bottom)

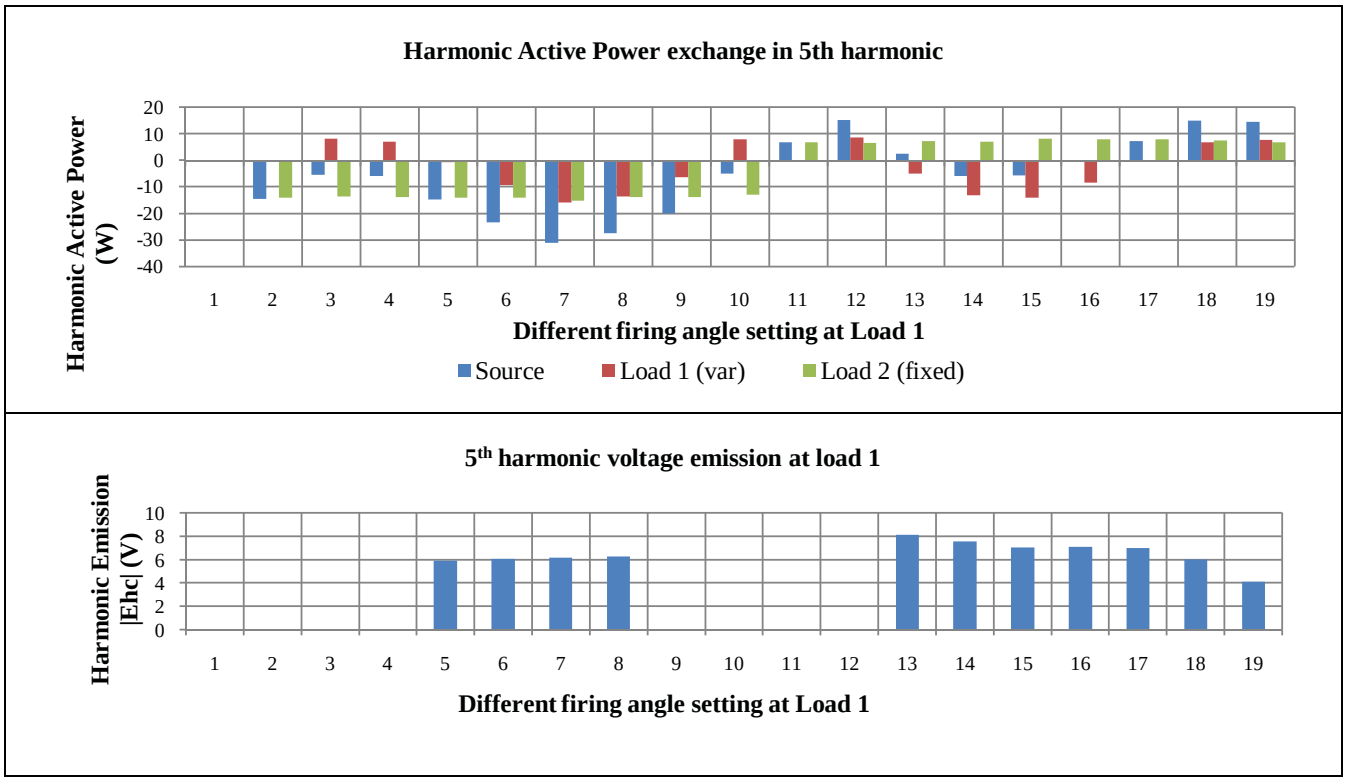

Fig. 6. Active power exchange in 5th harmonic (top) and emission at 5th harmonic per Harmonic Vector Method (bottom)

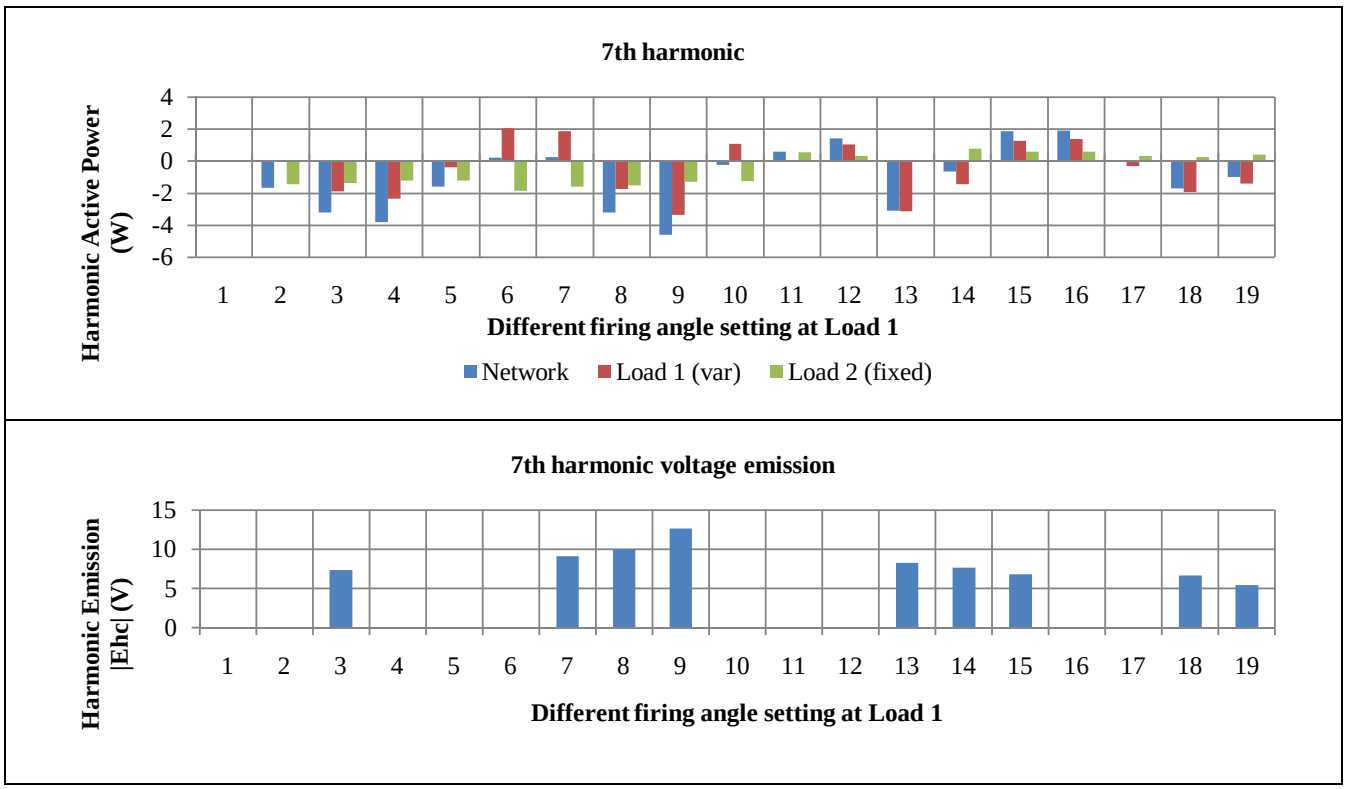

Fig. 7. Active power exchange in 7th harmonic (top) and emission at 7th harmonic per Harmonic Vector Method (bottom)

VI. REFERENCES

[1] E. D. Jaeger, "Disturbance emission level assessment techniques (CIGRE-CIRED joint working group C4.109)," pp. 1-2, 2009.

[2] E. D. Jaeger, "Review of Emission Assessment Techniques (CIGRE-CIRED joint working group C4.109)," 2011.

[3] W. Xu and Y. Liu, "A method for determining customer and utility harmonic contributions at the point of common coupling," *Power Delivery, IEEE Transactions on*, vol. 15, pp. 804-811, 2000.

[4] T. Pfajfar, B. Blazic, and I. Papic, "Harmonic Contributions Evaluation With the Harmonic Current Vector Method," *Power Delivery, IEEE Transactions on*, vol. 23, pp. 425-433, 2008.

[5] T. Pfajfar, B. Blazic, and I. Papic, "Methods for estimating customer voltage harmonic emission levels," in , 2008, pp. 1-6.

[6] P. H. Swart, J. D. van Wyk, and M. J. Case, "On the technique for localization of sources producing distortion in transmission networks.," *ETEP*, vol. 6, no. 5, Sep. 1996.

[7] A. P. J. Rens and P. H. Swart, "On Techiniques for the Localisation of Multiple Distortion Sources in Three-Phase Networks: Time Domain Verification.," *ETEP*, vol. 11, no. 5, Aug. 2001.

[8] I. S. 1459-2010, "IEEE Standard Definitions for the Measurement of Electric Power Quantities Under Sinusoidal, Nonsinusoidal, Balanced, or Unbalanced Conditions.".

[9] L. Cristaldi and A. Ferrero, "Harmonic power flow analysis for the measurement of the electric power quality," *Instrumentation and Measurement, IEEE Transactions on*, vol. 44, pp. 683-685, 1995.

[10] W. Xu, E. E. Ahmed, X. Zhang, and X. Liu, "Measurement of network harmonic impedances: practical implementation issues and their solutions," *Power Delivery, IEEE Transactions on*, vol. 17, pp. 210-216, 2002.

[11] K. O. H. Pedersen, A. H. Nielsen, and N. K. Poulsen, "Short-circuit impedance measurement," *Generation, Transmission and Distribution, IEE Proceedings-*, vol. 150, pp. 169-174, 2003.

[12] F. M. Fernandez and P. S. C. Nair, "Estimation of supply side harmonics by using network impedance data," in , 2010, pp. 1-6.

[13] W. Xu, X. Liu, and Y. Liu, "An investigation on the validity of power-direction method for harmonic source determination," *Power Delivery, IEEE Transactions on*, vol. 18, pp. 214-219, 2003.

[14] L. Cristaldi, A. Ferrero, and S. Salicone, "A distributed system for electric power quality measurement," *Instrumentation and Measurement, IEEE Transactions on*, vol. 51, pp. 776-781, 2002.